

Engineered bispecific antibodies as cancer therapy

Shuyu Huang

黄书煜

© 2023 Shuyu Huang

All rights reserved. Published papers were reprinted in this publication under CC license. No parts of this thesis may be reproduced or transmitted in any form or by any means without prior permission of the author.

ISBN:

The research described in this thesis was performed at the Faculty of Veterinary Medicine, Department of Infectious Diseases and Immunology, Utrecht University, The Netherlands; the Institute of Immunology and Infection Research, School of Biological Sciences, University of Edinburgh, Edinburgh, UK; Aduro Biotech Europe, Oss, the Netherlands.

Cover design: Shuyu Huang conceives the idea and makes the final layout. All the elements are relevant to the content of this thesis.

Layout and design: Shuyu Huang

Printing: proefschriftmaken | www.proefschriftmaken.nl

Printing of this thesis was financially supported by Infection & Immunity Center Utrecht and by the Immunology Section, Department of Biomolecular Health Science, Faculty of Veterinary Medicine, Utrecht University.

Engineered bispecific antibodies as cancer therapy

Geavanceerde bispecifieke antilichamen als kankertherapie

(met een samenvatting in het Nederlands)

Proefschrift

ter verkrijging van de graad van doctor aan de Universiteit Utrecht
op gezag van de rector magnificus, prof.dr. H.R.B.M. Kummeling,
ingevolge het besluit van het college voor promoties
in het openbaar te verdedigen op 13 juni 2023 des middags te 12.15 uur

door

Shuyu Huang

geboren op 3 juli 1992 te Jiangxi provincie, China

Promotoren:

Prof. dr. F. Broere

Prof. dr. E.J.A.M. Sijts

Beoordelingscommissie:

Dr. M.L. Boes

Prof. dr. T. van Hall

Prof. dr. H.P. Haagsman

Prof. dr. A. Gröne

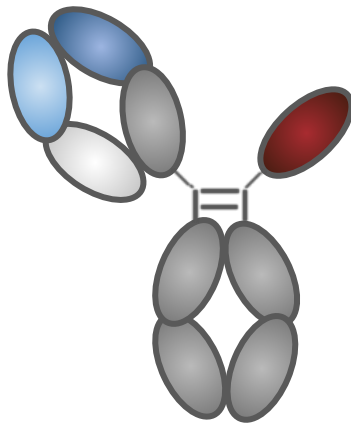
Prof. dr. S.G.D. Rüdiger

Shuyu Huang was financially supported by European Union, Horizon 2020 research and innovation programme under the Marie Skłodowska-Curie Innovative Training Networks.

Table of contents

Chapter 1	General introduction	7
Chapter 2	Bispecific antibodies targeting dual tumor - associated antigens in cancer therapy	32
Chapter 3	A novel efficient bispecific antibody format, combining a conventional antigen-binding fragment with a single domain antibody, avoids potential heavy-light chain mis-pairing	60
Chapter 4	Shortened Hinge Design of Fab x sdAb-Fc Bispecific Antibodies Enhances Redirected T-Cell Killing of Tumor Cells.....	90
Chapter 5	In a therapeutic setting, mouse IgG2a isotype is superior to mIgG1 or mIgE in controlling tumor growth	123
Chapter 6	General discussion	153
Chapter 7	Summary/Overzicht	167
Appendix	Acknowledgements/Curriculum vitae/List of publications	173

1



General introduction

The immune system protects the body from infections and foreign substances by triggering an immune response. Immunology was established in the nineteenth century based on two major findings. One is the identification of phagocytic cells by Elias Metchnikoff, who discovered that phagocytic cells could eat and digest many microorganisms, providing nonspecific defenses against infection [1]. The innate immunity was established as a result of this. Another one is the identification of antibodies by Emil Behring and Paul Ehrlich, which neutralize microbial toxins [2]. The adaptive immunity was founded based on this. From then on, the immune system is divided into an adaptive and innate immune system.

The innate immune system responds rapidly but not specifically to pathogens. Instead of being tailored to a specific pathogen, inborn responses are generic. Every pathogen that the innate system encounters receives the same response strength. In most organisms, the host's primary defense mechanism is the innate immune system [3]. Adaptive immunity is an antigen-specific defense against infections. The adaptive immune system is unique in that it can generate immunological memory, which means that after being exposed to a pathogen once, the immune system will respond more quickly and effectively to it on subsequent occasions. For instance, the creation of antibodies or experienced T cells recognizing a specific pathogen, which develop throughout the course of an individual's lifetime as an adaptation to infection with that pathogen. In the past, innate immunity and adaptive immunity are thought to be two irrelevant parts. It took a long time before it changed into a view of complementary binarity, which views innate and acquired immunity as partners in interaction [4].

Monoclonal antibody

In the early 1890s, Emil von Behring and Shibasaburo Kitasato discovered that the transfer of serum of animals could mediate resistant to diphtheria or tetanus. Thus, the serum contained a particular "antitoxic activity" that could provide temporary protection against the effects of diphtheria or tetanus toxins in humans. It was eventually discovered that this activity was brought about by proteins that are now known as antibodies, which bind specifically to the toxins and inhibit their activity [5].

An antibody (Ab), produced by plasma cells, is a large immunoglobulin (Ig) used by the immune system to execute various biological functions. Based on the differences in the heavy chain constant regions, antibodies

can be classified into 5 types, also called “isotypes”. These include IgG, IgM, IgA, IgD, and IgE which all fulfill different functions in the body [6]. Within the 5 types, IgG isotype antibody is the most abundant antibody in blood, which plays an important role in the biological defense system, including but not limited to recognizing and killing foreign objects such as pathogenic bacteria and viruses. IgG antibodies are “Y” shaped proteins with a molecular weight of ~ 150 kDa, made up of two pairs of heavy-light chain polypeptide chains. Based on the function, an IgG antibody can be divided into two parts: an antigen-binding fragment (Fab) that consists of two variable and two constant regions (C-region), with the two variable regions (V-region) making up the variable fragment (Fv), which provides the antigen specificity of the antibody and a crystallizable fragment (Fc) that drives biological activity (**Fig. 1**).

The large repertoire of antigen-specific antibodies protects human beings against an almost unlimited variety of pathogens. The diversity of the immunoglobulin repertoire is generated by four main processes. First, the variable region of the immunoglobulin heavy and light chain is encoded by multiple gene segments that are combined by gene rearrangement to form functional Fv. Thus, in different rearrangement events different gene segment combinations can be used. A significant portion of the diversity found in V regions can be attributed to this combinatorial diversity. Second, the process of recombination adds and subtracts nucleotides at the junctions between the various gene segments, introducing junctional diversity. The numerous possible combinations of heavy- and light-chain V regions that pair to form the antigen-binding site in the immunoglobulin molecule constitute a third source of diversity and are referred to as combinatorial diversity. As will be discussed further down, each of the two methods for generating combinatorial diversity could theoretically result in approximately 1.9×10^6 distinct antibody molecules. Depending on how junctional diversity is calculated, it is estimated that the repertoire of receptors expressed by naive B cells could include at least 10^{11} distinct receptors. Diversity could even be several orders of magnitude greater. Finally, point mutations in the rearranged V-region genes are introduced by somatic hypermutation, and only occurs in B cells following the initiation of an immune response. Somatic hypermutation happens in the germinal centers (GCs) of lymph nodes and spleen, and is accompanied by antibody isotype switching [7].

Somatic hypermutation drives affinity maturation, as B cells producing the highest affinity antibodies are selected for survival. Antibody isotype

switching (or class switching) is a process of DNA recombination which changes the immunoglobulin constant region from IgM (the first Fc to be produced) into IgG, IgE, or IgA, which modulates Ig effector function as appropriate for defense against the invading pathogen. These two processes involve a specific subset of CD4 T helper cells, called follicular helper T cells (Tfh) [8]. Tfh directly stimulate B cells through the interaction of the co-stimulatory molecule CD40 with the B cell's CD40-ligand (CD40-L) and by producing the cytokine IL-21, which stimulates B cell proliferation. The isotype of antibody produced can be determined by additional cytokine production by Tfh [9]. Thus, in the GC reaction, somatic hypermutation in B cells modifies the Ig V region and isotype switching the Ig Fc tail to improve the protective capacity of the antibodies they produce. In the later stages of the primary immune response, these B cells will either differentiate into plasma cells that secrete class-switched antibody of a higher affinity or into memory B cells [8].

Due to the binding specificity, antibodies can help immune system to fight against pathogens. The first and most straightforward method is to bound pathogens or their products, thereby impair their ability to infect cells. This is known as neutralization and is an efficient way to prevent virus from entering cells and replicating, and against bacterial toxin [10]. In addition, an antibody is able to bind to a microbe or an abnormal/foreign cell and kill it by Fc induced secondary immune functions. These mechanisms can be separated in i) Antibody-dependent cell-mediated cytotoxicity (ADCC, lysis of target cells coated with antibody by effector cells with cytolytic activity that recognize the antibody coat through specific immunoglobulin receptors called Fc receptors, including NK cells, macrophages, and granulocytes), ii) Antibody-dependent cellular phagocytosis (ADCP, an immunological mechanism of elimination whereby tumor cells are targeted with mAbs to be digested by phagocytic immune cells) and iii) Complement-dependent cytotoxicity (CDC, i.e. specific target cell lysis through recruitment of complement to the targeted cell surface, initiating the complement cascade). Furthermore, the Fc region also interacts with the neonatal Fc receptor, which is involved in recycling the IgG molecules, leading to prolonged half-life of antibodies [11,12]. Different Fc receptors as determined by the isotype of IgG mAb could induce distinct immune responses. Therefore, in cancer therapy, the isotype of IgG mAb plays a critical role. The IgG Fc-induced secondary immune functions are mediated via complement and FcγRs including activating FcγRs (FcγRI, FcγRIIa/IIc,

FcγRIIIa, FcγRIIIb) and inhibitory FcγR (FcγRIIb) [13,14]. Since both activating and inhibitory FcRs are usually co-expressed on effector cells, the outcome of IgG-mediated secondary immune functions is largely determined by its Fc relative binding affinity and Fc receptor availability. Thus, the activating-to-inhibitory (A/I) ratio is used to describe an antibody's relative affinity for its receptors [15]. In mice, there are four IgG subclasses (mIgG1, mIgG2a, mIgG2b and mIgG3) which differ from one another in their capacity to bind to Fc receptors on immune cells and to activate complement. Therefore, the expected mode of action of therapeutic mAbs influences the choice of antibody isotype. Based on data generated in mice, mIgG2a showed a high A/I, mIgG1 showed a low A/I, and intermediate A/I was observed for mIgG2b [15]. Because of this, it has been demonstrated in numerous in vivo model systems that therapeutic antibodies of the mIgG2a subclass are more effective at clearing tumors. As a result, in numerous in vivo model systems, therapeutic antibodies of the mIgG2a subclass have been demonstrated to be more potent in eliminating tumor cells [16].

Antibodies contribute both to passive immunity as well as to active immunity. Passive immunity refers to the transfer of antibodies to an unprotected individual for the purpose of disease prevention or treatment. Animal studies in 1890 were the first formal demonstration of passive immunization as a successful treatment for diphtheria and tetanus, and diphtheria-specific antitoxin was successfully used in the hospital to reduce mortality during diphtheria outbreaks as early as the middle of the 1890s.

In order to utilize the characteristics of antibodies to protect humans from diseases, in 1975, hybridoma technology was invented to produce monoclonal antibodies (mAbs) artificially by Milstein and Köhler. In 1985, the first therapeutic mAb, muromonab-CD3 (OKT3) which against the CD3 antigen on mature peripheral human T cells, blocks T cell function, was approved by the Food and Drug Administration (FDA) for the treatment of acute organ transplant rejection [17]. In 1997, Rituximab became the first therapeutic monoclonal antibody that was approved for clinical use in cancer therapies which significantly improved the clinical outcomes in non-Hodgkin's lymphoma. Since then, mAb-based therapeutic has revolutionized the field of cancer therapy and represented one of the fastest-growing classes of drugs on the market [18]. The mechanisms of tumor cell killing by antibodies can be summarized as being due to several mechanisms: 1) direct action of the antibody, through growth factor receptor blockade, induce apoptosis by agonist activity, or delivery of a drug or

cytotoxic agent; 2) immune-mediated cell killing mechanisms, inducing ADCC, ADCP and CDC, and regulation of T cell function by immune checkpoint modulation [19]. Due to the success of therapeutic mAb as cancer therapy, more mAb-based therapies have been developed for cancer treatment such as antibody drug conjugate (ADC) therapy, chimeric antigen receptor (CAR) T-cell therapy, etc.

In 2018, the worldwide therapeutic mAbs market was worth roughly \$115.2 billion and is anticipated to reach \$300 billion by 2025 [20].

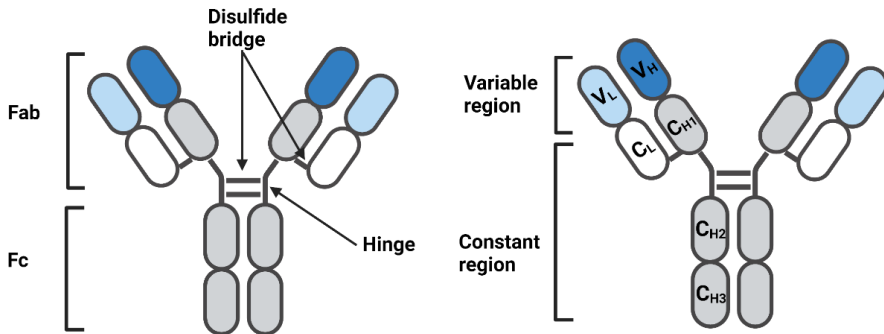


Figure 1. Schematic structure of an antibody. An antibody consists of an antigen-binding fragment (Fab) and a crystallizable component (Fc). Two heavy chains and two light chains fold into constant regions: constant region 1 (CH1), constant region 2 (CH2), constant region 3 (CH3) and light chain constant region (CL); variable regions: heavy chain variable region (VH) and light chain variable region (VL).

Bispecific antibodies

The success of Cetuximab (an anti-EGFR mAb) and Rituximab (an anti-CD20 mAb) in treating a variety of cancers are two examples of the impressive outcomes achieved with mAbs in cancer treatment. However, there are a few drawbacks to mAb-based treatments that limit their outcome as cancer therapeutics [21]. First of all, most tumor-associated antigens (TAAs) used as target are also expressed on healthy tissues. Therefore, many monospecific mAbs that target tumors not only kill tumor cells but also sometimes cause severe on-target damage to healthy tissues [22]. Secondly, multiple disease-causing proteins and cross-talking pathways are involved in cancer, which is a highly complex and multifactorial disease. Activation of

alternative pathways in a complex molecular network may mediate tumor escape from single pathway blockade by a mAb. Moreover, treatment induced downregulation or loss of antigen on tumor cells also leads to acquired monospecific mAb based therapy resistance [23].

In contrast to mono-specific antibody, bispecific antibodies (BsAbs) are a class of mAb that could target two different antigens/epitopes simultaneously. The potential advantages of BsAbs in comparison to monospecific monoclonal antibodies is that BsAbs could theoretically improve tumor selectivity while minimizing side effects in normal tissues by targeting two TAAs with each of them being not necessarily tumor-specific individually [24,25]. Dual targeting could also be used to modify two functional pathways in the tumor, thereby preventing treatment resistance because cancer is a complex and multifactorial disease [26,27]. The concept of BsAbs can be traced back to the 1960s, when it was proposed and described by Nisonoff et al., coupling two rabbit antigen binding fragments from two different polyclonal sera through mild re-oxidation [28]. Following the footprint of the development of mAbs, in 1983, hybrid hybridoma (also known as quodroma) technology, which fuses two antibody-producing hybridomas, was developed to generate BsAbs for clinical applications [29].

Bispecific antibody format

Although Nisonoff et al have already created the concept of BsAb in the 1960s, the first therapeutic BsAb was approved into the market almost 50 years later, in 2009, mainly due to manufacturing issues and clinical failure [28,30]. In addition, as heavy/light chain randomly form molecules during assembly the correct heavy/light chain association became an issue. The theoretical yield of desired BsAbs produced by quodroma technology was ~12.5%. Yet worse, the correct antigen-specific ones were extremely difficult to be purified. Therefore, the major issue for BsAb development had been the production of pure BsAbs free of undesirable by-products (**Fig. 2**) [31].

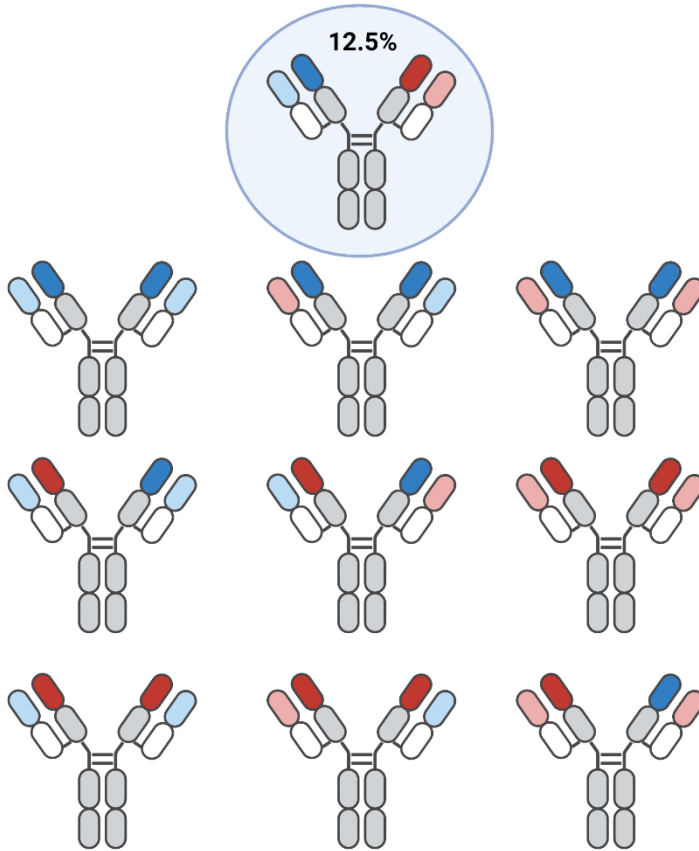


Figure 2. Chain association issue. Generating bispecific heterodimeric IgG antibodies from a single expression cell line with four different antibody chains—two heavy and two light chains results in the chain association issue. There is a total of 2^4 (16) possible chain combinations, resulting in 10 different bispecific antibody products, as the heavy/light chains can associate with each other in a stochastic manner. The yield of the only one desired product within this mixture is 12.5% maximum.

Over the past two decades, with the advent of protein engineering, the chain association issue of BsAbs was solved to a substantial extent which triggered a worldwide wave of bispecific antibody development. Heavy-heavy chain association issues were addressed by several heterodimerization methods which enforce the correct association of the two different heavy chains of a BsAb, such as the knobs-into-holes (KiH) heterodimerization method which creates a 'knob' and a 'hole' structure by

changing the size of amino acids in the CH3 domain of antibody. The 'knob' structure is created by replacing a small amino acid with a larger one (T366Y) while the 'hole' structure is created by the replacement of a large amino acid to a smaller one (Y407T). In this way, the 'knob' structure is able to insert into the 'hole' structure, thus facilitating heterodimerization. Knobs-into-holes technology has been widely used to help heterodimerization during bispecific antibody construction [32,33]. In parallel to KiH technology, other heterodimerization methods were developed. ART-Ig uses electrostatic steering of Fc tails to facilitate heterodimer formation by introducing mutations (D360K, D403K and K402D, K419D) in the Fc region of each heavy chain [34]; Leucine zipper platform (LUZ-Y) facilitates the heterodimerization of antibody heavy chains by an extra leucine zipper appending to the C terminus of the CH3 domain of the antibody [35]; Bispecific engagement by antibodies based on T-cell receptor (BEAT) achieves heterodimerization by a proprietary CH3 interface, mimicking the natural association of the T-cell surface receptors α and β between the two CH3 domains of IgG [36]; Strand-exchange engineered domain CH3 heterodimers (SEEDbody) supports heterodimerization of antibody heavy chains by creating complementary human strand-exchange engineered domain (SEED) CH3 heterodimers which are composed of alternating segments of human IgA and IgG CH3 sequences [37].

In addition to heavy-heavy chain association issues, heavy-light chain mis-pairing issues were overcome by emerging innovative strategies. One strategy is to use the common light chain approach, in which a pair of common light chains are shared by two different heavy chains [32,38]. Learned from the heterodimerization methods applied for heavy-heavy chain association, some approaches engineered the contact points of VH/VL, CH1/CL or both [39–41]; Other approaches exchanged the VH-VL or the CH1-CL domains between the heavy and light chain Fab domains [42].

Moreover, there are some strategies that have been invented to avoid heavy-heavy and/or heavy-light chain mis-pairing issues. For example, BsAbs generated by in vitro assembling of two half-antibodies derived from parental antibodies such as in duobody technology. Inspired by natural BsAbs formed by IgG4 antibodies via a in vivo process named Fab-arm exchange, the duobody technology introduces a K409R & T370K and F405L & R411T mutation in the CH3 region of the two parental antibodies, respectively, which enables in vitro controlled Fab-arm exchange (cFAE) to form BsAbs [43]; Notably, amivantamab, a BsAb targeting EGFR and c-MET

developed by duobody technology has been approved onto the market by the FDA in 2021 [44]. Similar to duobody technology, IgG1/IgG2 bispecific technology also relies on the Fab arm exchange mechanism for IgG4. The two parental antibodies can be expressed and purified in human IgG1 or IgG2 subtypes with desired mutations in Fc region. Stable bispecific antibody with high yields can be formed by mixing them together under proper redox conditions [45]. In addition, combining a conventional Fab with a nanobody or scFv is another way to avoid heavy-light chain mis-pairing, as scFv and nanobody do not naturally associate to a light chain [36,46]. Alternatively, various platforms such as appended IgG which fuses an additional binding site to either the heavy or light chain, could overcome the random heavy and light chain pairing as well [47].

With all these advances, currently over 100 different BsAb formats have become available for researchers to take advantage of for different applications [47,48]. The varied BsAb formats are usually divided into two classes: IgG-like and non-IgG-like. The IgG-like BsAbs often have a long serum half-life, display a relatively favourable solubility and stability and are able to induce secondary immune functions (ADCC, ADCP and CDC). Non-IgG-like BsAbs have the edge over IgG-like ones in immunogenicity, tissue-penetrating capacity and yield [49].

Of over 100 different BsAb formats, some have been further developed into mature commercial technology platforms for BsAb production (**Fig. 3**) [50]. The format of IgG-like BsAbs can be further divided into symmetric and asymmetric architecture. Asymmetric IgG-like BsAb platforms usually combine two methodologies which overcome heavy-heavy chain and heavy-light chain mis-pairing, respectively such as CrossMab [51] and DuetMab [52], which simultaneously use knobs-into-holes and Fab engineering methods. While there are also some asymmetric IgG-like BsAb platforms do not use heavy-light chain heterodimerization method as they avoid heavy-light chain mis-pairing issues by combining a Fab with scFv or nanobody, such as Ybody [53] and ITab [54]. Symmetric IgG-like BsAb platforms, as previously described, either perform in vitro antibody assembling or append additional binding site(s) to IgG backbones such as duobody or mAb-Trap [55]. Due to the absence of an Fc tail, the development of non-IgG-like BsAb platforms is relatively more diverse than IgG-like BsAbs since Fabs, scFvs or nanobodies can be tandemly linked one to another such as BiTE [56], DART [57] and TandAbs [58].

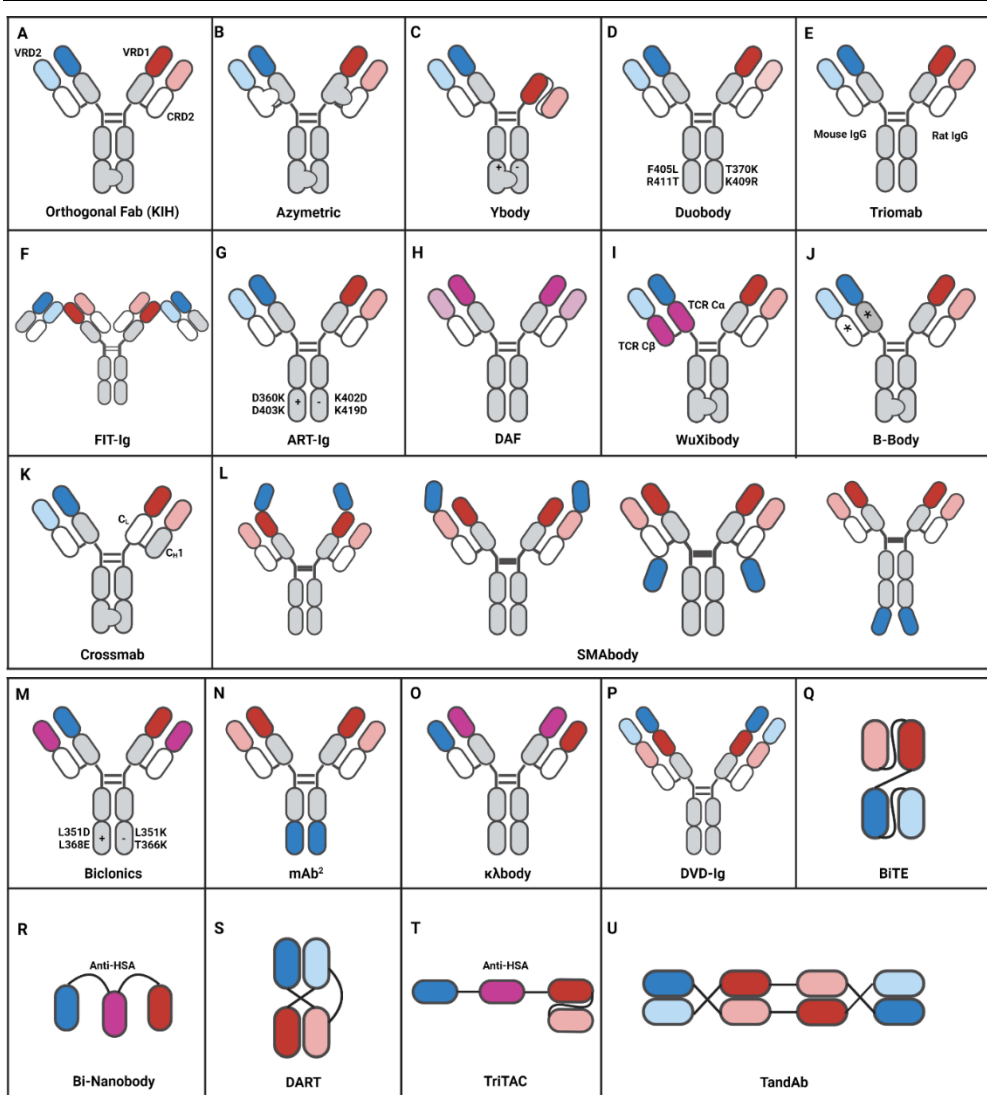


Figure 3. Schematic examples of different BsAbs platforms. (A) The Orthogonal Fab platform introduces charged amino acids into the Fab subdomains to enable correct heavy-light chain association. VRD1 (VL-Q38D VH-Q39K/VL-D1R VH-R62E), CRD2 (CL-L135Y S176W/CH1-H172A F174G) and VRD2 (VL-Q38R VH-Q39Y) mutations are introduced into each antibody. **(B)** The Azymetric platform introduces T350V-L351Y-F405A-Y407V x T350V-T366L-K392L-T394W mutations into CH3 to enhance heavy-heavy chain (H-HC) heterodimerization. **(C)** The Y-Body platform combines a Fab-Fc with a scFv-Fc which does not associate with a light chain, thus overcoming the heavy-light chain (H-LC) mis-pairing issue.

Knobs-in-Holes (KiH) and electrostatic steering effects technologies are applied simultaneously in the Fc region to facilitate heavy chain heterodimerization. **(D)** The Duobody platform introduces K409R, T370K and F405L, R411T mutations in the CH3 region of two parental antibodies respectively which enables a process named controlled Fab-arm exchange (cFAE) to form BsAbs. **(E)** The heavy and light chain constant regions of Triomab are originally from different isotypes or even species which allows fractionated purification by protein A chromatography and elution from the column at a specific pH. **(F)** The Fabs-In-Tandem immunoglobulin (FIT-Ig) platform is a tetravalent Fabs tandem immunoglobulin technology platform developed by Epimab Bio; with two Fabs connected to the N-terminus of the two heavy chains to form a bispecific antibody with a unique structure. **(G)** The ART-Ig platform uses electrostatic steering of Fc tails to facilitate heterodimer formation by introducing mutations (D360K, D403K and K402D, K419D) in the Fc region of each heavy chain. **(H)** The dual action fab (DAF) platform uses phage display technology to optimize the CDRs of a certain antibody to create a new binding ability while retaining the affinity to original antigen. **(I)** The WuXiBody platform uses classic KiH technology to achieve a desired heavy chain heterodimerization and uses the TCR constant α and β chains to replace the heavy chain constant region CH1 and the light chain constant region to avoid H-LC mismatches. **(J)** The B-Body platform applies KiH for correct Fc heterodimer assembly and overcomes H-LC mispairing by substituting the CH1 and CL of one arm for domains derived from another human antibody (marked by *). **(K)** The CrossMab platform resolves H-LC mispairing by exchanging the CH1 for CL within one Fab of the BsAb and overcomes H-HC mis-pairing by combination with another Fc heterodimer technology such as KiH. **(L)** The single-domain antibody fused to monoclonal Ab (SMABody) platform fuses a pair of single-domain antibodies to a conventional monoclonal antibody backbone, thus forming a symmetric bispecific antibody. **(M)** The Biclomics platform utilizes shared common light chain strategy and electrostatic steering effects. Positively charged mutations (L351D and L368E) and negatively charged mutations (L351K and T366K) are introduced in CH3 of each heavy chain. **(N)** The mAb² platform grafts a second antigen binding site into the Fc tail of a monospecific antibody. **(O)** In contrast to common light chain strategy, the $\kappa\lambda$ -body platform applies a shared common heavy chain to solve the H-LC mispairing issue. **(P)** Similar to the FIT-Ig platform, the dual variable domain immunoglobulin (DVD-Ig) platform is symmetrical with four antigen binding

sites, obtained by fusion of a pair of VH/VL domains as a second antigen binding site to each arm of an IgG antibody. **(Q)** The bispecific T cell engager (BiTE) platform consists of a scFv targeting CD3 and another TAA (tumor-associated antigen) targeting scFv linked by G4S linker. **(R)** The Bi-Nanobody platform assembles three nanobodies into a trivalent antibody by two G4S linkers, with one nanobody against human serum albumin (HSA) for half-life extension and the other two specific to therapeutic targets. **(S)** The dual-affinity retargeting (DART) platform covalently links VH and VL sequences with the VL and VH sequences of another antibody through C-terminal cysteine residues. **(T)** The trispecific T-cell activating construct (TriTAC) is made by two nanobodies and a scFv specific for CD3, HSA and a TAA, respectively. **(U)** The tandem diabody (TandAb) platform is a tetravalent antibody molecule which forces two polypeptide chains to fold in a head-to-tail pattern to form 2+2 BsAb fragment.

Cancer therapy with CD3-T cell redirecting bispecific antibody (CD3-TbsAb)

Compared to monospecific antibodies (mAbs), BsAbs appear and show distinct advantages due to their capability to mediate new mechanism(s) of action (MoAs). An example is the T cell redirecting bispecific antibodies (TbsAbs). Taking advantage of the ability of binding two different antigens simultaneously, TbsAbs could target one receptor (usually CD3 ϵ) expressed on the T cell surface with one arm and an antigen on tumor cell with the other arm, thus redirecting T cells to tumor cells which leads to specific tumor cell elimination (**Fig. 4**). Instead of being activated by TCR signaling, T cells then are activated by CD3-TbsAb via CD3, thus any T cells could serve as effector cells [59]. Furthermore, in cell-based tumor cell lysis assays, CD3-TbsAb have shown a 100 ~ 10,000-fold higher efficacy than other BsAbs and mAbs with a low ratio of T cells to target tumor cells [38]. Due to the success of CD3-TbsAbs in hematological cancers, TbsAbs receive extensive attention nowadays. As of December 2020, there are more than 193 BsAbs in clinical study, the majority of which are TbsAbs [60].

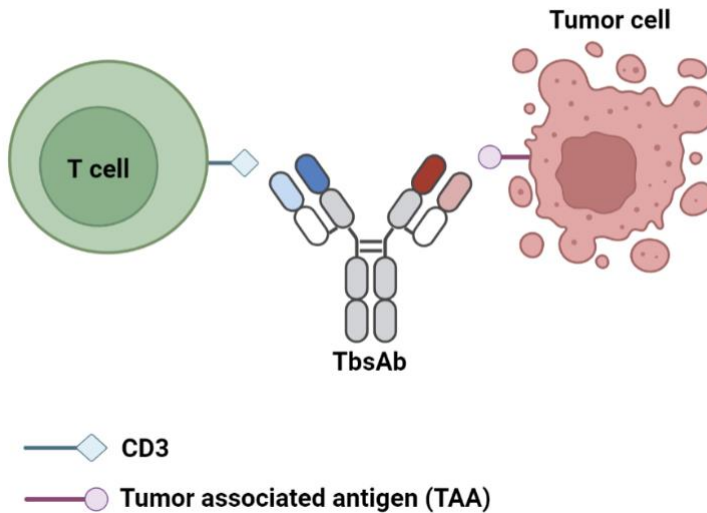


Figure 4. Schematic of mechanisms of action of T cell redirecting bispecific antibodies (TbsAb). TbsAb could engage T cells and tumor cells by simultaneously targeting CD3 and tumor associated antigen (TAA), resulting in the formation of immune synapse and release of cytokines, perforins, and granzymes, which ultimately causes the death of malignant cell.

Unlike the superior efficacy observed in hematological malignancies, CD3-TbsAbs have been reported to be associated with specific challenges in therapy of solid tumors.

A) On-target off-tumor toxicities: Compared to tumor-associated antigens (TAAs) in hematological malignancies (such as CD19, CD20 etc.), the selection of TAAs in solid tumors is more challenging. For instance, B cell lymphoma treated with CD19 or CD20 targeted therapy could cause temporary depletion of B cells which is acceptable and reversible since B cells can be regenerated by hematopoietic stem cells [61]. However, TAAs in solid tumor usually are not only expressed on tumor cells but also on healthy tissue, which can lead to severe T cell infiltration and even organ failure when treated with CD3-TbsAbs [62].

B) T cells in the tumor micro-environment (TME): Unlike the endless T cell pool in hematological malignancies, based on the statuses of immune cells infiltration, solid tumor can be classified into 3 different types, i) “inflamed” tumors, which are infiltrated with functional immune cells; ii)

“immune excluded” tumors, which have CD8⁺ T cells accumulated in the stroma but have not efficiently infiltrated; and iii) “immune desert” tumors, which CD8⁺ T cells are absent from tumor and its periphery [63–65].

C) The functioning of infiltrating T cells: Due to the existence of immunosuppressive cells in the TME (such as Tregs and MDSCs) and immunosuppressive cytokines (such as TGF- β and IL-10), sometimes even there are T cells infiltrated, they can be dysfunctional and not able to eliminate tumor cells [66]. This issue might be addressed or partially addressed by using optimal format TbsAbs to induce enhanced T cell activation (see chapter 4).

In 2018, the global market of BsAbs have already reached approximately \$1 billion [67]. According to Frost & Sullivan’s prediction, with the potential approval of new BsAbs and indications, the BsAb market scale will grow rapidly and surpass \$8 billion by 2025. Due to the huge market of BsAb and increasingly competitive in mono-specific antibody area, in the coming years, it is anticipated that the number of BsAb drugs in development will expand at a rate three times faster than that of conventional monoclonal antibody drugs.

Scope of this thesis

Given the increasing evidence suggesting the potential superiority of bispecific antibodies over conventional monospecific antibodies as cancer therapy, the main aim of this thesis was to develop a novel bispecific format facilitating the production of bispecific antibodies and to apply this format for cancer treatment. In this thesis, we developed and characterized a novel bispecific antibody format which could avoid potential heavy-light chain mispairing. Afterwards, we demonstrated that shortened hinge design of this format could enhance redirected T-cell killing of tumor cells. Furthermore, we investigated the efficacy of different isotypes of mouse tumor-targeting antibodies in a model therapeutic setting.

In the **first chapter**, we introduced the background for the studies in this thesis and summarized the latest research progress on bispecific antibodies as cancer therapy.

In **chapter 2**, as it is challenging to keeping track of all the new BsAb clinical studies that come out on a regular basis. Of all kinds of BsAbs, dual TAA targeting BsAbs have been demonstrated superior anti-tumor efficacy in both solid tumors and hematologic malignancies in early clinical studies,

making dual TAA targeting BsAbs a valuable class of biologics. Furthermore, dual TAA targeting BsAbs offer a number of advantages, including improved payload delivery, increased tumor selectivity, and the capacity to simultaneously alter two functional pathways in the tumor cell. Therefore, in this chapter, we summarized the clinical development of dual TAAs targeting BsAbs, discussed the factors that need to be carefully considered when designing BsAb targeting two TAAs and provided future perspectives for this field.

In **chapter 3**, we described a novel BsAb format (sdAb x Fab-Fc) composed of a conventional antigen-binding fragment (Fab), a single domain antibody (sdAb) and a mouse IgG2a Fc. We demonstrated that sdAb x Fab-Fc format BsAbs can avoid the issue of heavy-light chain mis-pairing without any additional protein engineering and can be functionally expressed and assembled in a single 293-F host cell, using knobs-into-holes and charge-pairs dimerization. Alternatively, they can be formed artificially by controlled Fab-arm exchange; reaching high purity and retaining their capacity to bind both their target antigens simultaneously. The novel sdAb x Fab-Fc format we reported provides a rapid and efficient strategy to generate BsAb with high purity and it comes with a unique mass-based possibility to further purify desired BsAbs from undesired side-products. This is significant because a major challenge in the development of BsAbs is the difficulty in producing a pure BsAb without the presence of contaminating antibodies (by-products during assembling, non-functional or monospecific molecules). Compared to conventional BsAb formats, the advantages of the sdAb x Fab-Fc format may thus open an opportunity to apply this novel sdAb x Fab-Fc BsAb format for academic and clinical study application.

In **chapter 4**, we have generated two T-cell redirecting bispecific antibodies (TbsAbs) targeting mEGFR and mCD3E in the Fab x sdAb-Fc format which we previously reported, with two different lengths of hinges. Subsequently, we compared their anti-tumor activity and demonstrated that a TbsAb with a shorter hinge showed a significantly better T cell redirected tumor cell elimination than the TbsAb with a longer hinge. Moreover, the TbsAb.short form mediated much more T cell-tumor cell clusters and increased expression level of T cell activation markers (CD69 and CD25) on T cells compared to the TbsAb long form. Taken together, according to our findings, even minor modifications to the hinge design of TbsAbs can have a great impact on the anti-tumor activity of TbsAbs and similar antibodies may benefit from this design.

In **chapter 5**, the mouse mIgG2a is the most common Ig isotype used in tumor mouse models. However, in mice, the efficacy of antibody-based tumor therapy is largely restricted to a prophylactic application of the antibodies. In therapeutic settings tumor-antigen targeting antibodies normally fail to show efficacy. In this study, we assessed the efficacy of different isotypes of mouse tumor-targeting antibodies in a therapeutic setting using a highly systematic approach. To this end, we engineered and expressed antibodies of the same specificity but different isotypes, targeting the artificial tumor antigen CD90.1 / Thy1.1 expressed by B16 melanoma cells. As wild type C57BL/6 mice express only Thy1.2, the anti-Thy1.1 antibody treatment was tumor-selective. Our experiments revealed that also in a therapeutic setting, mIgG2a was superior to both mIgE and mIgG1 in controlling tumor growth. Furthermore, the observed mIgG2a anti-tumor effect was entirely Fc-mediated as the protection was lost when antibodies with an Fc silenced mIgG2a isotype (LALA-PG mutations) were used. These data confirm mIgG2a superiority in immune interventions in tumour models. Taken together, these data clearly demonstrate that the choice of isotype is a critical parameter determining the efficacy of tumor-targeting antibody therapy. We feel that consideration of these findings should substantially improve the efficacy of therapeutic antibody-based cancer treatments and should, therefore, substantially influence the work of a wide range of researchers in the field of tumor immunotherapy.

Finally, in **chapter 6**, all findings in this thesis as well as future perspectives and applications are discussed.

Reference

1. Kaufmann, S.H.E. Immunology's Foundation: The 100-Year Anniversary of the Nobel Prize to Paul Ehrlich and Elie Metchnikoff. *Nat Immunol* **2008**, *9*, 705–712, doi:10.1038/ni0708-705.
2. Kaufmann, S.H.E. Emil von Behring: Translational Medicine at the Dawn of Immunology. *Nat Rev Immunol* **2017**, *17*, 341–343, doi:10.1038/nri.2017.37.
3. Place, D.E.; Kanneganti, T.-D. The Innate Immune System and Cell Death in Autoinflammatory and Autoimmune Disease. *Curr Opin Immunol* **2020**, *67*, 95–105, doi:10.1016/j.coi.2020.10.013.
4. Kaufmann, S.H.E. Immunology's Coming of Age. *Front Immunol* **2019**, *10*, 684, doi:10.3389/fimmu.2019.00684.
5. Haas, L.F. Emil Adolph von Behring (1854-1917) and Shibasaburo Kitasato (1852-1931). *J Neurol Neurosurg Psychiatry* **2001**, *71*, 62, doi:10.1136/jnnp.71.1.62.
6. Goulet, D.R.; Atkins, W.M. Considerations for the Design of Antibody-Based Therapeutics. *Journal of Pharmaceutical Sciences* **2020**, *109*, 74–103, doi:10.1016/j.xphs.2019.05.031.
7. Gearhart, P.J. Immunology: The Roots of Antibody Diversity. *Nature* **2002**, *419*, 29–31, doi:10.1038/419029a.
8. Gatto, D.; Brink, R. The Germinal Center Reaction. *J Allergy Clin Immunol* **2010**, *126*, 898–907; quiz 908–909, doi:10.1016/j.jaci.2010.09.007.
9. Fazilleau, N.; Mark, L.; McHeyzer-Williams, L.J.; McHeyzer-Williams, M.G. Follicular Helper T Cells: Lineage and Location. *Immunity* **2009**, *30*, 324–335, doi:10.1016/j.immuni.2009.03.003.
10. Dowd, K.A.; Pierson, T.C. Antibody-Mediated Neutralization of Flaviviruses: A Reductionist View. *Virology* **2011**, *411*, 306–315, doi:10.1016/j.virol.2010.12.020.
11. Chiu, M.L.; Gilliland, G.L. Engineering Antibody Therapeutics. *Current Opinion in Structural Biology* **2016**, *38*, 163–173, doi:10.1016/j.sbi.2016.07.012.
12. Wang, Q.; Chung, C.-Y.; Chough, S.; Betenbaugh, M.J. Antibody Glycoengineering Strategies in Mammalian Cells. *Biotechnology and Bioengineering* **2018**, *115*, 1378–1393, doi:10.1002/bit.26567.
13. Treffers, L.W.; van Houdt, M.; Bruggeman, C.W.; Heineke, M.H.; Zhao, X.W.; van der Heijden, J.; Nagelkerke, S.Q.; Verkuijlen, P.J.J.H.; Geissler, J.;

Lissenberg-Thunnissen, S.; et al. FcγRIIIb Restricts Antibody-Dependent Destruction of Cancer Cells by Human Neutrophils. *Frontiers in Immunology* **2019**, *9*.

14. Bruhns, P.; Jönsson, F. Mouse and Human FcR Effector Functions. *Immunological Reviews* **2015**, *268*, 25–51, doi:10.1111/imr.12350.

15. Nimmerjahn, F.; Ravetch, J.V. Divergent Immunoglobulin G Subclass Activity Through Selective Fc Receptor Binding. *Science* **2005**, *310*, 1510–1512, doi:10.1126/science.1118948.

16. Nimmerjahn, F.; Ravetch, J.V. Fcγ Receptors: Old Friends and New Family Members. *Immunity* **2006**, *24*, 19–28, doi:10.1016/j.immuni.2005.11.010.

17. Monoclonal Antibodies Defining Distinctive Human T Cell Surface Antigens | Science Available online: https://www.science.org/doi/abs/10.1126/science.314668?casa_token=8zSD8mj0Y6MAAAAAA:B2tuNX8aJ9sjGNhBQCcFg_JioFWmBE6kBIDLJj6VMEbq8vbs8JPo0RawZ9zUDJa6zVplzP_xL1GskDeS (accessed on 10 October 2022).

18. Coulson, A.; Levy, A.; Gossell-Williams, M. Monoclonal Antibodies in Cancer Therapy: Mechanisms, Successes and Limitations. *West Indian Med J* **2014**, *63*, 650–654, doi:10.7727/wimj.2013.241.

19. Scott, A.M.; Wolchok, J.D.; Old, L.J. Antibody Therapy of Cancer. *Nat Rev Cancer* **2012**, *12*, 278–287, doi:10.1038/nrc3236.

20. Rawat, S.; Hussain, M.S.; Mohapatra, C.; Kaur, G. An Overview Of Monoclonal Antibodies And Their Therapeutic Applications. *NVEO - NATURAL VOLATILES & ESSENTIAL OILS Journal* | *NVEO* **2021**, 4121–4130.

21. Chames, P.; Van Regenmortel, M.; Weiss, E.; Baty, D. Therapeutic Antibodies: Successes, Limitations and Hopes for the Future. *Br J Pharmacol* **2009**, *157*, 220–233, doi:10.1111/j.1476-5381.2009.00190.x.

22. Aleksakhina, S.N.; Kashyap, A.; Imyanitov, E.N. Mechanisms of Acquired Tumor Drug Resistance. *Biochim Biophys Acta Rev Cancer* **2019**, *1872*, 188310, doi:10.1016/j.bbcan.2019.188310.

23. Iorgulescu, J.B.; Braun, D.; Oliveira, G.; Keskin, D.B.; Wu, C.J. Acquired Mechanisms of Immune Escape in Cancer Following Immunotherapy. *Genome Med* **2018**, *10*, 87, doi:10.1186/s13073-018-0598-2.

24. Mazor, Y.; Hansen, A.; Yang, C.; Chowdhury, P.S.; Wang, J.; Stephens, G.; Wu, H.; Dall'Acqua, W.F. Insights into the Molecular Basis of a Bispecific

Antibody's Target Selectivity. *MAbs* **2015**, *7*, 461–469, doi:10.1080/19420862.2015.1022695.

25. Mazor, Y.; Sachsenmeier, K.F.; Yang, C.; Hansen, A.; Filderman, J.; Mulgrew, K.; Wu, H.; Dall'Acqua, W.F. Enhanced Tumor-Targeting Selectivity by Modulating Bispecific Antibody Binding Affinity and Format Valence. *Sci Rep* **2017**, *7*, 40098, doi:10.1038/srep40098.

26. Lopez-Albaitero, A.; Xu, H.; Guo, H.; Wang, L.; Wu, Z.; Tran, H.; Chandarlapaty, S.; Scaltriti, M.; Janjigian, Y.; de Stanchina, E.; et al. Overcoming Resistance to HER2-Targeted Therapy with a Novel HER2/CD3 Bispecific Antibody. *Oncoimmunology* **2017**, *6*, e1267891, doi:10.1080/2162402X.2016.1267891.

27. Moores, S.L.; Chiu, M.L.; Bushey, B.S.; Chevalier, K.; Luistro, L.; Dorn, K.; Brezski, R.J.; Haytko, P.; Kelly, T.; Wu, S.-J.; et al. A Novel Bispecific Antibody Targeting EGFR and cMet Is Effective against EGFR Inhibitor-Resistant Lung Tumors. *Cancer Research* **2016**, *76*, 3942–3953, doi:10.1158/0008-5472.CAN-15-2833.

28. Nisonoff, A.; Wissler, F.C.; Lipman, L.N. Properties of the Major Component of a Peptic Digest of Rabbit Antibody. *Science* **1960**, *132*, 1770–1771, doi:10.1126/science.132.3441.1770.

29. Milstein, C.; Cuello, A.C. Hybrid Hybridomas and Their Use in Immunohistochemistry. *Nature* **1983**, *305*, 537–540, doi:10.1038/305537a0.

30. Garber, K. Bispecific Antibodies Rise Again: Amgen's Blinatumomab Is Setting the Stage for a Bispecific-Antibody Revival, Enabled by New Formats That May Solve the Field's Long-Standing Problems. *Nature Reviews Drug Discovery* **2014**, *13*, 799–802.

31. Klein, C.; Sustmann, C.; Thomas, M.; Stubenrauch, K.; Croasdale, R.; Schanzer, J.; Brinkmann, U.; Kettenberger, H.; Regula, J.T.; Schaefer, W. Progress in Overcoming the Chain Association Issue in Bispecific Heterodimeric IgG Antibodies. *mAbs* **2012**, *4*, 653–663, doi:10.4161/mabs.21379.

32. Merchant, A.M.; Zhu, Z.; Yuan, J.Q.; Goddard, A.; Adams, C.W.; Presta, L.G.; Carter, P. An Efficient Route to Human Bispecific IgG. *Nat Biotechnol* **1998**, *16*, 677–681, doi:10.1038/nbt0798-677.

33. Atwell, S.; Ridgway, J.B.B.; Wells, J.A.; Carter, P. Stable Heterodimers from Remodeling the Domain Interface of a Homodimer Using a Phage Display Library. Edited by P.E. Wright. *Journal of Molecular Biology* **1997**, *270*, 26–35, doi:10.1006/jmbi.1997.1116.

34. Sampei, Z.; Igawa, T.; Soeda, T.; Okuyama-Nishida, Y.; Moriyama, C.;

Wakabayashi, T.; Tanaka, E.; Muto, A.; Kojima, T.; Kitazawa, T.; et al. Identification and Multidimensional Optimization of an Asymmetric Bispecific IgG Antibody Mimicking the Function of Factor VIII Cofactor Activity. *PLOS ONE* **2013**, *8*, e57479, doi:10.1371/journal.pone.0057479.

35. Wranik, B.J.; Christensen, E.L.; Schaefer, G.; Jackman, J.K.; Vendel, A.C.; Eaton, D. LUZ-Y, a Novel Platform for the Mammalian Cell Production of Full-Length IgG-Bispecific Antibodies *. *Journal of Biological Chemistry* **2012**, *287*, 43331–43339, doi:10.1074/jbc.M112.397869.

36. Moretti, P.; Skegro, D.; Ollier, R.; Wassmann, P.; Aebischer, C.; Laurent, T.; Schmid-Printz, M.; Giovannini, R.; Blein, S.; Bertschinger, M. BEAT® the Bispecific Challenge: A Novel and Efficient Platform for the Expression of Bispecific IgGs. *BMC Proceedings* **2013**, *7*, O9, doi:10.1186/1753-6561-7-S6-O9.

37. SEEDbodies: Fusion Proteins Based on Strand-Exchange Engineered Domain (SEED) CH3 Heterodimers in an Fc Analogue Platform for Asymmetric Binders or Immunofusions and Bispecific Antibodies† | Protein Engineering, Design and Selection | Oxford Academic Available online: <https://academic.oup.com/peds/article/23/4/195/1590881> (accessed on 10 October 2022).

38. Jackman, J.; Chen, Y.; Huang, A.; Moffat, B.; Scheer, J.M.; Leong, S.R.; Lee, W.P.; Zhang, J.; Sharma, N.; Lu, Y.; et al. Development of a Two-Part Strategy to Identify a Therapeutic Human Bispecific Antibody That Inhibits IgE Receptor Signaling *. *Journal of Biological Chemistry* **2010**, *285*, 20850–20859, doi:10.1074/jbc.M110.113910.

39. Igawa, T.; Tsunoda, H.; Kikuchi, Y.; Yoshida, M.; Tanaka, M.; Koga, A.; Sekimori, Y.; Orita, T.; Aso, Y.; Hattori, K.; et al. VH/VL Interface Engineering to Promote Selective Expression and Inhibit Conformational Isomerization of Thrombopoietin Receptor Agonist Single-Chain Diabody. *Protein Engineering, Design and Selection* **2010**, *23*, 667–677, doi:10.1093/protein/gzq034.

40. Lewis, S.M.; Wu, X.; Pustilnik, A.; Sereno, A.; Huang, F.; Rick, H.L.; Guntas, G.; Leaver-Fay, A.; Smith, E.M.; Ho, C.; et al. Generation of Bispecific IgG Antibodies by Structure-Based Design of an Orthogonal Fab Interface. *Nat Biotechnol* **2014**, *32*, 191–198, doi:10.1038/nbt.2797.

41. Bönisch, M.; Sellmann, C.; Maresch, D.; Halbig, C.; Becker, S.; Toleikis, L.; Hock, B.; Rüker, F. Novel CH1:CL Interfaces That Enhance Correct Light Chain Pairing in Heterodimeric Bispecific Antibodies. *Protein Engineering, Design and Selection* **2017**, *30*, 685–696, doi:10.1093/protein/gzx044.

42. Schanzer, J.M.; Wartha, K.; Croasdale, R.; Moser, S.; Künkele, K.-P.;

Ries, C.; Scheuer, W.; Duerr, H.; Pompiani, S.; Pollman, J.; et al. A Novel Glycoengineered Bispecific Antibody Format for Targeted Inhibition of Epidermal Growth Factor Receptor (EGFR) and Insulin-like Growth Factor Receptor Type I (IGF-1R) Demonstrating Unique Molecular Properties. *J Biol Chem* **2014**, *289*, 18693–18706, doi:10.1074/jbc.M113.528109.

43. Labrijn, A.F.; Meesters, J.I.; de Goeij, B.E.C.G.; van den Bremer, E.T.J.; Neijssen, J.; van Kampen, M.D.; Strumane, K.; Verploegen, S.; Kundu, A.; Gramer, M.J.; et al. Efficient Generation of Stable Bispecific IgG1 by Controlled Fab-Arm Exchange. *Proc. Natl. Acad. Sci. U.S.A.* **2013**, *110*, 5145–5150, doi:10.1073/pnas.1220145110.

44. Syed, Y.Y. Amivantamab: First Approval. *Drugs* **2021**, *81*, 1349–1353, doi:10.1007/s40265-021-01561-7.

45. Strop, P.; Ho, W.-H.; Boustany, L.M.; Abdiche, Y.N.; Lindquist, K.C.; Farias, S.E.; Rickert, M.; Appah, C.T.; Pascua, E.; Radcliffe, T.; et al. Generating Bispecific Human IgG1 and IgG2 Antibodies from Any Antibody Pair. *J Mol Biol* **2012**, *420*, 204–219, doi:10.1016/j.jmb.2012.04.020.

46. Huang, S.; Segués, A.; Hulsik, D.L.; Zaiss, D.M.; Sijts, A.J.A.M.; van Duijnhoven, S.M.J.; van Elsas, A. A Novel Efficient Bispecific Antibody Format, Combining a Conventional Antigen-Binding Fragment with a Single Domain Antibody, Avoids Potential Heavy-Light Chain Mis-Pairing. *Journal of Immunological Methods* **2020**, *483*, 112811, doi:10.1016/j.jim.2020.112811.

47. Brinkmann, U.; Kontermann, R.E. The Making of Bispecific Antibodies. *mAbs* **2017**, *9*, 182–212, doi:10.1080/19420862.2016.1268307.

48. Godar, M.; de Haard, H.; Blanchetot, C.; Rasser, J. Therapeutic Bispecific Antibody Formats: A Patent Applications Review (1994-2017). *Expert Opinion on Therapeutic Patents* **2018**, *28*, 251–276, doi:10.1080/13543776.2018.1428307.

49. Fan, G.; Wang, Z.; Hao, M.; Li, J. Bispecific Antibodies and Their Applications. *Journal of Hematology & Oncology* **2015**, *8*, 130, doi:10.1186/s13045-015-0227-0.

50. Ma, J.; Mo, Y.; Tang, M.; Shen, J.; Qi, Y.; Zhao, W.; Huang, Y.; Xu, Y.; Qian, C. Bispecific Antibodies: From Research to Clinical Application. *Frontiers in Immunology* **2021**, *12*.

51. Schaefer, W.; Regula, J.T.; Böhner, M.; Schanzer, J.; Croasdale, R.; Dürr, H.; Gassner, C.; Georges, G.; Kettenberger, H.; Imhof-Jung, S.; et al. Immunoglobulin Domain Crossover as a Generic Approach for the Production of Bispecific IgG Antibodies. *Proc. Natl. Acad. Sci. U.S.A.* **2011**, *108*, 11187–11192, doi:10.1073/pnas.1019002108.

52. Mazor, Y.; Oganessian, V.; Yang, C.; Hansen, A.; Wang, J.; Liu, H.; Sachsenmeier, K.; Carlson, M.; Gadre, D.V.; Borrok, M.J.; et al. Improving Target Cell Specificity Using a Novel Monovalent Bispecific IgG Design. *mAbs* **2015**, *7*, 377–389, doi:10.1080/19420862.2015.1007816.
53. Zhou, P.; Zhang, J.; Yan, Y. Bispecific Antibody 2017.
54. Chen, H.; Cui, Y.; Huang, Z.; Qi, B.; Yan, X.; Zhang, X. Multispecific Fab Fusion Proteins and Use Thereof 2018.
55. Yu, J.; Song, Y.; Tian, W. How to Select IgG Subclasses in Developing Anti-Tumor Therapeutic Antibodies. *Journal of Hematology & Oncology* **2020**, *13*, 45, doi:10.1186/s13045-020-00876-4.
56. Wolf, E.; Hofmeister, R.; Kufer, P.; Schlereth, B.; Baeuerle, P.A. BiTEs: Bispecific Antibody Constructs with Unique Anti-Tumor Activity. *Drug Discovery Today* **2005**, *10*, 1237–1244, doi:10.1016/S1359-6446(05)03554-3.
57. Johnson, S.; Burke, S.; Huang, L.; Gorlatov, S.; Li, H.; Wang, W.; Zhang, W.; Tuaille, N.; Rainey, J.; Barat, B.; et al. Effector Cell Recruitment with Novel Fv-Based Dual-Affinity Re-Targeting Protein Leads to Potent Tumor Cytolysis and in Vivo B-Cell Depletion. *Journal of Molecular Biology* **2010**, *399*, 436–449, doi:10.1016/j.jmb.2010.04.001.
58. Völkel, T.; Korn, T.; Bach, M.; Müller, R.; Kontermann, R.E. Optimized Linker Sequences for the Expression of Monomeric and Dimeric Bispecific Single-Chain Diabodies. *Protein Eng* **2001**, *14*, 815–823, doi:10.1093/protein/14.10.815.
59. Wu, Z.; Cheung, N.V. T Cell Engaging Bispecific Antibody (T-BsAb): From Technology to Therapeutics. *Pharmacology & Therapeutics* **2018**, *182*, 161–175, doi:10.1016/j.pharmthera.2017.08.005.
60. Zhang, Z.; Luo, F.; Cao, J.; Lu, F.; Zhang, Y.; Ma, Y.; Zeng, K.; Zhang, L.; Zhao, H. Anticancer Bispecific Antibody R&D Advances: A Study Focusing on Research Trend Worldwide and in China. *Journal of Hematology & Oncology* **2021**, *14*, 124, doi:10.1186/s13045-021-01126-x.
61. Ellerman, D. Bispecific T-Cell Engagers: Towards Understanding Variables Influencing the in Vitro Potency and Tumor Selectivity and Their Modulation to Enhance Their Efficacy and Safety. *Methods* **2019**, *154*, 102–117, doi:10.1016/j.ymeth.2018.10.026.
62. Lutterbuese, R.; Raum, T.; Kischel, R.; Hoffmann, P.; Mangold, S.; Rattel, B.; Friedrich, M.; Thomas, O.; Lorenczewski, G.; Rau, D.; et al. T Cell-Engaging BiTE Antibodies Specific for EGFR Potentially Eliminate KRAS- and BRAF-Mutated Colorectal Cancer Cells. *Proceedings of the National*

Academy of Sciences **2010**, *107*, 12605–12610, doi:10.1073/pnas.1000976107.

63. Groeneveldt, C.; van Hall, T.; van der Burg, S.H.; ten Dijke, P.; van Montfoort, N. Immunotherapeutic Potential of TGF- β Inhibition and Oncolytic Viruses. *Trends in Immunology* **2020**, *41*, 406–420, doi:10.1016/j.it.2020.03.003.

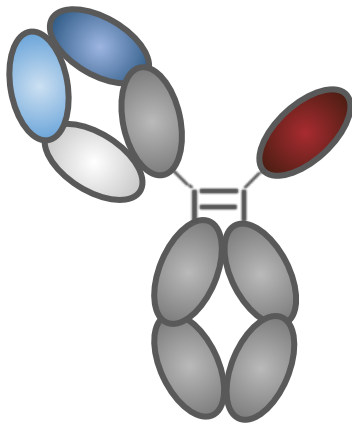
64. Lanitis, E.; Dangaj, D.; Irving, M.; Coukos, G. Mechanisms Regulating T-Cell Infiltration and Activity in Solid Tumors. *Annals of Oncology* **2017**, *28*, xii18–xii32, doi:10.1093/annonc/mdx238.

65. Kuczek, D.E.; Larsen, A.M.H.; Thorseth, M.-L.; Carretta, M.; Kalvisa, A.; Siersbæk, M.S.; Simões, A.M.C.; Roslind, A.; Engelholm, L.H.; Noessner, E.; et al. Collagen Density Regulates the Activity of Tumor-Infiltrating T Cells. *Journal for ImmunoTherapy of Cancer* **2019**, *7*, 68, doi:10.1186/s40425-019-0556-6.

66. Tormoen, G.W.; Crittenden, M.R.; Gough, M.J. Role of the Immunosuppressive Microenvironment in Immunotherapy. *Adv Radiat Oncol* **2018**, *3*, 520–526, doi:10.1016/j.adro.2018.08.018.

67. Hosseini, S.S.; Khalili, S.; Baradaran, B.; Bidar, N.; Shahbazi, M.-A.; Mosafar, J.; Hashemzaei, M.; Mokhtarzadeh, A.; Hamblin, M.R. Bispecific Monoclonal Antibodies for Targeted Immunotherapy of Solid Tumors: Recent Advances and Clinical Trials. *International Journal of Biological Macromolecules* **2021**, *167*, 1030–1047, doi:10.1016/j.ijbiomac.2020.11.058.

2



Bispecific antibodies targeting dual tumor - associated antigens in cancer therapy

Shuyu Huang^{1,2}, Sander M. J. van Duijnhoven¹, Alice J. A. M. Sijts², Andrea van Elsas¹

¹ Aduro Biotech Europe, Oss, the Netherlands

² Faculty of Veterinary Medicine, Department of Infectious Diseases and Immunology, Utrecht University, Utrecht, the Netherlands

J Cancer Res Clin Oncol 146, 3111–3122 (2020).

Contribution statement: Shuyu Huang conceived the idea and drafted the manuscript.

Abstract

Purpose Bispecific antibodies (BsAbs) have emerged as a leading drug class for cancer therapy and are becoming increasingly of interest for therapeutic applications. As of April 2020, over 123 BsAbs are under clinical evaluation for use in oncology (including the two marketed BsAbs Blinatumomab and Catumaxomab). The majority (82 of 123) of BsAbs under clinical evaluation can be categorized as bispecific immune cell engager whereas a second less well-discussed subclass of BsAbs targets two tumor-associated antigens (TAAs). In this review, we summarize the clinical development of dual TAAs targeting BsAbs and provide an overview of critical considerations when designing dual TAA targeting BsAbs.

Methods Herein the relevant literature and clinical trials published in English until April 1st, 2020, were searched using PubMed and ClinicalTrials.gov database. BsAbs were considered to be active in clinic if their clinical trials were not terminated, withdrawn or completed before 2018 without reporting results. Data missed by searching ClinicalTrials.gov was manually curated.

Results Dual TAAs targeting BsAbs offer several advantages including increased tumor selectivity, potential to concurrently modulate two functional pathways in the tumor cell and may yield improved payload delivery.

Conclusions Dual TAAs targeting BsAbs represent a valuable class of biologics and early stage clinical studies have demonstrated promising anti-tumor efficacy in both hematologic malignancies and solid tumors.

Keywords: bispecific antibodies, dual targeting, cancer therapy, clinical trials, literature review.

Introduction

The first therapeutic monoclonal antibody (mAb), muromonab-CD3 (OKT3), was approved by the Food and Drug Administration (FDA) more than 30 years ago, which marked the launch of a long mAb-based therapeutics campaign (Kung et al. 1979). Currently, antibody therapeutics represent the fastest growing class of drugs on the market with more than 70 antibody drugs approved and more than 550 in clinical study (Carter and Lazar 2018; Suurs et al. 2019). Within the large antibody-based therapeutic family, recently, bispecific antibodies have gained much interest in cancer therapeutic applications (Garber 2014). Compared to monospecific monoclonal antibodies, the potential advantages of BsAbs are listed here. By targeting two tumor-associated antigens (TAAs) that individually are not necessarily tumor-specific, in theory BsAbs achieve improved selectivity towards tumor, minimizing the side effects in normal tissues (Mazor et al. 2015, 2017). Since cancer is a complex and multifactorial disease, dual targeting could also be used to modulate two functional pathways in the tumor, thus avoiding resistance to the treatment (Lopez-Albaitero et al. 2017; Moores et al. 2016). Furthermore, BsAbs provided added functionality that cannot be achieved with a combination of two monospecific mAbs, such as redirecting specific immune cells to tumor cells (Zhukovsky et al. 2016), pre-targeting strategies (Boerman et al. 2003), half-life extension (Kontermann 2011) and delivery through the blood–brain barrier (Yu et al. 2011).

The first bispecific antibody, with the ability to bind to two different antigens at the same time, was generated by coupling rabbit antigen-binding fragments (Fabs) from two different polyclonal sera via mild re-oxidation 1960s (Nisonoff et al. 1960). At the time hope for this next generation, BsAb therapy were dampened due to manufacturing issues and clinical failure (Garber 2014). Over the past two decades, advances in biotechnology leading to improved protein engineering and manufacturing techniques have fueled the development of increasingly complex BsAbs with defined structure and biochemical, functional, and pharmacological properties (Brinkmann and Kontermann 2017). In oncology, two BsAbs have been approved for clinical treatment. Catumaxomab [CD3 × EpCAM (epithelial cell adhesion molecule)], was approved by the European Medicines Agency (EMA) in 2009 for the intraperitoneal treatment of malignant ascites although withdrawn in 2017 for commercial reasons. Blinatumomab (CD3 × CD19), was approved by the FDA in 2014 for the treatment of Philadelphia chromosome-negative B cell acute lymphoblastic leukemia (ALL)

(Przepiorka et al. 2015; Seimetz et al. 2010). The approval of these two BsAbs has stimulated further attention and investment by pharmaceutical and biotech companies.

Bispecific antibodies are one of the rapidly growing new drug classes. With new BsAb clinical studies constantly emerging, keeping track is a challenging task. The various BsAbs including cell bridging, receptor inhibition/activation, co-factor mimicking and piggybacking BsAbs in oncology and autoimmune disease were summarized excellently in a recent review (Labrijn et al. 2019). Therefore, we focus this review on the current state of the art of a less well-discussed subclass of BsAbs, targeting two tumor-associated antigens for oncology clinical development. We also discuss the factors that need to be carefully considered when designing BsAb targeting two TAAs and provide future perspectives for this field.

Bispecific antibody formats

Antibodies are grouped into five classes according to their constant region: IgG, IgM, IgA, IgD, and IgE. The basic structure of an IgG antibody is composed of two pairs of heavy-light chain polypeptide chains connected by interchain disulfide bonds and noncovalent bonds, resembling a “Y” shape complex, with a total molecular weight of ~ 150 kDa. An antibody can be also divided into functional parts: the antigen-binding fragments (Fab) and the fragment crystallizable (Fc) region (Fig. 1a). The Fc region is the tail region of an antibody that interacts with a receptor called the neonatal receptor, which is involved in regulating the IgG serum levels to prolong the antibody half-life. The Fc region also induces secondary immune functions that lead to immune-mediated target-cell killing, such as Antibody-dependent cell-mediated cytotoxicity (ADCC), Antibody-dependent cellular phagocytosis (ADCP) and Complement-dependent cytotoxicity (CDC) (Chiu and Gilliland 2016; Wang et al. 2018).

Typical antibodies are symmetric and monospecific, with two identical heavy-light chain polypeptide chains binding to the same epitope, while BsAbs are composed of two different antigen-binding regions. Hence, the formats of BsAb are much more complex and diverse than mAb. As a result of advances in protein and gene engineering, more than 100 different BsAb formats have been invented, with around one-fourth of those further developed into commercial platforms for bispecific antibody generation (Brinkmann and Kontermann 2017; Godar et al. 2018). The varied BsAb

formats can be roughly divided into two classes depending on the presence of an Fc domain.

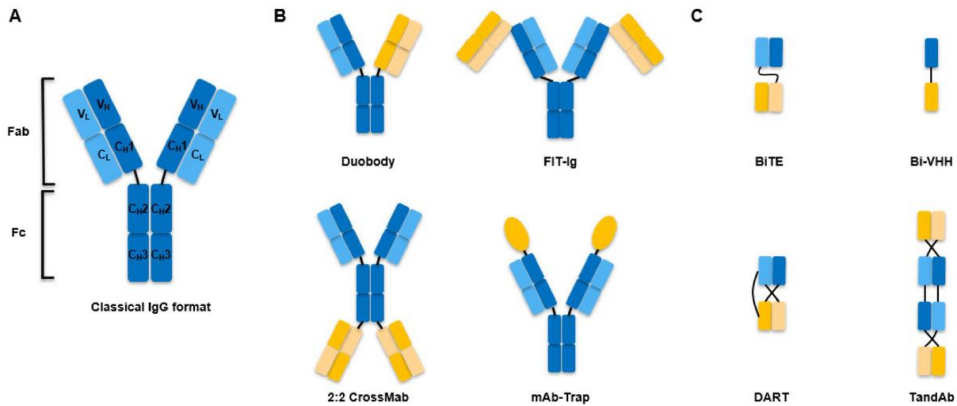


Fig. 1 Schematic overview of the antibody structure and representations of several dual TAAs targeting BsAb formats with/without Fc tail. **a** The classical IgG structure; **b** representative Fc containing BsAb formats; **c** representative Fc less BsAb formats. *FIT-Ig* Fab in-tandem immunoglobulin, *scFv* Single-chain variable fragment, *BITE* Bispecific T cell engager, *VHH* variable domain of heavy chain, *DART* dual-affinity retargeting molecule, *TandAb* tandem diabody.

Fc containing architecture

Fc region containing BsAbs mainly include Duobody(Labrijn et al. 2013), FIT-Ig (Gong et al. 2017), 2:2 Cross-Mab (Brunker et al. 2016), mAb-Trap (J. Yu et al. 2020)(Fig. 1b). Fc presence provides them with a relatively long in vivo half-life owing to its neonatal Fc receptor (FcRn)-mediated recycling processes (Roopenian and Akilesh 2007). In addition, the Fc region can also be designed to mediate secondary immune functions in accordance with the required mode-of-action (Table 1) (Scott et al.2012). On the other hand, to address the chain association issues, protein engineering of Fc region containing BsAbs requires more effort which might compromise the physicochemical and biological characteristics or even affinity of the BsAb, eventually requiring additional analytical and quality testing (Klein et al. 2012).

Fc less architecture

Fc-less BsAbs are composed of either single-chain variable fragment

(scFv), variable domain of heavy chain of heavy chain(VHH) or Fab fragment of two different antibodies, but without Fc region such as BiTE (Wolf et al. 2005), DART (Johnson et al. 2010), TandAb (Kipriyanov et al. 1999), Bi-VHH (Conrath et al. 2001), etc. (Fig. 1c). In the absence of an Fc region, these types of BsAbs are smaller in size and heavy-heavy chain mis-pairing issues are avoided, leading to relatively high yield, better tissue-penetrating capacity and less immunogenicity. But along with it came certain disadvantages such as the short in vivo half-life, decreased stability and a higher probability of aggregate formation (Table 1) (Ayyar et al. 2016; Kontermann and Brinkmann 2015; Velasquez et al. 2018).

Table 1 Comparison of Fc containing and Fc less bispecific antibodies

	Fc containing	Fc less
Representative platform	Duobody, CrossMab, FIT-Ig	BiTE, DART, TandAb
Representative drug	Catumaxomab	Bilncyto
Advantages	CMC: Good solubility and stability Curative effect: Induce secondary immune functions (ADCC, ADCP and CDC); long in vivo half-life	CMC: Small size, high yield, easy to produce Curative effect: Low immunogenicity; Fewer side-effects; Better tissue-penetrating capacity; For CD3×antigen format, T cell mediated tumor cell killing is better than which Fc mediated
Disadvantages	Mis-pairing and purification problems; relatively poor permeability of tumor tissue	Requires specific purification technology; require half-life extension or frequent dosing

CMC chemistry, manufacturing, and controls

Dual TAAs targeting BsAbs

As of April 2020, over 123 BsAbs are under clinical evaluation in cancer patients (including marketed Blinatumomab and Catumaxomab). Among the 123 BsAbs, bispecific immune cell engagers (BICEs) are the dominant class of BsAbs (82 of 123), which target a receptor expressed on the immune cell surface with one arm and a tumor cell surface receptor with the other arm. Thus, they redirect specific immune effector cells to tumor cells. In this review, we focus on the dual TAAs targeting BsAbs. The strategy of dual TAAs targeting with a BsAb offers several advantages including increased tumor selectivity, modulation of two functional pathways in the tumor cell at the same time and improved payload delivery (Fig. 2). Although dual TAAs targeting BsAbs only represent a small portion of the 123 BsAbs undergoing clinical trials (9 of 123), the limited number of targets involved indicates its huge growth potential (Table 2).

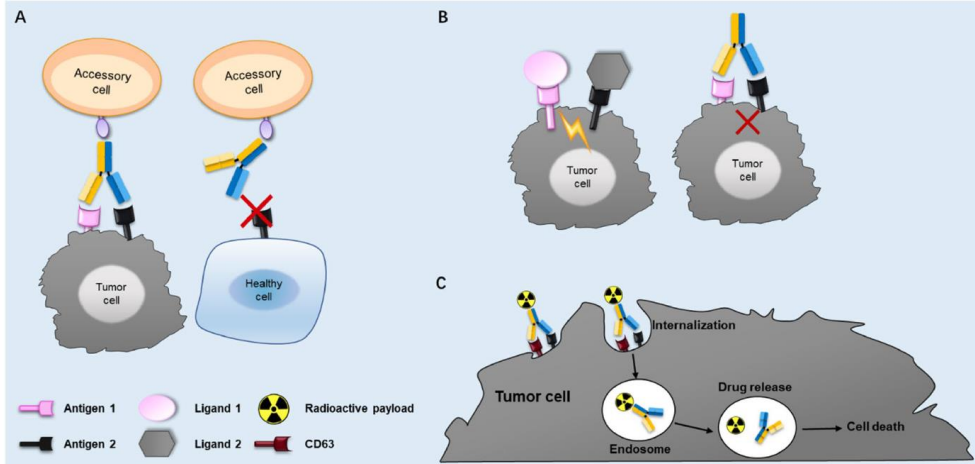


Fig. 2 Proposed mechanisms of action (MOA) for dual TAAs targeting BsAbs. **a** Dual TAAs targeting BsAb binds to double antigen-positive cancer cells, but not single antigen-positive healthy cells; **b** dual signaling blockade; **c** enhanced payload delivery mediated by CD63 targeted BsAb.

Table 2 Clinical trials of dual tumor-associated antigens targeting bispecific antibodies

Antibody Name	Sponsor	Targets	Format	Diseases	Clinical studies
Zenocutuzumab, MCLA-128 PB4188	Merus	HER2×HER3	Fab×Fab-Fc, IgG1, 1+1	Solid tumors harboring NRG1 fusion NSCLC harboring NRG1 fusion Pancreatic cancer Harboring NRG1 fusion	Phase II (NCT03321981)
OXS-1550, DT2219ARL	GT biopharma	CD19×CD22	scFv×scFv, 1+1	Refractory B-lineage leukemia Relapsed B-lineage leukemia	Phase I/II (NCT02370160)
EMB01	EpimAb Biotherapeutics	EGFR×c-MET	Fab×Fab-Fc, IgG1, 2+2	Neoplasms Neoplasm metastasis Non-small-cell lung cancer	Phase I/II (NCT03797391)
JNJ-61186372	Janssen	EGFR×c-MET	Fab×Fab-Fc, IgG1, 1+1	Non-small-cell lung cancer	Phase I (NCT02609776 and NCT04077463)
TG-1801, NI-1701	TG Therapeutics	CD47×CD19	Fab×Fab-Fc, IgG1, 1+1	B cell lymphoma	Phase I (NCT03804996)
IBI322	Innovent biologics	CD47×PDL-1	Undisclosed	Advanced malignancies	Phase I (NCT04338659 and NCT04328831)
MCLA-158	Merus	EGFR×LGR5	Fab×Fab-Fc, IgG1, 1+1	Advanced/metastatic solid tumors Colorectal Cancer	Phase I (NCT03526835)
IMM0306	ImmuneOnco	CD20×CD47	Fab×Ligand-Fc, IgG1, 2+2	Non-hodgkin lymphoma	Phase I (CTR20192612)
RO6874813 (RO7386)	Roche	DR5×FAP	Fab×Fab-Fc, IgG1, 2+2	Advanced and/or metastatic solid tumors	Phase I (NCT02558140)

Increased tumor selectivity

Many tumor-targeting monospecific mAbs not only eliminate tumor cells

but also induce sometimes severe on-target toxicity towards healthy tissues. For example, anti-CD47 mAbs block a 'do not eat me' signal upregulated on tumor cells to evade macrophage-mediated phagocytosis but is also present on erythrocytes, platelets, and other healthy cells. Anti-CD47 mAbs induce severe anemia and thrombocytopenia contributing to decision by Celgene to terminate the Phase I clinical study of CC-90002 (NCT02641002). To circumvent this, BsAbs were designed with a tumor-specific targeting arm to drive tumor-selective binding of an affinity optimized second arm targeting CD47. For instance, the TG-1801 (NI-1701), is a 1:1 IgG1 BsAb targeting CD19, a biomarker exclusively expressed on normal B cells and B-cell lineage malignancies, and CD47. BsAb TG-1801 could potentially overcome the limitation of CD47 monospecific targeting therapy by specifically blocking the 'do not eat me' signal only on B-cells. This is achieved by combining a low-affinity CD47 arm with a high-affinity CD19 arm, thereby reducing the risk of unwanted CD47 blockade in healthy cells (Buatois et al. 2018; Hatterer et al. 2019). Similarly, IMM0306, a CD20 x CD47 BsAb developed by ImmuneOnco has achieved remarkable therapeutic effects in various tumor models and showed no binding to human erythrocytes in pre-clinical study (Yu et al. 2020). Besides hematological malignancies, there are also BsAbs that work in a similar way to increase blockade/activation specificity in solid tumors, such as IBI322 and RO6874813 (RO7386). Whereas the depletion of healthy B cells can be tolerated to a certain degree in the treatment of B cell-derived tumors (e.g., by targeting CD19), this is not necessarily the case for targeting TAA expressed on solid tumors and associated healthy tissues. IBI322 is a CD47 x PDL-1 BsAb developed by Innovent Biologics which preferentially accumulated in PD-L1 positive solid tumors, thereby reducing the potential side effects due to the CD47 pathway blockade in healthy cells (Wang et al. 2020). In another example, RO6874813 is a 2:2 CrossMab that binds with high to fibroblast activation protein (FAP) on cancer-associated fibroblasts in tumor stroma and low affinity to death receptor 5 (DR5). The TNFR family member DR5 is often expressed on tumor cells and its activation induces apoptosis. FAP-driven binding enables docking of RO6874813 on cancer-associated fibroblasts increasing the local concentration of DR5 binding hyperclustering to potently induce apoptosis in tumor cells but not in normal cells (Brunker et al. 2016).

Strictly tumor-specific antigens useful for antibody targeting have yet to be identified in solid tumors. Although dual targeting of two tumor-selective antigens increases tumor selectivity over healthy cells expressing one

antigen, it can be further improved. To address this, Mazor et al. generated different variants of EGFR × HER2 BsAbs each with, respectively, affinity optimized EGFR binding arms. Eventually, one EGFR × HER2 BsAb displayed much more preferential binding to EGFR-HER2 double-positive cells over EGFR single-positive cells (Mazor et al. 2017). Although the binding profile of this BsAb over HER2 single-positive cells was not reported, this study indicates that dual tumor-associated antigen targeting BsAb might require further tuning of binding affinity of one or both variable domains to achieve adequate tumor selectivity or specificity. In another example to achieve tumor-specific targeting, Banaszek et al. developed a Trispecific T cell-engaging antibody derivative consists of two TAA targeting scFv and a CD3 binding fragment. Remarkably, this antibody comes in two complementary halves. Each half contains a TAA binding scFv fused to either the variable light (VL) or variable heavy (VH) chain domain of an anti-CD3 antibody. When the two complementary halves simultaneously bind their respective antigens on the same cell, they reconstitute the original CD3-binding site to engage T cells (Banaszek et al. 2019).

Dual receptor signaling blockade

Cancer is a highly complex and multifactorial disease, involving multiple disease-driving proteins and crosstalking pathways. Cross-talk between different pathways supports a complex molecular network which may mediate tumor escape (Aleksakhina et al. 2019). Facilitated by inherent tumor heterogeneity, acquisition of drug resistance is often observed in patients who relapse after treatment with a single molecular targeted therapy.

Epidermal growth factor receptor (EGFR) is the first identified receptor tyrosine kinase, which plays essential roles in regulating cell proliferation, survival and differentiation. EGFR overexpression is associated with the development of epithelial malignancies, such as non-small cell lung cancer, ovarian cancer, colorectal cancer, and prostate cancer (Nicholson et al. 2001). Tyrosine kinase inhibitors (TKIs) such as Gefitinib and Erlotinib that target the EGFR signaling cascade have been a clinical success over the past two decades, but also faced the challenge of drug resistance (Mok et al. 2009; Steins et al. 2018). For instance, in non-small cell lung cancer (NSCLC) patients demonstrated clinically meaningful response to first-generation EGFR tyrosine kinase inhibitors, but drug resistance was found to occur within a year or less (Kobayashi et al. 2005; Pérez-Soler et al. 2004). Although the second/third generation TKIs demonstrates activity in drug-

resistant patients, eventually they also develop acquired resistance to the TKIs due to new EGFR mutations (van der Wekken et al. 2016). Another important cause of drug resistance to TKIs is the activation of parallel RTK (Receptor Tyrosine Kinase) pathways. For instance, activation of Hepatocyte Growth Factor/Mesenchymal-Epithelial Transition factor (HGF/MET) pathway was shown to occur frequently bypassing EGFR TKI inhibitors (Bean et al. 2007; Engelman et al. 2007). With this in mind, two BsAbs (JNJ-61186372, Janssen; EMB01, EpimAb) targeting EGFR and c-MET were derived independently and are currently being tested in clinical studies. JNJ-61186372 is a humanized EGFR × c-MET BsAb generated using Fab arm exchange technology (Labrijn et al. 2013). JNJ-61186372 simultaneously blocks ligand-induced phosphorylation of EGFR and c-MET, and induces enhanced ADCC activity owing to the low-fucose-containing Fc carbohydrate. Moreover, JNJ-61186372 downregulated receptor expression on tumor cells thus preventing the drug resistance mediated by new emerging mutations of EGFR or c-MET (Castoldi et al. 2013; Moores et al. 2016). In a Phase I study (NCT02609776) which included 108 patients with advanced NSCLC, JNJ-61186372 has shown manageable safety profile and broad-spectrum anti-tumor efficacy in patients with EGFR exon 20 insertion, EGFR C797S mutation, MET amplification or resistance to Osimertinib, a third generation EGFR TKI (Park et al. 2020). Based on these data, FDA recently granted Breakthrough Therapy Designation (BTD) to JNJ-61186372 in NSCLC.

In another example, a HER2 × HER3 BsAb (Zenocutuzumab, also named MCLA-128, PB4188) is undergoing clinical evaluation for the treatment of patients with solid tumors harboring Neuroregulin1 (NRG1) fusion. NRG1 is a member of the EGF family that binds HER3 leading to the formation of a heterodimeric complex between HER2 and HER3. Patients treated for HER2 driven cancers are frequently found to escape from HER2 targeting agents via NRG1 activation of the HER3 pathway. NRG1 fusions represent actionable oncogenic driver mutations potentially useful to select patients most likely to respond to Zenocutuzumab. NRG1 fusions occur in ~ 3% NSCLC, ~ 1.5% pancreatic cancer and less than 1% of other cancers, and are detected frequently in KRAS-wildtype pancreatic ductal adenocarcinomas (PDAC) providing a potential drug target for those patients who do not benefit from KRAS inhibitors. Due to the high affinity to HER2, MCLA-128 docks on HER2 and blocks the formation of HER2/3 heterodimers and NRG1-fusion binding to HER3 simultaneously, thus

inhibiting tumor cell proliferation (de Vries Schultink et al. 2020; Geuijen et al. 2018; Editorial 2019).

Tumor delivery of toxic payloads

Antibody–drug conjugate (ADC) therapeutics combine the targeting precision of an antibody with the cytotoxic activity of a highly potent cytotoxic payload by conjugation to mAbs. Once the drug conjugated antibodies bind the antigens on tumor cell surface, ADCs are internalized by receptor-mediated endocytosis, and the toxic payload is released (Shim 2020). In the apparent absence of tumor-specific mAb targets or because tumor-selective targets not always internalize well, BsAbs may provide improved options compared to monospecific antibody-based ADC for tumor-selective delivery of highly potent chemical payloads.

For instance, the abundant clinical experience and approval of trastuzumab emtansine for the treatment of metastatic breast cancer confirmed that HER2 can be an effective ADC target. However, the internalization of HER2 targeted ADCs often relied on cross-linking of HER2 molecules while monomeric HER2 does not internalize well (de Goeij et al. 2016). To improve the internalization of HER2 targeted ADCs, a BsAb-based ADC targeting CD63 and HER2 was designed. CD63, also named lysosome-associated membrane glycoprotein 3 (LAMP3), is a member of the tetraspanin superfamily demonstrated to shuttle between the plasma membrane and intracellular compartments and is overexpressed in pancreatic cancer, gastric cancer and melanoma. The HER2 × CD63 BsAb showed strong internalization, lysosomal accumulation and cytotoxicity in HER2-positive tumor cells, and minimal internalization into HER2-negative cells (de Goeij et al. 2016).

CD19 and CD22 targeted therapy have been successful in the treatment of B cell lymphomas and rare Hairy Cell Leukemia (HCL), respectively, (Kochenderfer and Rosenberg 2013; Kreitman and Arons 2018). However, for CD19 targeted therapy, a sub-population of cancer cells in B-Lineage Leukemia patients turned to express CD22, thus escaped the killing mediated by CD19 targeted therapy (Fry et al. 2018). For CD22 targeted therapy, HCL represents only a small portion of patients with leukemia and expanding the use of the drug to a wider population of patients is critical. To overcome these resistance mechanisms, OXS-1550 (DT2219ARL), a CD19 × CD22 BsAb conjugated to a modified form of diphtheria toxin was developed and is currently being evaluated in Phase I

study in patients with relapsed/refractory B cell lymphoma or leukemia (Bachanova et al. 2015; Schmohl et al. 2018).

Taken together, ADC-BsAbs can be designed to increase the selectivity of payload delivery, enhance its internalization or overcome the escape mechanisms of tumor cells, and may have huge potential as next-generation ADCs providing substantial advantage over monospecific antibody-based ADCs.

Challenges and considerations for the development of dual TAAs targeting BsAbs

Abundant scientific rationale supports the development of BsAb for the treatment of multifactorial disease, such as cancer. BsAb have unique advantages compared to monospecific antibody, but there are also a number of specific challenges regarding bispecific antibodies development that need to be addressed (Li et al. 2020). In this respect, although the regulatory process for evaluation of monoclonal antibodies is well established, FDA published additional guidance for BsAb development programs in April 2019. The guidance for BsAb development programs highlighted additional consideration unique to BsAb development that address scientific rationale, chemistry, manufacturing, and controls (CMC), nonclinical pharmacology and clinical study. To support the development of a particular bispecific antibody, a strong scientific rationale should be provided including, but not limited to, adequate description of the two targets and the rationale for bispecific targeting [mechanism of action (MOA)], dose rationale and increased safety and/or efficacy as compared to similar monospecific products and available therapies. Diverse formats and engineering strategies enabling the design of BsAbs supporting a proposed MOA and the intended clinical application may also cause (1) unexpected attribute changes in BsAbs such as immunogenicity, antigen specificity, affinity and half-life or (2) production-related challenges including production yield, process-related impurities and stability (Atwell et al. 1997; Chailyan et al. 2011; Herold et al. 2017; Masuda et al. 2006). Different formats of BsAbs may require unique development considerations or technologies for each of them, but eventually, the BsAb products should be developed in accordance with standard monoclonal antibody development practices posing new challenges to CMC. Furthermore, during BsAb clinical studies, in addition to comparing the BsAb to the standard of care or placebo, in some cases, FDA

may request a comparison of the BsAb to an approved monospecific product against the same antigen to inform the risk–benefit ratio. Based on the general indications provided in this FDA guidance, several critical factors need to be carefully considered when developing dual TAAs targeting BsAbs. These include (1) selection of target antigens, (2) affinity and biological effects of each arm, and (3) format utilized.

Selection of target antigens

Rational target selection basically determines the MOA of BsAb and is the most important step for success. The preferred BsAb should enable novel biological function and therapeutic MOA which cannot be achieved using mAbs alone or in combination. Basic science supported a key role of c-MET in NSCLC patients developing resistance to EGFR TKIs, supporting design of JNJ-61186372 (EGFR × c-MET BsAb) and patient selection criteria leading to demonstrated anti-tumor activity in NSCLC patients with resistance to EGFR TKIs (Park et al. 2020; Yun et al. 2020). Interestingly, duligotuzumab (MEHD7945A), a BsAb targeting EGFR and HER3, showed no clinical benefit in comparison to cetuximab (anti-EGFR mAb) in phase 2 trials in patients with metastatic colorectal cancer or head and neck squamous cell carcinoma. Expression of HER3 determined by RNA or protein in tumor biopsies did not correlate with the response rate to duligotuzumab. Therefore, the researchers concluded that HER3 has a minor role in EGFR inhibitor naïve mCRC patients (Fayette et al. 2016; Hill et al. 2018). However, others believe that the disappointing results of the study were mainly due to improper selection of patients that were not resistant to prior cetuximab exposure (Saba 2017). Similarly, a phase III study (NCT02134015) of patritumab (HER3 inhibitor) in combination with erlotinib (EGFR inhibitor) for the treatment of NSCLC patients had failed before duligotuzumab (Liu et al. 2019; Yonesaka et al. 2017). Thus, the rationality of selecting EGFR and HER3 as targets for BsAb development requires further investigations. So far, BsAbs targeting dual TAAs have only involved a limited number of targets, with a main focus on ErbB family proteins. It will be interesting to assess BsAbs targeting novel target combinations developed for unmet clinical need.

Affinity and biology effects of each arm

The affinity and biological activity of BsAb to each of the two antigens could have a critical impact on the final clinical outcome. Before JNJ-

61186372, a BsAb against EGFR and c-MET (LY3164530) developed by Eli Lilly, did not enter phase II study due to toxicity and lack of data supporting a predictive biomarker. LY3164530 consisted of an IgG4 antibody targeting c-MET (emibetuzumab, LY2875358) and a single-chain variable fragment targeting EGFR (cetuximab) fused to the N-terminus of each heavy chain. By making use of these two existing antibodies (cetuximab and emibetuzumab), the affinity and activity for each individual arm in LY3164530 were fixed and the relative inhibition of EGFR versus c-MET and affinity to each individual antigen could not be adjusted to improve functionality. Significant toxicities of LY3164530 were recorded and found to be associated with EGFR inhibition but not c-MET inhibition, indicating that engineering the functionality of each arm might have improved its overall toxicity profile (Patnaik et al. 2018). In contrast, JNJ-61186372 was selected from a panel of EGFR × c-MET BsAbs based on functional activity and, similarly, zenocutuzumab came from an unbiased functional screening of a panel of 545 BsAbs (Geuijen et al. 2018; Grugan et al. 2017). Moreover, a BsAb can sometimes exert a completely opposite activity compared to its two parental mAbs due to its format of conformation. For instance, a dual-variable-domain immunoglobulin (DVD-Ig) BsAb, generated by combining two well-validated antagonist anti-HER2 antibodies trastuzumab and pertuzumab, was shown to be a functional agonist of HER2 (Gu et al. 2014). Therefore, activity of a BsAb should not be assumed based on its parental mAbs, instead both affinity and biological activity should be investigated in an unbiased fashion following construction of the BsAb.

Format utilized

The format of BsAb greatly influences its final physicochemical properties and biological functions. Over 100 different BsAb formats have been invented to solve many scientific or technical issues and their diversity enabled researchers to use them for various applications. A BsAb format suitable for all applications does not exist—the best format is the one that works well for desired application specifically (Brinkmann and Kontermann 2017). BsAbs properly designed with a well-chosen backbone can demonstrate enhanced anti-tumor efficacy and/or reduced side effects. Currently, the human IgG1 backbone is commonly used for dual TAAs targeting BsAbs mainly due to its well-known capacity to confer high exposure and long terminal half-life as well as inducing strong secondary immune functions. Many studies have demonstrated that small differences

in the amino acid sequence of the CH2 and CH3 domain as well as the glycosylation profile of the Fc domain highly impact antibody thermal stability, pharmacokinetic properties and FcγR-mediated effector functions (Haraya et al. 2019; Kapelski et al. 2019; Regula et al. 2016; Roux et al. 1997; Zheng et al. 2011). The human FcγRIII, expressed on macrophages, monocytes, neutrophils, mast cells, and NK cells, binds antibodies with low glycosylation more tightly, thus inducing more potent ADCC effects (Satoh et al. 2006). For instance, ADCC of MCLA-128 was enhanced by low fucose glycoengineering using the GlymaxX Technology (ProBiogen) while retaining its binding to FcRn (de Vries Schultink et al. 2018); JNJ-61186372 was produced by a CHO cell line defective for protein fucosylation to enhance ADCC (Moores et al. 2016). However, in addition to differences in Fc region, variation in the variable region presentation and flexibility of the hinge region affect the functional activity of the IgG class. As reported by Kapelskia et al. the hinge region of human IgG subclasses showed different flexibility (IgG1 > IgG4 > IgG2, IgG1 being the most flexible) which significantly influenced the T cell redirection capacity of BsAb (Kapelski et al. 2019). Furthermore, in another example, eight anti-HER2 biparatopic BsAbs were generated from the same parental mAbs by DVD-Ig platform with different variable domain orientations or linker lengths. Interestingly, four BsAbs with same variable domain orientation showed strong agonistic activity while another four BsAbs with opposite orientation were antagonists. Further experiments demonstrated that the BsAb with a particular variable domain orientation could specifically prevent the heterodimer formation of EGFR/HER2 and HER2/HER3, thus forming more HER2 homodimers which lead to the activation of HER2 signal pathway (Gu et al. 2014). Unlike the factors influencing the potency of T cell engager antibodies which are well studied and reviewed (Ellerman 2019), the factors such as IgG subclass, variable domain orientation and length of hinge influencing BsAbs targeting dual TAAs are still largely unknown due to the completely different epitope topology, target geometry and distribution.

Compared to conventional monovalent BsAbs, more and more BsAb formats designed with multi-valence for each target have appeared and showed distinct advantages in particular cases. Cibisatamab (RG7802), a 2:1 CEA × CD3 BsAb, was optimized to have two CEA binding arms with low affinity individually but high avidity when combined, to increase the specificity to CEA^{high} tumor cells but spare CEA^{low} healthy cells. This setup facilitated Cibisatamab to bind to cells with > 10,000 CEA-binding sites/cell,

which are most likely tumor cells (Bacac et al. 2016). For dual TAAs targeting BsAbs, the valence for each targeted TAAs should be considered individually based on specific properties of the targeted product profile. For instance, in the case of RO7386, a 2:2 BsAb targeting FAP and DR5 using high-affinity bivalent FAP arms ensured tumor-selective targeting, whereas bivalent low-affinity DR5 arms facilitated DR5 hyperclustering and killing of tumor cells (Brunker et al. 2016). Interestingly, for two BsAbs targeting EGFR and c-MET JNJ-61186372 used a 1:1 format while EMB01 used a 2:2 format. Early evidence supporting 1:1 design was that bivalent binding of c-MET invariably induced activation rather than inhibition due to dimerization (Wang et al. 2016). However, in pre-clinical studies, with bivalent binding to c-MET, EMB01 showed no c-MET activation in the absence of HGF. Furthermore, EMB01 achieved significant and sustainable tumor regression in the NCI-H1975-HGF CDX model, which was claimed to be more striking than the one achieved by JNJ-61186372 in a similar model. Such differences may be due to clustering induced by tetravalent antibody binding, which was demonstrated to enhance internalization and degradation for many receptors, including EGFR (Gong et al. 2017).

Besides IgG formats, the IgM format is also used for the development of BsAbs which by design provides more antigen binding sites than IgG format (Kaveri et al. 2012). For instance, IgM-2323 is a CD20 × CD3 bispecific IgM antibody developed by IGM Biosciences currently under clinical evaluation in Phase I for the treatment of patients with B cell Non-Hodgkin's lymphoma (NHL) and other B cell malignancies (NCT04082936). In contrast to BsAb in other formats, IGM-2323 has 10 binding units to CD20 and one binding unit to CD3. Due to its 10 binding units for CD20, IGM-2323 is speculated to display very high avidity for CD20 expressing cancer cells including those with low CD20 expression that would escape from conventional anti-CD20 therapy (Keyt et al. 2020).

Conclusions and prospects

Whereas, as a drug class monospecific mAbs have been established as a potent and credible option for cancer therapy, BsAbs are still in the exploration stage. Due to their unique design and structure, BsAbs bring unparalleled advantages compared to the monospecific mAbs, but also the challenges with respect to characterization and production. A challenge for the development of BsAbs is that each design and concept require unbiased

analysis on a case-by-case basis. The different permutations and potential combinations of formats and targets makes every BsAb unique, requiring sound scientific exploration without drawing too many conclusions based on other experience. For the treatment of a multi-factorial disease, such as cancer, monospecific mAb-based therapy is always at risk of inducing drug resistance and tumor escape. Theoretically, BsAb based therapy could be a better solution and clinical data obtained so far supported this assumption, but much more is still needed. In this review, we have summarized the selection of target antigens, binding affinity, avidity and functional activity towards the two selected antigens as three critical factors to be considered in addition to the actual format for selection of clinical BsAb candidate drugs. BsAbs have huge potential to emerge as one of the most effective therapeutic biologicals and we firmly believe that BsAb-based therapies may revolutionize existing cancer treatment options in the future representing a big step forward in our fight against cancer.

Author contributions The first draft of the manuscript was written by SH and all authors commented on previous versions of the manuscript. All authors read and approved the final manuscript.

Funding This project has received funding from the European Union's Horizon 2020 research and innovation programme under the Marie Skłodowska-Curie grant agreement No 765394.

Conflict of interest A. van Elsas owns stock in Aduro Biotech, Inc. The other authors declare that they have no conflict of interest.

References

Aleksakhina SN, Kashyap A, Imyanitov EN (2019) Mechanisms of acquired tumor drug resistance. *Biochim Biophys Acta BBA Rev Cancer* 1872(2):188310. <https://doi.org/10.1016/j.bbcan.2019.188310>

Atwell S, Ridgway JBB, Wells JA, Carter P (1997) Stable heterodimers from remodeling the domain interface of a homodimer using a phage display library. *J Mol Biol* 270(1):26–35. <https://doi.org/10.1006/jmbi.1997.1116>

Ayyar BV, Arora S, O’Kennedy R (2016) Coming-of-age of antibodies in cancer therapeutics. *Trends Pharmacol Sci* 37(12):1009–1028. <https://doi.org/10.1016/j.tips.2016.09.005>

Bacac M, Fauti T, Sam J, Colombetti S, Weinzierl T, Ouaret D, Bodmer W, Lehmann S, Hofer T, Hosse RJ, Moessner E, Ast O, Bruenker P, Grau-Richards S, Schaller T, Seidl A, Gerdes C, Perro M, Nicolini V, Umana P (2016) A novel carcinoembryonic antigen T cell bispecific antibody (CEA TCB) for the treatment of solid tumors. *Clin Cancer Res* 22(13):3286–3297. <https://doi.org/10.1158/1078-0432.CCR-15-1696>

Bachanova V, Frankel AE, Cao Q, Lewis D, Grzywacz B, Verneris MR, Ustun C, Lazaryan A, McClune B, Warlick ED, Kantarjian H, Weisdorf DJ, Miller JS, Vallera DA (2015) Phase I Study of a bispecific ligand-directed toxin targeting CD22 and CD19 (DT2219) for refractory B cell malignancies. *Clin Cancer Res* 21(6):1267–1272. <https://doi.org/10.1158/1078-0432.CCR-14-2877>

Banaszek A, Bumm TGP, Nowotny B, Geis M, Jacob K, Wofl M, Trebing J, Kucka K, Kouhestani D, Gogishvili T, Krenz B, Lutz J, Rasche L, Hoemann D, Neuweiler H, Heiby JC, Bargou RC, Wajant H, Einsele H, Stuhler G (2019) On-target restoration of a split T cell-engaging antibody for precision immunotherapy. *Nat Commun* 10(1):5387. <https://doi.org/10.1038/s41467-019-13196-0>

Bean J, Brennan C, Shih J-Y, Riely G, Viale A, Wang L, Chitale D, Motoi N, Szoke J, Broderick S, Balak M, Chang W-C, Yu C-J, Gazdar A, Pass H, Rusch V, Gerald W, Huang S-F, Yang P-C, Pao W (2007) MET amplification occurs with or without T790M mutations in EGFR mutant lung tumors with acquired resistance to gefitinib or erlotinib. *Proc Natl Acad Sci* 104(52):20932–20937. <https://doi.org/10.1073/pnas.0710370104>

Boerman OC, van Schaijk FG, Oyen WJ, Corstens FH (2003) Pretargeted radioimmunotherapy of cancer: progress step by step. *J Nucl Med* 44(3):400–411

Brinkmann U, Kontermann RE (2017) The making of bispecific antibodies.

MAbs 9(2):182–212. <https://doi.org/10.1080/19420862.2016.1268307>

Brunker P, Wartha K, Friess T, Grau-Richards S, Waldhauer I, Koller CF, Weiser B, Majety M, Runza V, Niu H, Packman K, Feng N, Daouti S, Hosse RJ, Mossner E, Weber TG, Herting F, Scheuer W, Sade H, Umana P (2016) RG7386, a novel tetravalent FAPDR5 antibody, effectively triggers FAP-dependent, avidity-driven DR5 hyperclustering and tumor cell apoptosis. *Mol Cancer Ther* 15(5):946–957. <https://doi.org/10.1158/1535-7163.MCT-15-0647>

Buatois V, Johnson Z, Salgado-Pires S, Papaioannou A, Hatterer E, Chauchet X, Richard F, Barba L, Daubeuf B, Cons L, Broyer L, D'Asaro M, Matthes T, LeGallou S, Fest T, Tarte K, Clarke Hinojosa RK, Genescà Ferrer E, Ribera JM, Ferlin WG (2018) Preclinical development of a bispecific antibody that safely and effectively targets CD19 and CD47 for the treatment of B cell lymphoma and leukemia. *Mol Cancer Ther* 17(8):1739–1751. <https://doi.org/10.1158/1535-7163.MCT-17-1095>

Carter PJ, Lazar GA (2018) Next generation antibody drugs: pursuit of the “high-hanging fruit”. *Nat Rev Drug Dis* 17(3):197–223. <https://doi.org/10.1038/nrd.2017.227>

Castoldi R, Ecker V, Wiehle L, Majety M, Busl-Schuller R, Asmussen M, Nopora A, Jucknischke U, Osl F, Kobold S, Scheuer W, Venturi M, Klein C, Niederfellner G, Sustmann C (2013) A novel bispecific EGFR/Met antibody blocks tumor-promoting phenotypic effects induced by resistance to EGFR inhibition and has potent antitumor activity. *Oncogene* 32(50):5593–5601. <https://doi.org/10.1038/onc.2013.245>

Chailyan A, Marcatili P, Tramontano A (2011) The association of heavy and light chain variable domains in antibodies: implications for antigen specificity: analysis of VH-VL interface in antibodies. *FEBS J* 278(16):2858–2866. <https://doi.org/10.1111/j.1742-4658.2011.08207.x>

Chiu ML, Gilliland GL (2016) Engineering antibody therapeutics. *Curr Opin Struct Biol* 38:163–173. <https://doi.org/10.1016/j.sbi.2016.07.012>

Conrath EK, Lauwereys M, Wyns L, Muyldermans S (2001) Camel single-domain antibodies as modular building units in bispecific and bivalent antibody constructs. *J Biol Chem* 276(10):7346–7350. <https://doi.org/10.1074/jbc.M007734200>

de Goeij BECG, Vink T, ten Napel H, Breij ECW, Satijn D, Wubbolts R, Miao D, Parren PWHI (2016) Efficient payload delivery by a bispecific antibody-drug conjugate targeting HER2 and CD63. *Mol Cancer Ther* 15(11):2688–2697. <https://doi.org/10.1158/1535-7163.MCT-16-0364>

de Vries Schultink AHM, Doornbos RP, Bakker ABH, Bol K, Throsby M,

Geuijen C, Maussang D, Schellens JHM, Beijnen JH, Huitema ADR (2018) Translational PK-PD modeling analysis of MCLA-128, a HER2/HER3 bispecific monoclonal antibody, to predict clinical efficacious exposure and dose. *Invest New Drugs* 36(6):1006–1015. <https://doi.org/10.1007/s10637-018-0593-x>

de Vries Schultink AHM, Bol K, Doornbos RP, Murat A, Wasserman E, Dorlo TPC, Schellens JHM, Beijnen JH, Huitema ADR (2020) Population pharmacokinetics of MCLA-128, a HER2/HER3 bispecific monoclonal antibody, in patients with solid tumors. *Clin Pharmacokinet*. <https://doi.org/10.1007/s40262-020-00858-2>

Editorial (2019) MCLA-128 fights *NRG1* fusion-positive cancers. *Cancer Discov* 9(12):1636. <https://doi.org/10.1158/2159-8290.CD-NB2019-128>

Ellerman D (2019) Bispecific T cell engagers: towards understanding variables influencing the in vitro potency and tumor selectivity and their modulation to enhance their efficacy and safety. *Methods* 154:102–117. <https://doi.org/10.1016/j.ymeth.2018.10.026>

Engelman JA, Zejnullahu K, Mitsudomi T, Song Y, Hyland C, Park JO, Lindeman N, Gale C-M, Zhao X, Christensen J, Kosaka T, Holmes AJ, Rogers AM, Cappuzzo F, Mok T, Lee C, Johnson BE, Cantley LC, Janne PA (2007) MET amplification leads to gefitinib resistance in lung cancer by activating ERBB3 signaling. *Science* 316(5827):1039–1043. <https://doi.org/10.1126/science.1141478>

Fayette J, Wirth L, Oprean C, Udrea A, Jimeno A, Rischin D, Nutting C, Harari PM, Csozsi T, Cernea D, O'Brien P, Hanley WD, Kapp AV, Anderson M, Penuel E, McCall B, Pirzkall A, Vermorken JB (2016) Randomized phase II study of duligotuzumab (MEHD7945A) vs cetuximab in squamous cell carcinoma of the head and neck (MEHGAN study). *Front Oncol*. <https://doi.org/10.3389/fonc.2016.00232>

Fry TJ, Shah NN, Orentas RJ, Stetler-Stevenson M, Yuan CM, Ramakrishna S, Wolters P, Martin S, Delbrook C, Yates B, Shalabi H, Fountaine TJ, Shern JF, Majzner RG, Stroncek DF, Sabatino M, Feng Y, Dimitrov DS, Zhang L, Mackall CL (2018) CD22-targeted CAR T cells induce remission in B-ALL that is naïve or resistant to CD19-targeted CAR immunotherapy. *Nat Med* 24(1):20–28. <https://doi.org/10.1038/nm.4441>

Garber K (2014) Bispecific antibodies rise again. *Nat Rev Drug Discovery* 13(11):799–801. <https://doi.org/10.1038/nrd4478>

Geuijen CAW, De Nardis C, Maussang D, Rovers E, Gallenne T, Hendriks LJA, Visser T, Nijhuis R, Logtenberg T, de Kruif J, Gros P, Throsby M (2018) Unbiased combinatorial screening identifies a bispecific IgG1 that potently

inhibits HER3 signaling via HER2-guided ligand blockade. *Cancer Cell* 33(5):922–936.e10. <https://doi.org/10.1016/j.ccell.2018.04.003>

Godar M, de Haard H, Blanchetot C, Rasser J (2018) Therapeutic bispecific antibody formats: a patent applications review (1994–2017). *Expert Opin Ther Pat* 28(3):251–276. <https://doi.org/10.1080/13543776.2018.1428307>

Gong S, Ren F, Wu D, Wu X, Wu C (2017) Fabs-in-tandem immunoglobulin is a novel and versatile bispecific design for engaging multiple therapeutic targets. *MAbs* 9(7):1118–1128. <https://doi.org/10.1080/19420862.2017.1345401>

Grugan KD, Dorn K, Jarantow SW, Bushey BS, Pardinas JR, Laquerre S, Moores SL, Chiu ML (2017) Fc-mediated activity of EGFR x c-Met bispecific antibody JNJ-61186372 enhanced killing of lung cancer cells. *MAbs* 9(1):114–126. <https://doi.org/10.1080/19420862.2016.1249079>

Gu J, Yang J, Chang Q, Lu X, Wang J, Chen M, Ghayur T, Gu J (2014) Identification of anti-ErbB2 dual variable domain immunoglobulin (DVD-IgTM) proteins with unique activities. *PLoS ONE* 9(5):e97292. <https://doi.org/10.1371/journal.pone.0097292>

Haraya K, Tachibana T, Igawa T (2019) Improvement of pharmacokinetic properties of therapeutic antibodies by antibody engineering. *Drug Metab Pharmacokinet* 34(1):25–41. <https://doi.org/10.1016/j.dmpk.2018.10.003>

Hatterer E, Barba L, Noraz N, Daubeuf B, Aubry-Lachainaye J-P, von der Weid B, Richard F, Kosco-Vilbois M, Ferlin W, Shang L, Buatois V (2019) Co-engaging CD47 and CD19 with a bispecific antibody abrogates B-cell receptor/CD19 association leading to impaired B-cell proliferation. *MAbs* 11(2):322–334. <https://doi.org/10.1080/19420862.2018.1558698>

Herold EM, John C, Weber B, Kremser S, Eras J, Berner C, Deubler S, Zacharias M, Buchner J (2017) Determinants of the assembly and function of antibody variable domains. *Sci Rep* 7(1):12276. <https://doi.org/10.1038/s41598-017-12519-9>

Hill AG, Findlay MP, Burge ME, Jackson C, Alfonso PG, Samuel L, Ganju V, Karthaus M, Amatu A, Jeffery M, Bartolomeo MD, Bridgewater J, Coveler AL, Hidalgo M, Kapp AV, Sufan RI, McCall BB, Hanley WD, Penuel EM, Taberero J (2018) Phase II study of the dual EGFR/HER3 inhibitor duligotuzumab (MEHD7945A) versus cetuximab in combination with FOLFIRI in second-line *RAS* wild-type metastatic colorectal cancer. *Clin Cancer Res* 24(10):2276–2284. <https://doi.org/10.1158/1078-0432.CCR-17-0646>

Johnson S, Burke S, Huang L, Gorlatov S, Li H, Wang W, Zhang W, Tuailon N, Rainey J, Barat B, Yang Y, Jin L, Ciccarone V, Moore PA, Koenig S,

Bonvini E (2010) Effector cell recruitment with novel Fv-based dual-affinity re-targeting protein leads to potent tumor cytotoxicity and in vivo B cell depletion. *J Mol Biol* 399(3):436–449. <https://doi.org/10.1016/j.jmb.2010.04.001>

Kapelski S, Cleiren E, Attar RM, Philippar U, Hasler J, Chiu ML (2019) Influence of the bispecific antibody IgG subclass on T cell redirection. *MAbs* 11(6):1012–1024. <https://doi.org/10.1080/19420862.2019.1624464>

Kaveri SV, Silverman GJ, Bayry J (2012) Natural IgM in immune equilibrium and harnessing their therapeutic potential. *J Immunol* 188(3):939–945. <https://doi.org/10.4049/jimmunol.1102107>

Keyt B, Baliga R, Li K, Manlusoc M, Hinton P, Ng D, Tran M, Shan B, Lu H, Rahman S, Saini A, Cao Y, Saraiya C, Peterson M, Godfrey WR (2020) Lymphoma cell-killing activity and cytokine release by CD20-directed bispecific IgM antibody-based T cell engager (IGM-2323). *J Clin Oncol*. https://doi.org/10.1200/JCO.2020.38.15_suppl.e15007

Kipriyanov SM, Moldenhauer G, Schuhmacher J, Cochlovius B, Von der Lieth C-W, Matys ER, Little M (1999) Bispecific tandem diabody for tumor therapy with improved antigen binding and pharmacokinetics. *J Mol Biol* 293(1):41–56. <https://doi.org/10.1006/jmbi.1999.3156>

Klein C, Sustmann C, Thomas M, Stubenrauch K, Croasdale R, Schanzer J, Brinkmann U, Kettenberger H, Regula JT, Schaefer W (2012) Progress in overcoming the chain association issue in bispecific heterodimeric IgG antibodies. *MAbs* 4(6):653–663. <https://doi.org/10.4161/mabs.21379>

Kobayashi S, Janne PA, Meyerson M, Eck MJ (2005) EGFR mutation and resistance of non-small-cell lung cancer to gefitinib. *N Engl J Med* 352:792

Kochenderfer JN, Rosenberg SA (2013) Treating B cell cancer with T cells expressing anti-CD19 chimeric antigen receptors. *Nat Rev Clin Oncol* 10(5):267–276. <https://doi.org/10.1038/nrclinonc.2013.46>

Kontermann RE (2011) Strategies for extended serum half-life of protein therapeutics. *Curr Opin Biotechnol* 22(6):868–876. <https://doi.org/10.1016/j.copbio.2011.06.012>

Kontermann RE, Brinkmann U (2015) Bispecific antibodies. *Drug Discovery Today* 20(7):838–847. <https://doi.org/10.1016/j.drudis.2015.02.008>

Kreitman RJ and Arons E (2018) Update on hairy cell leukemia. *19 Kung P, Goldstein G, Reinherz E, Schlossman S (1979) Monoclonal antibodies defining distinctive human T cell surface antigens. Science* 206(4416):347–349. <https://doi.org/10.1126/science.314668>

Labrijn AF, Meesters JI, de Goeij BECG, van den Bremer ETJ, Neijssen J, van Kampen MD, Strumane K, Verploegen S, Kundu A, Gramer MJ, van Berkel PHC, van de Winkel JGJ, Schuurman J, Parren PWHI (2013) Efficient generation of stable bispecific IgG1 by controlled Fab-arm exchange. *Proc Natl Acad Sci* 110(13):5145–5150. <https://doi.org/10.1073/pnas.1220145110>

Labrijn AF, Janmaat ML, Reichert JM, Parren PWHI (2019) Bispecific antibodies: a mechanistic review of the pipeline. *Nat Rev Drug Discovery* 18(8):585–608. <https://doi.org/10.1038/s41573-019-0028-1>

Li H, Er Saw P, Song E (2020) Challenges and strategies for next generation bispecific antibody-based antitumor therapeutics. *Cell Mol Immunol* 17(5):451–461. <https://doi.org/10.1038/s41423-020-0417-8>

Liu X, Liu S, Lyu H, Riker AI, Zhang Y, Liu B (2019) Development of effective therapeutics targeting her3 for cancer treatment. *Biol Proc Online* 21(1):5. <https://doi.org/10.1186/s12575-019-0093-1>

Lopez-Albaitero A, Xu H, Guo H, Wang L, Wu Z, Tran H, Chandarlapaty S, Scaltriti M, Janjigian Y, de Stanchina E, Cheung N-KV (2017) Overcoming resistance to HER2-targeted therapy with a novel HER2/CD3 bispecific antibody. *Oncolmmunology* 6(3):e1267891. <https://doi.org/10.1080/2162402X.2016.1267891>

Masuda K, Sakamoto K, Kojima M, Aburatani T, Ueda T, Ueda H (2006) The role of interface framework residues in determining antibody VH/VL interaction strength and antigen-binding affinity. *FEBS J* 273(10):2184–2194. <https://doi.org/10.1111/j.1742-4658.2006.05232.x>

Mazor Y, Hansen A, Yang C, Chowdhury PS, Wang J, Stephens G, Wu H, Dall'Acqua WF (2015) Insights into the molecular basis of a bispecific antibody's target selectivity. *MAbs* 7(3):461–469. <https://doi.org/10.1080/19420862.2015.1022695>

Mazor Y, Sachsenmeier KF, Yang C, Hansen A, Filderman J, Mulgrew K, Wu H, Dallacqua WF (2017) Enhanced tumor-targeting selectivity by modulating bispecific antibody binding affinity and format valence. *Sci Rep* 7(1):40098. <https://doi.org/10.1038/srep40098>

Mok TS, Wu Y-L, Thongprasert S, Yang C-H, Chu D-T, Saijo N, Sunpaweravong P, Han B, Margono B, Ichinose Y, Nishiwaki Y, Ohe Y, Yang J-J, Chewaskulyong B, Jiang H, Duffield EL, Watkins CL, Armour AA, Fukuoka M (2009) Gefitinib or carboplatin-paclitaxel in pulmonary adenocarcinoma. *N Engl J Med* 361(10):947–957. <https://doi.org/10.1056/NEJMoa0810699>

Moores SL, Chiu ML, Bushey BS, Chevalier K, Luistro L, Dorn K, Brezski

RJ, Haytko P, Kelly T, Wu S-J, Martin PL, Neijssen J, Parren PWHI, Schuurman J, Attar RM, Laquerre S, Lorenzi MV, Anderson GM (2016) A Novel Bispecific antibody targeting EGFR and cMet is effective against EGFR inhibitor-resistant lung tumors. *Can Res* 76(13):3942–3953. <https://doi.org/10.1158/0008-5472.CAN-15-2833>

Nicholson RI, Gee JMW, Harper ME (2001) EGFR and cancer prognosis. *Eur J Cancer* 37:9–15. [https://doi.org/10.1016/S0959-8049\(01\)00231-3](https://doi.org/10.1016/S0959-8049(01)00231-3)

Nisonoff A, Wissler F, Lipman L (1960) Properties of the major component of a peptic digest of rabbit antibody.pdf. *Science* 132:1770–1771. <https://doi.org/10.1126/science.132.3441.1770>

Park K, John T, Kim S-W, Lee JS, Shu CA, Kim D-W, Ramirez SV, Spira AI, Sabari JK, Han J-Y, Trigo JM, Lee CK, Lee KH, Girard N, Lorenzini PA, Xie J, Roshak A, Thayu M, Knoblauch RE, Cho BC (2020) Amivantamab (JNJ-61186372), an anti-EGFR-MET bispecific antibody, in patients with EGFR exon 20 insertion (exon20ins)-mutated non-small cell lung cancer (NSCLC). *J Clin Oncol* 38(15):suppl 9512. https://doi.org/10.1200/JCO.2020.38.15_suppl.9512

Patnaik A, Gordon M, Tsai F, Papadopoulos K, Rasco D, Beeram SM, Fu S, Janku F, Hynes SM, Gundala SR, Willard MD, Zhang W, Lin AB, Hong D (2018) A phase I study of LY3164530, a bispecific antibody targeting MET and EGFR, in patients with advanced or metastatic cancer. *Cancer Chemother Pharmacol* 82(3):407–418. <https://doi.org/10.1007/s00280-018-3623-7>

Pérez-Soler R, Chachoua A, Hammond LA, Rowinsky EK, Huberman M, Karp D, Rigas J, Clark GM, Santabarbara P, Bonomi P (2004) Determinants of tumor response and survival with erlotinib in patients with non-small-cell lung cancer. *J Clin Oncol* 22(16):3238–3247. <https://doi.org/10.1200/JCO.2004.11.057>

Przepiorka D, Ko C-W, Deisseroth A, Yancey CL, Candau-Chacon R, Chiu H-J, Gehrke BJ, Gomez-Broughton C, Kane RC, Kirshner S, Mehrotra N, Ricks TK, Schmiel D, Song P, Zhao P, Zhou Q, Farrell AT, Pazdur R (2015) FDA approval: blinatumomab. *Clin Cancer Res* 21(18):4035–4039. <https://doi.org/10.1158/1078-0432.CCR-15-0612>

Regula JT, Lundh von Leithner P, Foxton R, Barathi VA, Cheung CMG, Bo Tun SB, Wey YS, Iwata D, Dostalek M, Moelleken J, Stubenrauch KG, Nogoceke E, Widmer G, Strassburger P, Koss MJ, Klein C, Shima DT, Hartmann G (2016) Targeting key angiogenic pathways with a bispecific Cross ma b optimized for neovascular eye diseases. *EMBO Mol Med* 8(11):1265–1288. <https://doi.org/10.15252/emmm.201505889>

Roopenian DC, Akilesh S (2007) FcRn: The neonatal Fc receptor comes of age. *Nat Rev Immunol* 7(9):715–725. <https://doi.org/10.1038/nri2155>

Roux KH, Strelets L, Michaelsen TE (1997) Flexibility of human IgG subclasses. *J Immunol.* 159(7):3372–3382

Saba NF (2017) Commentary: randomized phase II study of duligotuzumab (MEHD7945A) vs cetuximab in squamous cell carcinoma of the head and neck (MEHGAN Study). *Front Oncol.* <https://doi.org/10.3389/fonc.2017.00031>

Satoh M, Iida S, Shitara K (2006) Non-fucosylated therapeutic antibodies as next-generation therapeutic antibodies. *Expert Opin Biol Ther* 6(11):1161–1173. <https://doi.org/10.1517/14712598.6.11.1161>

Schmohl J, Todhunter D, Taras E, Bachanova V, Vallera D (2018) Development of a deimmunized bispecific immunotoxin

dDT2219 against B cell malignancies. *Toxins* 10(1):32. <https://doi.org/10.3390/toxins10010032>

Scott AM, Wolchok JD, Old LJ (2012) Antibody therapy of cancer. *Nat Rev Cancer* 12(4):278–287. <https://doi.org/10.1038/nrc3236>

Seimetz D, Lindhofer H, Bokemeyer C (2010) Development and approval of the trifunctional antibody catumaxomab (anti-EpCAM×anti-CD3) as a targeted cancer immunotherapy. *Cancer Treat Rev* 36(6):458–467. <https://doi.org/10.1016/j.ctrv.2010.03.001>

Shim H (2020) Bispecific antibodies and antibody-drug conjugates for cancer therapy: technological considerations. *Biomolecules* 10(3):360. <https://doi.org/10.3390/biom10030360>

Steins M, Thomas M, Geiger M (2018) Erlotinib. In: Martens UM (ed) *Small molecules in oncology*, vol 211. Springer International Publishing. pp 1–17. https://doi.org/https://doi.org/10.1007/978-3-319-91442-8_1

Suurs FV, Lub-de Hooge MN, de Vries EGE, de Groot DJA (2019) A review of bispecific antibodies and antibody constructs in oncology and clinical challenges. *Pharmacol Ther* 201:103–119. <https://doi.org/10.1016/j.pharmthera.2019.04.006>

van der Wekken AJ, Saber A, Hiltermann TJN, Kok K, van den Berg A, Groen HJM (2016) Resistance mechanisms after tyrosine kinase inhibitors afatinib and crizotinib in non-small cell lung cancer, a review of the literature. *Crit Rev Oncol/Hematol* 100:107–116. <https://doi.org/10.1016/j.critrevonc.2016.01.024>

Velasquez MP, Bonifant CL, Gottschalk S (2018) Redirecting T cells to

hematological malignancies with bispecific antibodies. *Blood* 131(1):30–38. <https://doi.org/10.1182/blood-2017-06-741058>

Wang J, Goetsch L, Tucker L, Zhang Q, Gonzalez A, Vaidya KS, Oleksijew A, Boghaert E, Song M, Sokolova I, Pestova E, Anderson M, Pappano WN, Ansell P, Bhatena A, Naumovski L, Corvaia N, Reilly EB (2016) Anti-c-Met monoclonal antibody ABT-700 breaks oncogene addiction in tumors with MET amplification. *BMC Cancer* 16(1):105. <https://doi.org/10.1186/s12885-016-2138-z>

Wang Q, Chung C-Y, Chough S, Betenbaugh MJ (2018) Antibody glycoengineering strategies in mammalian cells. *Biotechnol Bioeng* 115(6):1378–1393. <https://doi.org/10.1002/bit.26567>

Wang Y, Pan D, Huang C, Chen B, Li M, Zhou S, Wang L, Wu M, Wang X, Bian Y, Yan J, Liu J, Yang M, Miao L (2020) Dose escalation PET imaging for safety and effective therapy dose optimization of a bispecific antibody. *MAbs* 12(1):1748322. <https://doi.org/10.1080/19420862.2020.1748322>

Wolf E, Hofmeister R, Kufer P, Schlereth B, Baeuerle PA (2005) BiTEs: Bispecific antibody constructs with unique anti-tumor activity. *Drug Discovery Today* 10(18):1237–1244. [https://doi.org/10.1016/S1359-6446\(05\)03554-3](https://doi.org/10.1016/S1359-6446(05)03554-3)

Yonesaka K, Hirotsu K, von Pawel J, Dediu M, Chen S, Copigneaux C, Nakagawa K (2017) Circulating heregulin level is associated with the efficacy of patritumab combined with erlotinib in patients with non-small cell lung cancer. *Lung Cancer* 105:1–6. <https://doi.org/10.1016/j.lungcan.2016.12.018>

Yu YJ, Zhang Y, Kenrick M, Hoyte K, Luk W, Lu Y, Atwal J, Elliott JM, Prabhu S, Watts RJ, Dennis MS (2011) Boosting brain uptake of a therapeutic antibody by reducing its affinity for a transcytosis target. *Sci Transl Med* 3(84):8444. <https://doi.org/10.1126/scitranslmed.3002230>

Yu J, Song Y, Tian W (2020) How to select IgG subclasses in developing anti-tumor therapeutic antibodies. *J Hematol Oncol* 13(1):45. <https://doi.org/10.1186/s13045-020-00876-4>

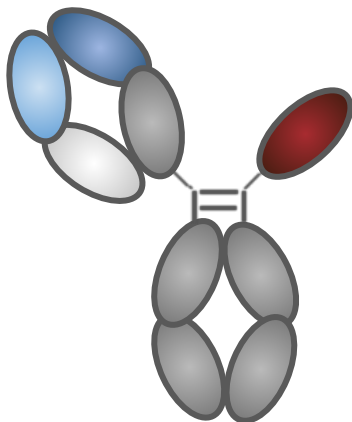
Yun J, Lee S-H, Kim S-Y, Jeong S-Y, Kim J-H, Pyo K-H, Park C-W, Heo SG, Yun MR, Lim S, Lim SM, Hong MH, Kim HR, Thayu M, Curtin JC, Knoblauch RE, Lorenzi MV, Roshak A, Cho BC (2020) Antitumor activity of amivantamab (JNJ-61186372), an EGFR-cMet bispecific antibody, in diverse models of EGFR Exon 20 Insertion-Driven NSCLC. *Cancer Discov*. <https://doi.org/10.1158/2159-8290.CD-20-0116>

Zheng K, Bantog C, Bayer R (2011) The impact of glycosylation on monoclonal antibody conformation and stability. *MAbs* 3(6):568–576.

<https://doi.org/10.4161/mabs.3.6.17922>

Zhukovsky EA, Morse RJ, Maus MV (2016) Bispecific antibodies and CARs: generalized immunotherapeutics harnessing T cell redirection. *Curr Opin Immunol* 40:24–35. <https://doi.org/10.1016/j.coi.2016.02.006>

3



A novel efficient bispecific antibody format, combining a conventional antigen-binding fragment with a single domain antibody, avoids potential heavy-light chain mis-pairing

Shuyu Huang^{a,b}, Aina Segués^{a,b}, David Lutje Hulsik^a, Dietmar M. Zaiss^c, Alice J.A.M. Sijts^b, Sander M.J. van Duijnhoven^a, Andrea van Elsas^a

^a Aduro Biotech Europe, Oss, the Netherlands

^b Faculty of Veterinary Medicine, Department of Infectious Diseases and Immunology, Utrecht University, Utrecht, the Netherlands

^c Institute of Immunology and Infection Research, School of Biological Sciences, University of Edinburgh, Ashworth Laboratories, Edinburgh, UK

Journal of immunological methods 483 (2020): 112811.

Contribution statement: Shuyu Huang and his supervisors conceived the original idea. Shuyu Huang carried out the experiments, analyzed the data and wrote the manuscript with support from his supervisors.

Abstract

Due to the technical innovations in generating bispecific antibodies (BsAbs) in recent years, BsAbs have become important reagents for diagnostic and therapeutic applications. However, the difficulty of producing a heterodimer consisting of two different arms with high yield and purity constituted a major limitation for their application in academic and clinical settings. Here, we describe a novel Fc-containing BsAb format (Fab x sdAb-Fc) composed of a conventional antigen-binding fragment (Fab), and a single domain antibody (sdAb), which avoids heavy-light chain mis-pairing during antibody assembly. In this study, the Fab x sdAb-Fc BsAbs were efficiently produced by three widely used heavy-heavy chain heterodimerization methods: Knobs-into-holes (KIH), Charge-pairs (CP) and controlled Fab-arm exchange (cFAE), respectively. The novel Fab x sdAb-Fc format provided a rapid and efficient strategy to generate BsAb with high purity and a unique possibility to further purify desired BsAbs from undesired antibodies based on molecular weight (MW). Compared to conventional BsAb formats, the advantages of Fab x sdAb-Fc format may thus provide a straightforward opportunity to apply bispecific antibody principles to research and development of novel targets and pathways in diseases such as cancer and autoimmunity.

Keywords: bispecific antibody, antibody chain association, knobs-into-holes, charge-pairs, controlled fab-arm exchange

1. Introduction

Bispecific antibodies (BsAbs) have been considered promising cancer therapeutics for a long period of time. The first artificial antibody-based molecule with the ability to bind to two different antigens at the same time was described by Nisonoff's team in 1960s, which marked the launch of a long BsAb generation campaign (Nisonoff et al., 1960). Compared to monospecific monoclonal antibodies, the potential advantages of BsAbs are undisputed. When applied to cancer therapy, BsAbs have shown potential to redirect specific immune cells to tumour cells to enhance tumour killing (Staerz et al., 1985). Furthermore, given that cancer is a complex, multifactorial and heterogenic disease involving many disease-driving proteins and cross-talking pathways, BsAbs can be used to target two antigens that each are not necessarily tumour specific but targeting the combination improves selectivity of tumour targeting over normal tissues (Mazor et al., 2015a) (Mazor et al., 2017). Moreover, dual targeting could be useful to modulate two separate functional pathways in the tumour, or to avoid resistance to the treatment (Lopez-Albaitero et al., 2017) (Moore et al., 2016). Nevertheless, BsAbs have not yet stimulated broad interest of pharmaceutical companies until recent years due to challenges in BsAb manufacturing (Garber, 2014). By the end of 2017, compared to the number of 57 clinically approved mAbs, there were only two BsAbs on the market (Grilo and Mantalaris, 2019). The major challenge in the development of BsAbs is the difficulty in producing a pure BsAb without the presence of contaminating antibody by-products such as non-functional or monospecific molecules formed during assembly.

Over the past two decades, with the development of protein and gene engineering, over 100 different formats of BsAbs have become available which fall into four classes: Fc containing asymmetric architecture, Fc-less asymmetric architecture, Fc containing symmetric architecture and Fc-less symmetric architecture (Brinkmann and Kontermann, 2017) (Ha et al., 2016). The diversification of BsAb formats allows researchers to modify the size, half-life, valency, flexibility, and biodistribution of BsAb for applications of different purposes. In many cases, the Fc region is needed to ensure a relatively long pharmacokinetic in vivo half-life and the ability to induce secondary immune functions of a given BsAb, such as Antibody-dependent cell mediated cytotoxicity (ADCC), Antibody-dependent cellular phagocytosis (ADCP) and Complement-dependent cytotoxicity (CDC). To form a Fc containing asymmetric BsAb, several methodologies have been

developed to enforce the correct association of the two different heavy chains of a BsAb during cellular expression. Well-known examples are knobs-into-holes (KIH) (Merchant et al., 1998) (Atwell et al., 1997), charge-pairs (CP) (Gunasekaran et al., 2010), leucine zipper induced heterodimerization (LUZ-Y) (Wranik et al., 2012), strand-exchange engineered domain CH3 heterodimers (SEEDbody) (Davis et al., 2010), and HA-TF (Moore et al., 2011).

These heterodimerization methods solved the heavy-heavy chain mis-pairing problem to a great extent, but inadvertent mis-pairing of heavy-light chain still remained a major limitation. One straightforward method to overcome heavy-light chain mis-pairing is to share common light chain by two different heavy chains (Merchant et al., 1998) (Jackman et al., 2010) (Krah et al., 2017). The latter approach provides a challenge when using pre-existing and validated ('benchmark') parental monospecific antibodies, and parental candidates must be (re-) generated to fit the common light chain approach. Alternatively, to enforce the correct heavy-light chain pairing, some approaches introduced amino acid mutations at the contact points of VH/VL, CH1/CL or both (Igawa et al., 2010) (Lewis et al., 2014) (Bönisch et al., 2017); some approaches exchanged the VH-VL or the CH1-CL domains by domain crossover between the heavy and light chain Fab domains such as CrossMab (Schaefer et al., 2011), DuetMab (Mazor et al., 2015b) and orthogonal Fab (Lewis et al., 2014). Alternatively, the heavy-light chain mis-pairing can be circumvented by producing the BsAb out of two parental mAbs as demonstrated for the Duobody (DB) technology which makes use of controlled Fab-arm exchange (cFAE) methodology to achieve correct heavy-heavy chain heterodimerization (Labrijn et al., 2013).

Importantly, in addition to introducing enhanced immunogenicity risk the extensive protein engineering required for most of these approaches to improve physicochemical, biological characteristics and even affinity lead to the requirement for additional analytical and quality testing (Atwell et al., 1997) (Masuda et al., 2006) (Chailyan et al., 2011) (Herold et al., 2017).

In this study, we describe a novel format of BsAb, the Fab x sdAb-Fc, which combines a conventional antigen-binding fragment (Fab) with a single domain antibody (sdAb), both linked to Fc domains optimized for heavy-heavy chain heterodimerization. This novel format avoids the issue of heavy-light chain mis-pairing and can be used in combination with common heavy-heavy chain heterodimerization strategies. As a proof of concept, we generated BsAbs, in a mouse IgG2a format, specific for two tumour antigens,

mEGFR and mPSMA, using well established cFAE, CP and KIH heavy-heavy chain heterodimerization methods. Since the sdAb domain does not bind light chains, the expressed light chain region of the BsAb can only associate with its corresponding heavy chain. Our results show that the Fab x sdAb-Fc BsAb can be generated with high purity, and the products are stable by all quality testing applied suggesting that this novel BsAb format constitutes a convenient and promising technology for exploration of bispecific concepts in the potential treatment of cancer, autoimmune, inflammatory and other diseases.

2. Materials and methods

2.1. Design of vectors

The anti-mEGFR sdAb (RR359) has been described before (Zaiss et al., 2013) and the amino acid sequence of anti-mPSMA antibody (Sam103) was obtained from patent US20170342169A1. The sequence of isotype control antibodies was obtained from the protein data bank, which PDB IDs were 2NY7 (B12, anti-gp120) and 4B50 (2H10, antigp41), respectively. The amino acid mutations introduced to each antibody to allow heavy-heavy chain heterodimerization are depicted in Fig. 1 for the various heterodimerization technologies. In short, for the Duobody (DB) method using the controlled Fab arm exchange, T370K and K409R point mutations were introduced to the CH3 region of a heavy chain only antibodies, F405L and R411T point mutations were introduced to the CH3 region of the conventional antibodies. Parental mAb expression vectors were constructed by de novo synthesis (GeneArt). For the CP method, E356K and D399K point mutations were introduced to the CH3 region of the heavy chain only antibody, K392D and K409D point mutations were introduced to the CH3 region of the conventional antibody. For the KIH method, T366S, L368A and Y407V point mutations were introduced to the CH3 region of the heavy chain only antibody, T366W point mutation was introduced to the CH3 region of the conventional antibody. Between the sdAb and the Fc part of the heavy chain only antibody (HcAb), a camelid/mouse chimeric linker was introduced (EPKIPQPQPKPQPQPQPKPQPKPCPPCKCPAPNLLGG). The expression vectors of these antibodies were constructed by de novo synthesis (GeneArt). Amino acid sequences of all antibodies are given in Supplementary Table 1.

2.2. Expression and purification of BsAbs by knobs-into-holes and charge pairs

The FreeStyle™ 293-F cells (Invitrogen) were grown in FreeStyle 293 Expression medium, (Invitrogen). Each relevant vector (described in Supplementary Table 1) was co-transfected into FreeStyle™ 293-F cells using the 293fectin reagent (Invitrogen) according to the conditions recommended by the manufacturer. 7 days post-transfection, cell suspensions were collected and centrifuged for 15 min at 2500g. The supernatant was passed through a 0.22 µm filter and stored at 4 °C. The amount of BsAbs in the supernatant was measured by a Cedex bioanalyzer (Roche). The supernatant was then mixed with MabSelect SuRe LX resin (GE Lifesciences) and rotated overnight at 4 °C. After overnight capturing, the BsAbs were purified from the supernatant by affinity chromatography using Pierce™ Centrifuge Columns (ThermoFisher Scientific) and re-buffering to PBS using PD-10 Desalting Columns (GE healthcare) according to the manufacturer's instructions. Antibody concentration was calculated based on Beer-Lambert Law, $A = \epsilon * b * c$, (A is the A280 absorbance, b is the path length, c is the analyte concentration and ϵ is the wavelength-dependent molar absorptivity coefficient with units of $M^{-1} \text{ cm}^{-1}$). A280 absorbance of each antibody was measured by spectrophotometry using a Nanodrop ND-1000 system.

2.3. Generation of BsAbs by controlled fab-arm exchange

Parental antibodies were produced under serum-free conditions by co-transfecting relevant heavy and light chain expression vectors in FreeStyle™ 293-F cells, using 293fectin™ according to the manufacturer's instructions. Antibodies were purified by protein A affinity chromatography, dialyzed overnight to PBS, and filter-sterilized over 0.22 µm filters. Antibody concentration was calculated as previously described. The bispecific antibody was produced by controlled Fab-arm exchange using the two purified bivalent parental antibodies, each with the respective complementary mutations: T370K, K409R or F405L, R411T (specific to mouse IgG2a isotype) (Labrijn et al., 2017). Equimolar amounts of relevant parental antibodies were mixed and incubated with 2-Mercaptoethylamine (2-MEA; Sigma) at a final concentration of 2mg/mL total antibody in PBS, with the final concentration of 2-MEA being 75mM. The mixtures were incubated for 5h at 31°C. To remove 2-MEA, the mixtures were buffer-exchanged against PBS using Slide-A-Lyzer cassettes (ThermoFisher

Scientific). Samples were stored overnight at 4°C to allow for the re-oxidation of the disulfide bonds. Antibody concentration was calculated as previously described. Three Fab x sdAb-Fc bispecific control antibodies were designed 1) DB.gp120 x EGFR containing the EGFR monovalent single domain antibody combined with a non-relevant isotype arm (antibody B12, anti-HIV-gp120); 2) DB.PSMA x gp41 containing the PSMA monovalent antibody combined with a non-relevant isotype single domain antibody arm (antibody 2H10, anti-HIV-gp41); 3) Non-functional bispecific DB.gp120 x gp41 containing single-domain antibody arm gp41 combined with arm gp120. The three bispecific control antibodies were produced by cFAE.

2.4. High performance size-exclusion chromatography (HP-SEC)

Aggregation and degradation of BsAbs was quantified by HP-SEC using a YMC-pack Diol-200 column (YMC) with Agilent 1100 series HPLC system. Separation was carried out in 10 mM HEPES, pH 7.4, containing 150 mM NaCl, 3.4 mM EDTA and 0.05% Tween 20.

2.5. SDS-page

Formation of BsAbs was analyzed using SDS-PAGE analysis in reducing and non-reducing conditions. Samples were diluted to a final concentration of 0.5 mg/mL with respectively Laemmli Sample Buffer (Bio-Rad) for analysis in non-reducing conditions or Laemmli Sample Buffer containing 200 mM DTT for analysis in reducing conditions. Samples were heated at 99 °C for 5 min. 5 µg of antibody and 10ul Precision Plus Protein All Blue Standards (Bio-Rad) were loaded onto NuPAGE® 4–12% Bis-Tris Gel (Invitrogen). Electrophoresis was run in NuPAGE® MOPS SDS Running Buffer (Invitrogen) at 150 V for 90 min for the non-reduced samples and NuPAGE® MES SDS Running Buffer (Invitrogen) at 150 V for 60 min for the reduced samples. Gels were stained using Coomassie protein assay reagent (Thermo Scientific), destained with distilled water and scanned using ChemiDoc™ Touch Imaging System (Bio-Rad).

2.6. Capillary electrophoresis sodium dodecyl sulfate (CE-SDS)

The purity of all BsAbs were tested by CE-SDS in non-reduced mode. CE-SDS analysis was carried out on a CE system PA800 Plus machine (Beckman Coulter). Samples were diluted to 1 mg/mL with 10 kDa internal

standard and 15 mM iodoacetamide in SDS-MW sample buffer and heated to 70 °C for 10 min. 95 µL were transferred into sample vials and loaded into the machine. Separations were performed in a barafused silica 50 µm I.D capillary at 22 °C. Effective separation length was 20 cm, run time 30 min and antibody fragments detected at a wavelength of 220 nm. The capillary was flushed with 0.1 M HCl, NaOH, water and running buffer before sample loading at 5 kV for 20 s. Data analysis was carried out with the 32Karat software (version 9.2).

2.7. Capillary isoelectric focusing (cIEF)

cIEF was performed on a Beckman Coulter PA 800 Plus using an amine-coated (eCAP™), 50 µm ID × 30 cm capillary. An ampholyte mixture containing 2.5% (w/v) Pharmalyte pH 3–10, 0.2% (w/v) (hydroxypropyl) methyl cellulose, 0.3% (v/v) N,N,N',N'-tetramethylethylenediamine, and pI 10 marker was combined with antibody diluted in water to obtain a final antibody concentration of 0.3 mg/mL. Analysis was performed at 25 kV and 20 °C with a 15 min focusing period under normal polarity during which isoforms migrate to their pI in the pH gradient. This was followed by a 30 min mobilization step using the Bio-Rad chemical mobilizer with the UV detector set at 280 nm.

2.8. Generation of CHO-K1 stable cell line

The CHO-K1 cells (ATCC) were grown in Dulbecco's Modified Eagle Medium: Nutrient Mixture F-12 (DMEM/F12), supplemented with 5% New Born Calf Serum (Biowest). 24 µg of pCI-neo mEGFR (UniProtKB - Q01279) and pCI-neo mPSMA (UniProtKB - O35409) plasmids constructed by de novo synthesis (GeneArt) were transfected into 5×10^6 cells using lipofectamine 2000 reagent (Invitrogen) according to the conditions recommended by the manufacturer. Subsequently, transfected cells were cultured in complete cell culture medium (DMEM/F12 + 5% New Born Calf Serum) with addition of 0.8 mg/ml G418 for 14 days. Selected cells were then stained by rabbit anti-mEGFR-PE (Cell Signalling Technology) or anti-mPSMA antibodies (Sam103), respectively. Positive stained cells were seeded into 96-well plate for clone formation by single cell sorting on a FACSMelody (BD). The clones CHO/mPSMA-HA(A6) and CHO/mEGFR-LA(A1) stably expressed mPSMA or mEGFR, respectively, for more than 2 months and were further used for the present study.

2.9. Cell binding assays

CHO/mEGFR and CHO/mPSMA cells were detached and washed 3 times with FACS buffer (PBS + 1% BSA + 1 mM EDTA). For CHO/mEGFR binding assay, BsAb DB.PSMA x EGFR, BsAb DB.gp120 x gp41 and EGFR HcAb were added in 5-fold serial dilution in FACS buffer, incubated on ice for 45 min. For CHO/mPSMA binding assay, BsAb DB.PSMA x EGFR, BsAb DB.gp120 x gp41 and PSMA mAb were added in 5-fold serial dilution in FACS buffer, incubated on ice for 45 min. Secondary antibody staining was performed using rat-anti-mouse IgG2a antibody conjugated with FITC (Biolegend) in 1:500 dilution in FACS buffer on ice for 45 min. Samples were analysed by FACS Canto™ II (BD) using the software program BD FACSDiva. Ten thousand events were collected. Flow cytometry was used to determine the simultaneous binding activity of BsAb DB.PSMA x EGFR to mEGFR and mPSMA using stable transfected cell lines (CHO/mPSMA and CHO/mEGFR). In order to prepare single-cell suspension, cells were detached from flasks using cell dissociation buffer enzyme-free, PBS-based (Gibco). Cells were washed twice with PBS and CHO/mPSMA and CHO/mEGFR cells were labelled by cell staining dye eFluor 450 or 670 (eBioscience), respectively, according to the conditions recommended by the manufacturer. 5×10^4 cells of cell staining dye eFluor 450 or 670 labelled cell line were mixed in 100 μ l FACS buffer (PBS + 1%BSA + 1 mM EDTA) and cells were incubated with bispecific control antibodies (50 μ g/ml, equivalent to 390.63 nM) or 5-fold serial dilution of BD.PSMA x EGFR (0.0032 μ g/ml to 50 μ g/ml, equivalent to 0.005 nM to 390.63 nM) at 4 °C for 45 mins. The stained cells were analysed on a FACS Canto™ II (BD) using the software program BD FACSDiva. Ten thousand events were counted. While the FACS Canto™ II counted every singlet and each cluster as one event, it was unclear from this analysis whether cellular clusters were formed by two cells(doublets), three cells (triplets) or even more, therefore the term “percentage of cellular cluster events” was used to quantify our results.

2.10. Octet

mEGFR-His recombinant protein (R&D systems) was diluted to 50 mM in 10 mM acetate pH 5.0 (ForteBio) and loaded on NHS/EDC activated AR2G biosensors (ForteBio). BsAb DB.PSMA x EGFR and bispecific control antibodies were diluted to 20 μ g/mL in 10 \times kinetic buffer (ForteBio) and associated to mEGFR-His protein. mPSMA-His recombinant protein (Sino Biologicals) was diluted to 50 mM in 10 \times kinetic buffer and associated to

each BsAb. Binding kinetics were measured by Octet system according to the manufacturer's instructions (ForteBio). Data was analysed using Data analysis software HT V10.0 (ForteBio).

3. Results

3.1. Design and expression of BsAbs

To test whether Fab x sdAb-Fc format BsAbs, which combine a conventional antigen-binding fragment (Fab) with a single domain antibody (sdAb) and a mouse IgG2a Fc, can be produced efficiently, we generated Fab x sdAb-Fc BsAbs, using three well-known heavy chain heterodimerization strategies, i.e., cFAE, CP, or KIH, respectively. For the cFAE strategy, parental monospecific bivalent antibodies (T370K and K409R for anti-EGFR antibody RR359; F405L and R411T for anti-PSMA antibody Sam103) were first expressed separately. The BsAb duobody DB.PSMA x EGFR was produced in a second step by cFAE from the purified bivalent parental antibodies (Fig. 1A). In case of the CP and KIH strategies, the CP mutations (K392D and K409D for CH3 domain of anti-PSMA antibody, E356K and D399K for CH3 domain of anti-EGFR antibody) and KIH mutations (T366W for CH3 domain of anti-PSMA antibody, T366S, L368A and Y407V for CH3 domain of anti-EGFR antibody) were introduced into the corresponding expression vectors, respectively. Relevant heavy chain and light chain expression vectors CP mutations or KIH mutations were co-transfected into FreeStyle™ 293-F cells, respectively. The BsAbs CP.PSMA x EGFR and KIH.PSMA x EGFR were expressed and purified as described in method 2.2 (Fig. 1BC). The anti-gp120 (HIV) Fab arm and anti-gp41 (HIV) sdAb were used to generate bispecific control antibodies by cFAE (Burton et al., 1994) (Hulsik et al., 2013) (Fig. 1D).

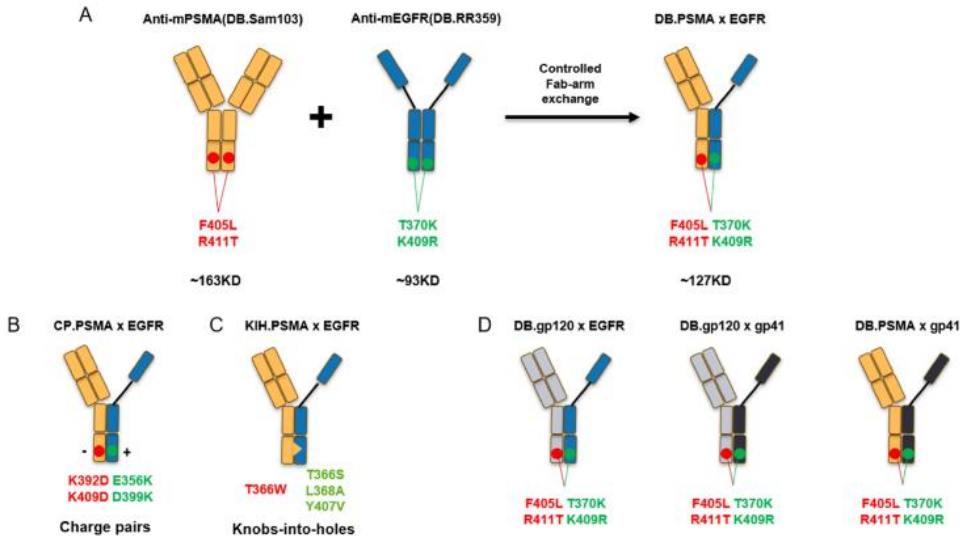


Fig. 1. Schematic diagram of mouse IgG2a-based Fab x sdAb-Fc BsAbs generated by using (A) controlled Fab-arm exchange (cFAE), (B) charge-pairs (CP) and (C) knobs-into-holes (KIH); (D) Design of bispecific control antibodies using the cFAE method.

3.2. Purity evaluation of BsAbs

In order to determine the purity of Fab x sdAb-Fc format BsAbs, we performed Capillary Electrophoresis Sodium Dodecyl Sulfate (CE-SDS) analysis. Under non-reducing conditions, the BsAbs generated by cFAE, CP and KIH showed clear separation from parental antibodies with a 95.9%, 94.6% and 88.9% purity for DB.PSMA x EGFR, CP.PSMA x EGFR or KIH.PSMA x EGFR, respectively. (Fig. 2A-C). The purity of three bispecific control antibodies DB.PSMA x gp41, DB.gp120 x EGFR, and DB.gp120 x gp41 was also evaluated by CE-SDS showing 94.8%, 94.2%, and 94.5% purity, respectively (data not shown). These data demonstrate that Fab x sdAb-Fc format BsAbs can be generated efficiently, and with high quality, using various heavy chain heterodimerization strategies. The BsAb KIH.PSMA x EGFR, which was produced with a relative low purity (88.9%), was produced by KIH using mutations T366W in the “knob” heavy chain and T366S, L368A, Y407V in the “hole” heavy chain (Fig. 1C). By introducing two additional mutations (S354C in the “knob” heavy chain and Y349C in the “hole” heavy chain) such a construct is expected to further increase the efficiency of heterodimerization and thus improve the purity of this BsAb construct (Merchant et al., 1998). Other than hydrophobic interaction

chromatography (HIC), Cation exchange chromatography (CIEX), Liquid chromatography–mass spectrometry (LC-MS), and CE-SDS, SDS-PAGE is a convenient and low demand in equipment method to assess the successful formation and estimate the purity of the Fab x sdAb-Fc BsAb format. Thus, SDS-PAGE analysis of each purified BsAb was performed. Under non-reducing conditions, the desired BsAbs are expected to show a predominant band with a MW of ~127 kDa, whereas parental antibodies should show predominant bands with a MW of ~93 kDa or ~ 163 kDa, respectively (Fig. 2D). For BsAb CP.PSMA x EGFR and BsAb KIH.PSMA x EGFR, additional minor bands were detected at a size of ~160 kDa, which indicated a minor contamination of the parental PSMA mAb in this batch. Under reducing conditions, one band for EGFR HcAb, two bands for PSMA mAb and three bands for BsAbs were detected, as expected (Fig. 2E). The bands at ~50 kDa detected in BsAbs and PSMA mAb represent the heavy chain of the PSMA mAb, while the MW bands at ~46 kDa detected in EGFR HcAb and BsAbs represent the heavy chain of the EGFR HcAb. The bands at ~25 kDa detected in BsAbs and PSMA mAb represent the light chain of the PSMA mAb. Taken together, these data indicate that BsAbs can be efficiently generated with high purity. Additionally, due to the MW difference between BsAbs and parental antibodies, this format of BsAb can be readily further purified from undesired by-products based on MW by preparative Size Exclusion Chromatography.

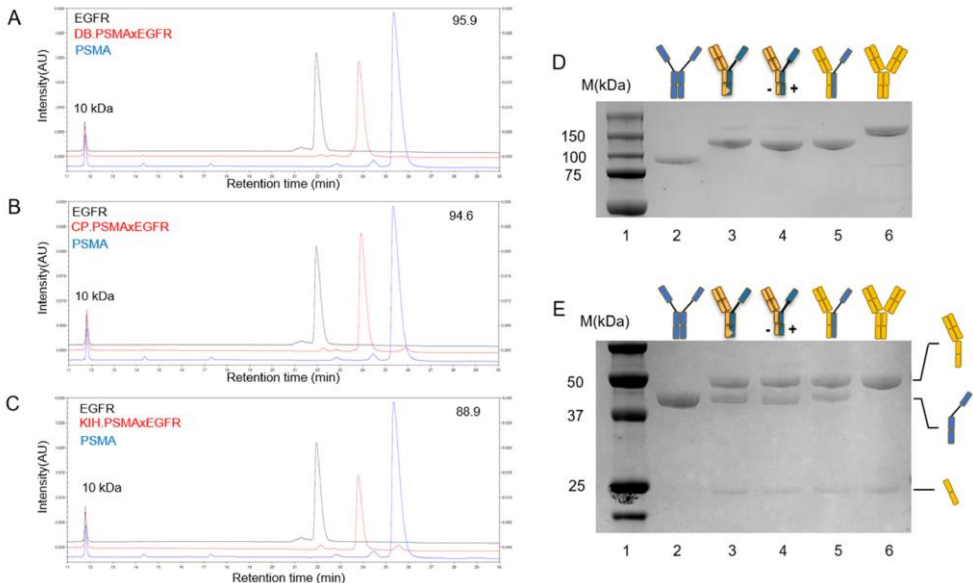


Fig. 2. CE-SDS and SDS-PAGE analysis for the various Fab x sdAb-Fc

BsAb formats. (A-C) Purity of (A) DB.PSMA x EGFR, (B) CP.PSMA x EGFR and (C) KIH.PSMA x EGFR evaluated by CE-SDS. 10 kDa standard marker was used for the calibration of retention time for each trace. Numbers represent percentage of BsAb product (middle red peaks). The peaks of parental antibody were shown in black (EGFR) or blue (PSMA) respectively; (D-E) Detection and separation of BsAbs and parental antibodies by coomassie blue staining of SDS-PAGE under (D) non-reducing or (E) reducing condition. Lane 1, MW ladder; lane 2, EGFR HcAb; lane 3, KIH.PSMA x EGFR; lane 4, CV.PSMA x EGFR; lane 5, DB.PSMA x EGFR; lane 6, PSMA mAb. (For interpretation of the references to colour in this figure legend, the reader is referred to the web version of this article.)

3.3. Monomericity evaluation of BsAbs

To further analyse the aggregation and degradation level of BsAbs in our purified batches, we performed analytical Size Exclusion Chromatography (HP-SEC). After HP-SEC gel filtration, a predominant peak with an area of 99% for BsAb DB.PSMA x EGFR, 98.5% for BsAb CP.PSMA x EGFR and 98.4% for BsAb KIH.PSMA x EGFR was detected (Supplementary Fig. 1). The aggregation and degradation level of three bispecific control antibodies DB.PSMA x gp41, DB.gp120 x EGFR, and DB.gp120 x gp41 were also evaluated by HP-SEC which showed 98.8%, 98.8%, and 99% monomericity, respectively (data not shown).

3.4. BsAbs analysis for isoelectric point

Generated BsAbs and parental antibodies were further analysed by Capillary Isoelectric Focusing cIEF (Fig. 3). The BsAbs and parental antibodies showed clearly different isoelectric points (pI). We observed that the peaks of BsAbs were not detected precisely in the middle of the peaks of two parental antibodies but were closer to the Sam103 peaks. The peak pattern in this novel BsAb format can be explained by the different mass contribution of each parental antibodies (~163 kDa versus ~93 kDa).

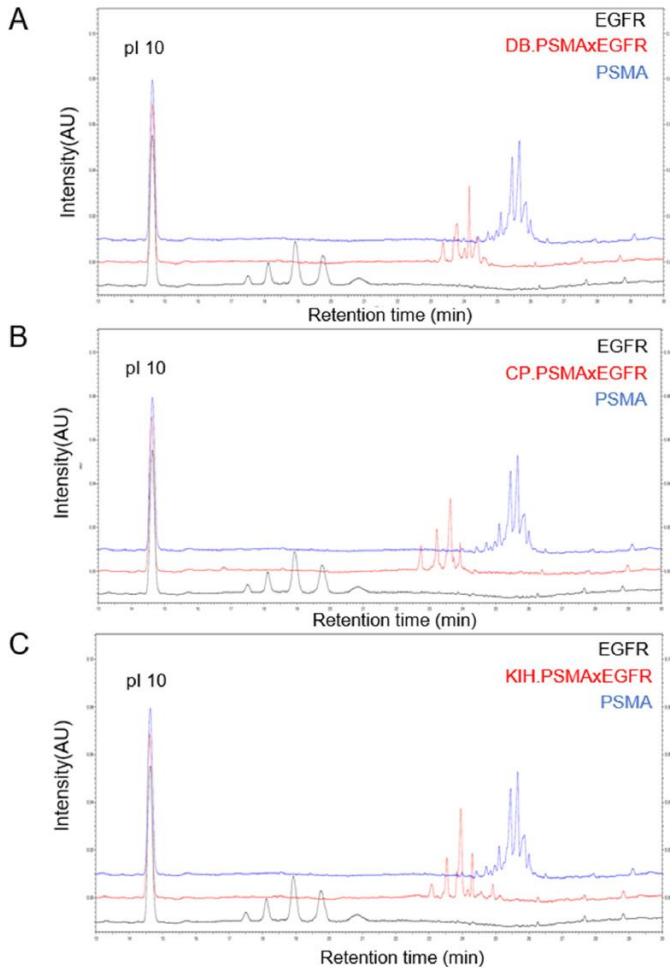


Fig. 3. cIEF analysis for the Fab x sdAb-Fc BsAbs. (A) DB.PSMA x EGFR, (B) CP.PSMA x EGFR (C) KIH.PSMA x EGFR and parental antibodies. A gel filtration standard (protein pI 10) was included for the calibration of retention time for each trace. The BsAbs are shown in red (middle line in each diagram). The parental antibodies are shown in blue for anti-PSMA mAb (top line in each diagram) and black for anti-EGFR HcAb (bottom line in each diagram), respectively. (For interpretation of the references to colour in this figure legend, the reader is referred to the web version of this article.)

3.5. Binding activity of BsAbs

To test the binding activity of each arm of the BsAbs, stably transfected CHO/mEGFR and CHO/mPSMA were generated and used for binding assays. Binding activity of BsAb DB.PSMA x EGFR and parental antibodies

specific for mEGFR or mPSMA were determined by flow cytometry, using unlabelled primary antibodies followed by FITC-labelled secondary antibody for detection. BsAb DB.PSMA x EGFR showed dose-dependent binding to both antigens. Monovalent binding activity of BsAb DB.PSMA x EGFR to CHO/mEGFR cells showed relative similar potency to bivalent binding by EGFR HcAb (EC₅₀ 0.87 nM versus 0.28 nM) (Fig. 4A-B). For mPSMA binding, BsAb DB.PSMA x EGFR showed strong reduction in binding to CHO/mPSMA compared to the parental bivalent PSMA mAb (EC₅₀ 219 nM versus 0.32 nM) (Fig. 4C-D). These data demonstrate that each antibody retained its specificity within the bi-specific construct. In addition, and in contrast to the EGFR specific sdAb RR359, the Sam103 PSMA antibody depends on avidity for high affinity binding to its target. Remarkably, a qualitative examination of the binding curves revealed a differential staining plateau for the two EGFR-specific antibody constructs. At a saturated concentration, BsAb DB.PSMA x EGFR binding to CHO/mEGFR cells plateaued at an MFI of ~1250, which was approximately 2 times as high as the plateau value for EGFR HcAb, which had an MFI of ~750 (Fig. 4A). The differences between MFI plateau reached by each antibody construct might be due to the difference between monovalent and bivalent binding, to be definitively confirmed using monovalent parental controls. In case of monovalent binding, one Ab construct binds one receptor. However, in case of bivalent binding one Ab construct is capable of binding two receptors resulting in a lower absolute amount of cell bound antibody. Correspondingly, in this experimental set-up, the higher staining plateau for BsAb compared to HcAb is likely the result of pure monovalent binding by the BsAb versus substantial bivalent binding for HcAb. Combined, these data demonstrate that each arm of BsAb DB.PSMA x EGFR maintained the binding activity to its corresponding antigen.

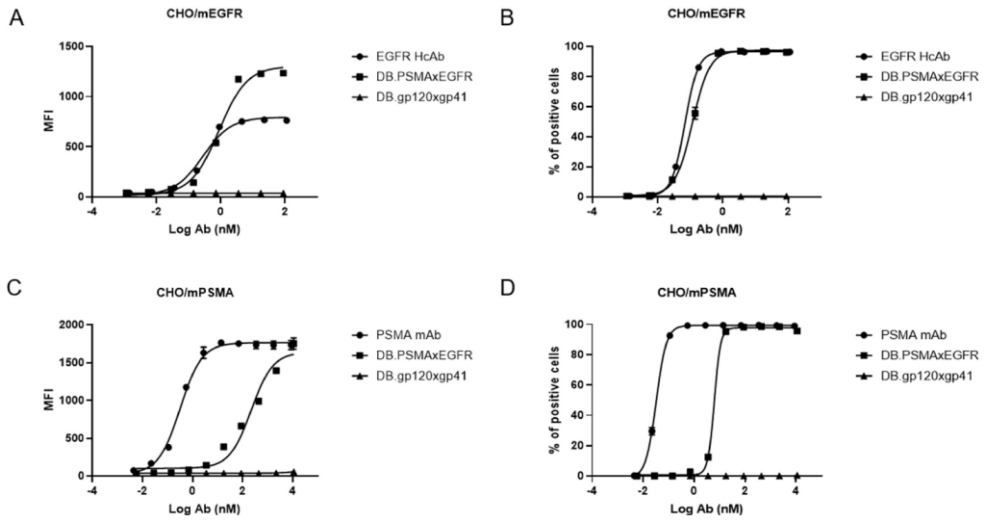


Fig. 4. Flow cytometry analysis of BsAbs and parental antibodies binding on CHO/mEGFR or CHO/mPSMA cells in a dose-dependent fashion. (A-B) CHO/mEGFR cells stained by parental anti-EGFR HcAb, DB.PSMA x EGFR or control antibody DB.gp120 x gp41 respectively. (C-D) CHO/mPSMA cells stained by parental anti-PSMA mAb, DB.PSMA x EGFR or control antibody DB.gp120 x gp41 respectively. Each data point is the mean \pm SD of triplicates.

3.6. Simultaneous binding of BsAb

To determine whether our bi-specific constructs retained their capacity to bind to both antigens simultaneously, we performed bio-layer interferometry (BLI), using an Octet machine, and physical cell-bridging experiments, using FACS analysis. The binding characteristics of the BsAb DB.PSMA x EGFR and three bispecific control antibodies to recombinant mEGFR-His and mPSMA-His were analysed using Octet. In short, mEGFR recombinant protein was loaded on the biosensor, followed by incubation of the various BsAbs to allow mEGFR specific binding. Thereafter, the biosensors were incubated with mPSMA recombinant protein to assess binding of mPSMA to the mEGFR-BsAb complex. As shown in Fig. 5, BsAb DB.PSMA x EGFR was able to bind both antigens, recombinant mEGFR and mPSMA, at the same time. Bispecific control DB.gp120 x EGFR showed only binding to mEGFR, while bispecific control DB.PSMA x gp41 showed no binding activity towards the mEGFR loaded biosensor (Fig. 5 and Supplementary Fig. 2).

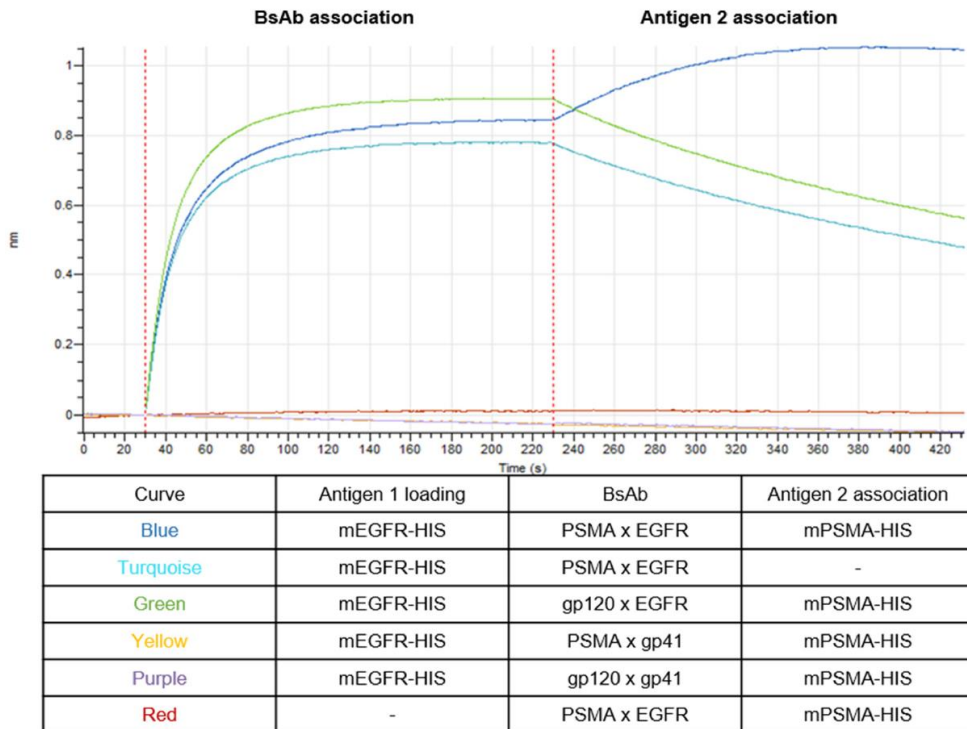


Fig. 5. BLI analysis of BsAb DB.PSMA x EGFR and BsAb controls for simultaneous binding to recombinant mEGFR and recombinant mPSMA. The BsAb association to mEGFR loaded biosensors is displayed, followed by the association of mPSMA to the BsAb-EGFR complex for the various BsAb antibodies as indicated in the table.

In addition, a cell bridging experiment was designed to test the ability of BsAb DB.PSMA x EGFR and three bispecific control antibodies to simultaneously bind to CHO/mEGFR and CHO/mPSMA cells. CHO/mEGFR and CHO/mPSMA cells were stained with two different cell staining dyes, subsequently mixed together at a 1:1 ratio, and incubated with BsAb (DB.PSMA x EGFR) or control antibodies. Flow cytometry results showed that only BsAb DB.PSMA x EGFR could serve as a bridge binding CHO/mEGFR and CHO/mPSMA cells together to form cell clusters in a dose dependent fashion leveling out at ~30% cell clusters (Fig. 6). Although we quantified ~30% cellular cluster events, the number of clustered cells is likely higher than 30% of total cells counted because the flow cytometry set up did not enable distinguishing between doublets, triplets, or higher order cell clusters. Clustering by BsAb is reported to be a direct function of absolute

number of target antigens expressed on each cell (Lopez-Albaitero et al., 2017; Oberst et al., 2014; Laszlo et al., 2014) and although we detected ~20,000 target molecules on average for mPSMA and mEGFR on the respective transfected clones (data not shown), a significant number of either clonal population would display a number of antigens below the clustering threshold. Moreover, stability of clustering is also determined by fluid shear force leading to disruption of weakly formed clusters before they pass the detector. Hence, a maximum of 100% cell clusters was not expected.

Combined, these data show that the BsAb DB.PSMA x EGFR is capable to simultaneously bind to its two antigens.

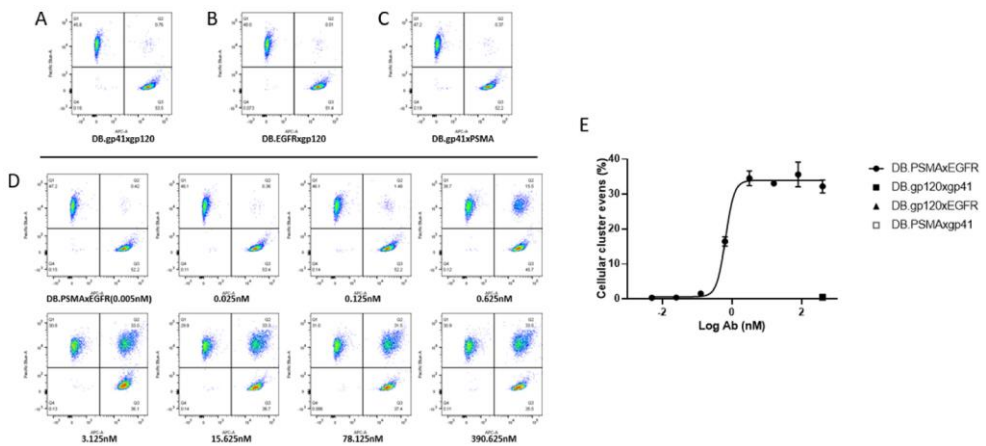


Fig. 6. Flow cytometry analysis of BsAbs inducing cellular clustering by simultaneous binding to CHO/mEGFR and CHO/mPSMA cells. (A-C) 1:1 mixed CHO/mEGFR and CHO/mPSMA cells incubated with 390.63 nM bispecific control antibodies; (D) 1:1 mixed CHO/mEGFR and CHO/mPSMA cells incubated with increasing concentration of DB.PSMA x EGFR. (E) Quantification of flow cytometry results by displaying the percentage of events that represents cellular clusters. Means \pm SD of a representative experiment ($n = 3$) performed in triplicates are shown.

4. Discussion

Although the concept of BsAb has been used for a very long time, the production and purification steps during BsAb development remain one of the major challenges for their application to research and clinical development. Specifically, heavy-light chain mis-pairing has remained one

of the major challenges to obtain pure BsAb. Approaches using a common light chain, present a challenge when making use of already pre-existing and validated antibodies (Merchant et al., 1998). Furthermore, approaches which introduce mutations at the contact points of VH/VL or CH1/CL sometimes compromise the stability of the BsAb (Atwell et al., 1997); while approaches that exchange the VH-VL or the CH1-CL domains by domain crossover between the heavy and light chain Fab domains can even damage antigen binding ability (Masuda et al., 2006) (Chailyan et al., 2011) (Herold et al., 2017). All these approaches require additional protein engineering and redetermination of the physicochemical and biological characteristics of engineered BsAb, making a standard mass production of novel bi-specific antibodies challenging.

In the present study, we describe a novel approach to overcome heavy-light chain mis-pairing, by establishing the Fab x sdAb-Fc format of BsAb composed of a conventional antigen-binding fragment (Fab), a single domain antibody (sdAb) and a mouse IgG2a Fc. We demonstrated that the Fab x sdAb-Fc BsAb format can functionally be expressed and assembled in a single FreeStyle™ 293-F host, using KI and CP dimerization strategies, or formed artificially by cFAE; reaching high purity and retaining their capacity to bind both their target antigens simultaneously.

This format of BsAb also provides additional advantages for further purification. As previously described, the Fab x sdAb-Fc format BsAbs showed ~35 kDa MW difference from each parental antibody which is sufficient for further separation based on size exclusion chromatography (SEC). Affinity chromatography might be another consideration to further purify this format of BsAb. Affinity chromatography is a type of chromatographic method used for purifying biological molecules within a mixture based on highly specific biological interactions between two molecules, for instance, interactions between antibody and antigen (Urh et al., 2009). Next, for the Fab x sdAb-Fc format, CH1 selective chromatography can help to remove HcAbs. An IgG CH1 domain specific antibody could be conjugated to a resin to capture BsAb and the parental antibody with CH1 domain, while HcAb cannot bind, in this way further improving the purity of BsAb.

In the present study, the hinge between the sdAb and Fc was designed to mimic the length of an entire CH1 domain, thus extending the length of the sdAb arm similar to that of conventional Fab. However, the hinge of the HcAb can be designed various for different applications. T cell-

redirecting BsAbs with Fc might benefit from a short hinge design. The distance between tumour cells and effector T cells has been demonstrated essential for T cell mediated tumour cell killing (Bluemel et al., 2010). A shorter distance between two arms can redirect T cells closer to tumour cells which might lead to better tumour cell elimination. For targeting of tumour associated antigens the hinge of Fab x sdAb-Fc BsAb can be optimized based on the distribution, density and extracellular size of antigens with special attention to the distance between two antigens expressed on the tumour cell surface. Nevertheless, how different hinges affect the functionality, stability and flexibility of this format of BsAb still needs to be investigated further.

Taken together, we describe here a novel approach of constructing bi-specific antibodies, which has a number of different advantages over traditional approaches. It is foreseeable that the potential applications for this format will only grow as the field of BsAb application in academic and clinical settings continues to evolve.

Declaration of Competing Interest

None.

Acknowledgments

We are grateful to Salim Harraou and Thomas Guyomard (Aduro Biotech Europe) for their technical assistance. This work was supported by the European Union, Horizon 2020 research and innovation programme under the Marie Skłodowska-Curie Innovative Training Networks [grant number 765394, 2018].

Appendix A. Supplementary data

Supplementary data to this article can be found online at <https://doi.org/10.1016/j.jim.2020.112811>.

Abbreviations

ADCC, Antibody-dependent cell-mediated cytotoxicity; ADCP, Antibody-dependent cellular phagocytosis; BsAb, Bispecific antibody; CDC, Complement-dependent cytotoxicity; CE-SDS, Capillary electrophoresis sodium dodecyl sulfate; cFAE, controlled Fab-arm exchange; cIEF, Capillary isoelectric focusing; CIEX, Cation exchange chromatography; CP, Charge-pairs; DB, Duobody; Fab, Antigen binding fragment; Fc, Fragment crystallizable; HcAb, heavy chain only antibody; HIC, hydrophobic

Chapter 3

interaction chromatography; HP-SEC, High performance size-exclusion chromatography; IgG, Immunoglobulin G; KIH, Knobs-into-holes; LC-MS, Liquid chromatography–mass spectrometry; mAbs, monoclonal antibodies; MW, molecular weight; pI, isoelectric point; sdAb, Single domain antibody.

Supplementary

Supplementary Table 1.

DB.RR359(anti-mEGFR).mi2a.T370K.K409R
MAVLGLLFCLVTFPSCVLSQVQLQESGGGLVQAGGSLRLSCAASGRT FTSYAMGWFRQVPGKEREFVAALSTRSAGNTYYADSVKGRFTISRDN AKNTVYLMQSSLKAEDTAVYYCAAGYMSSDADPSLAASLHPYDYWG QGTQVTVSSEPKIPQPKPQPKPQPKPQPKPQPKPCPPCKCPAPNLLG GPSVFIFPPKIKDVLMISSLSPMVTCTVVDVSEDDPDVQISWVFNVEVL TAQTQTHREDYNSTLRVVSALPIQHQDWMSGKEFKCKVNNKALPAPIE RTISKPKGSVRAPQVYVLPPEEEMTKKQVTLTCMVKDFMPEDIYVEW TNGKTELNYKNTEPVLDSGYSYFMYRSLRVEKKNWVERNSYSCSVV HEGLHNHHTTKSFSRTPGK
DB.SAM103(anti-mPSMA).mi2a.F405L.R411T (heavy chain)
EVKLVSEGGGLVQPGSSMKLSCTASGFTFSDYYMAWVRQVPEKGLE WVANINYDGTTTYLDLTKSRFIISRDNSKNILYLMQSSLKSEDTATYYC ARVLDGYYGYFDYWGQGTTLVSSAKTTAPSVYPLAPVCGDGTGSSV TLGCLVKGYFPEPVTLTWNSGSLSSGVHTFPAVLQSDLYTLSSSVTVT SSTWPSQSITCNVAHPASSTKVDKIEPRGPTIKPCPPCKCPAPNLLG GPSVFIFPPKIKDVLMISSLSPMVTCTVVDVSEDDPDVQISWVFNVEVL TAQTQTHREDYNSTLRVVSALPIQHQDWMSGKEFKCKVNNKALPAPIE RTISKPKGSVRAPQVYVLPPEEEMTKKQVTLTCMVDFMPEDIYVEW TNGKTELNYKNTEPVLDSGYSYLMYSKLTVEKKNWVERNSYSCSVV HEGLHNHHTTKSFSRTPGK
DB.SAM103(anti-mPSMA)(light chain)
QIVLTQSPAIMASAPGEKVTISCSASSSVSYMYWYQQKPGSSPKPWYI RTYNLASGVPARFSGSGSGTSYSLTISSEMEADAATYYCQQSHTYPPT FGGGTKLEIKRADAAPTVSIFPPSSEQLTSGGASVVCFLNFPKIDINV KWKIDGSRQNGVLNSWTDQDSKDYSTYSMSSTLTLTKDEYERHNSYT CEATHKTSTSPIVKSFNRNEC
KiH.RR359(anti-mEGFR).mi2a.T366S.L368A.Y407V
MAVLGLLFCLVTFPSCVLSQVQLQESGGGLVQAGGSLRLSCAASGRT FTSYAMGWFRQVPGKEREFVAALSTRSAGNTYYADSVKGRFTISRDN AKNTVYLMQSSLKAEDTAVYYCAAGYMSSDADPSLAASLHPYDYWG QGTQVTVSSEPKIPQPKPQPKPQPKPQPKPQPKPCPPCKCPAPNLLG GPSVFIFPPKIKDVLMISSLSPMVTCTVVDVSEDDPDVQISWVFNVEVL TAQTQTHREDYNSTLRVVSALPIQHQDWMSGKEFKCKVNNKALPAPIE RTISKPKGSVRAPQVYVLPPEEEMTKKQVTLSCAVTDFMPEDIYVEW TNGKTELNYKNTEPVLDSGYSYFMVSKLRVEKKNWVERNSYSCSVV HEGLHNHHTTKSFSRTPGK
KiH.SAM103(anti-mPSMA).mi2a.T366W
MAVLGLLFCLVTFPSCVLSEVKLVSEGGGLVQPGSSMKLSCTASGFTF SDYYMAWVRQVPEKGLEWVANINYDGTTTYLDLTKSRFIISRDNSKN

ILYLQMSSLKSEDTATYYCARVLDGYYGYFDYWGGTTLVSSAKTTA
 PSVYPLAPVCGDTTGSSVTLGCLVKGYFPEPVTLTWNSGSLSSGVHT
 FPAVLQSDLYTLSSSVTVTSSTWPSQSITCNVAHPASSTKVDKIEPRG
 PTIKPCPPCKCPAPNLLGGPSVFIFPPKIKDVLMLISLSPMVTVCVVVDVSE
 DDPDVQISWVFNVEVLTAQTQTHREDYNSTLRVVSALPIQHQDWMS
 GKEFKCKVNNKALPAPIERTISKPKGSVRAPQVYVLPPEEEMTKKQV
 TLWCMVTDMPEDIYVEWTNNGKTELNYKNTEPVLDSGYSYFMYSKL
 RVEKKNWVERNSYSCSVVHEGLHNHHTTKSFSRTPGK

CP.RR359(anti-mEGFR).mi2a.E356K.D399K

MAVLGLLFCLVTFPSCVLSQVQLQESGGGLVQAGGSLRLSCAASGRT
 FTSYAMGWFRQVPGKEREFVAALSTRSAGNTYYADSVKGRFTISRDN
 AKNTVYLQMSSLKAEDTAVYYCAAGYMSSDADPSLAASLHPYDYWG
 QGTQVTVSSEPKIPQPQPQPQPQPQPQPQPQPQPCKCPAPNLLG
 GPSVFIFPPKIKDVLMLISLSPMVTVCVVVDVSEDDPDVQISWVFNVEVL
 TAQTQTHREDYNSTLRVVSALPIQHQDWMSGKEFKCKVNNKALPAPIE
 RTISKPKGSVRAPQVYVLPPEKEMTKKQVTLTCMVTDMPEDIYVEW
 TNNGKTELNYKNTEPVLKSDGYSYFMYSKLRVEKKNWVERNSYSCSVV
 HEGLHNHHTTKSFSRTPGK

CP.SAM103(anti-mPSMA).mi2a.K392D.K409D

MAVLGLLFCLVTFPSCVLSQVQLVQSGAEGGLVQPGSSMKLSCTASGFTF
 SDYYMAWVRQVPEKGLEWVANINYDGTTTYLDLSKSRFIISRDN
 ILYLQMSSLKSEDTATYYCARVLDGYYGYFDYWGGTTLVSSAKTTA
 PSVYPLAPVCGDTTGSSVTLGCLVKGYFPEPVTLTWNSGSLSSGVHT
 FPAVLQSDLYTLSSSVTVTSSTWPSQSITCNVAHPASSTKVDKIEPRG
 PTIKPCPPCKCPAPNLLGGPSVFIFPPKIKDVLMLISLSPMVTVCVVVDVSE
 DDPDVQISWVFNVEVLTAQTQTHREDYNSTLRVVSALPIQHQDWMS
 GKEFKCKVNNKALPAPIERTISKPKGSVRAPQVYVLPPEEEMTKKQV
 TLTCMVTDMPEDIYVEWTNNGKTELNYDNTEPVLDSGYSYFMYSDL
 RVEKKNWVERNSYSCSVVHEGLHNHHTTKSFSRTPGK

DB.B12(anti-HIV-gp120).mi2a.F405L.R411T (heavy chain)

MAVLGLLFCLVTFPSCVLSQVQLVQSGAEVKKPGASVKVSCQASGYR
 FSNFVIHWVRQAPGQRFQFEWMGWINPYNGNKEFSQAKFQDRVTFTADT
 SANTAYMELRSLRSADTAVYYCARVGPYSWDDSPQDNYYMDVWGK
 GTTVIVSSAKTTAPSVYPLAPVCGDTTGSSVTLGCLVKGYFPEPVTLT
 WNSGSLSSGVHTFPAVLQSDLYTLSSSVTVTSSTWPSQSITCNVAHPA
 SSTKVDKIEPRGPTIKPCPPCKCPAPNLLGGPSVFIFPPKIKDVLMLISL
 SPMVTVCVVVDVSEDDPDVQISWVFNVEVLTAQTQTHREDYNSTLRV
 VSALPIQHQDWMSGKEFKCKVNNKALPAPIERTISKPKGSVRAPQVYV
 LPPPEEEMTKKQVTLTCMVTDMPEDIYVEWTNNGKTELNYKNTEPVL
 DSDGYSYFMYSKLTVKKNWVERNSYSCSVVHEGLHNHHTTKSFSRTP
 GK

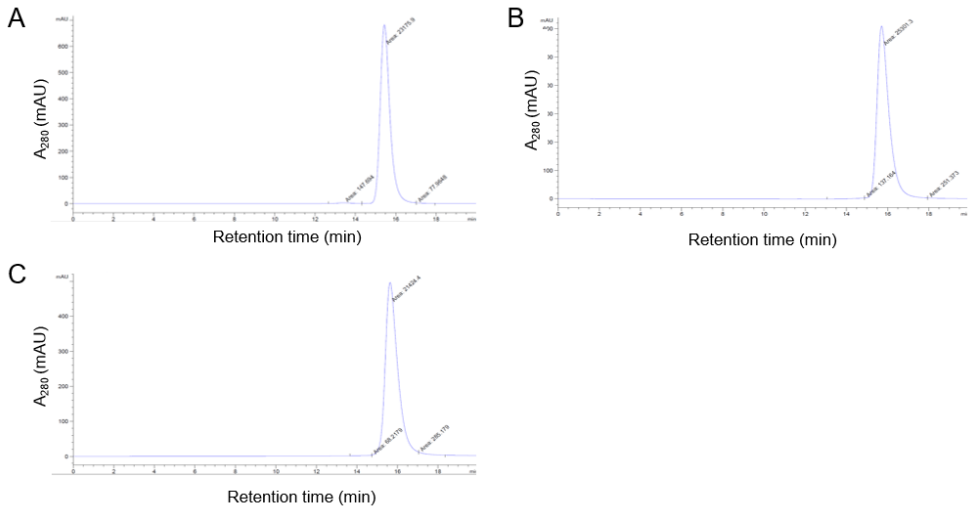
DB.B12(anti-HIV-gp120)(light chain)

EIVLTQSPGTLSLSPGERATFSCRSSHSIRSRVAVYQHKGQAPRLV
 IHGVSNRASGISDRFSGSGSGTDFTLTITRVEPEDFALYYCQVYGASSY

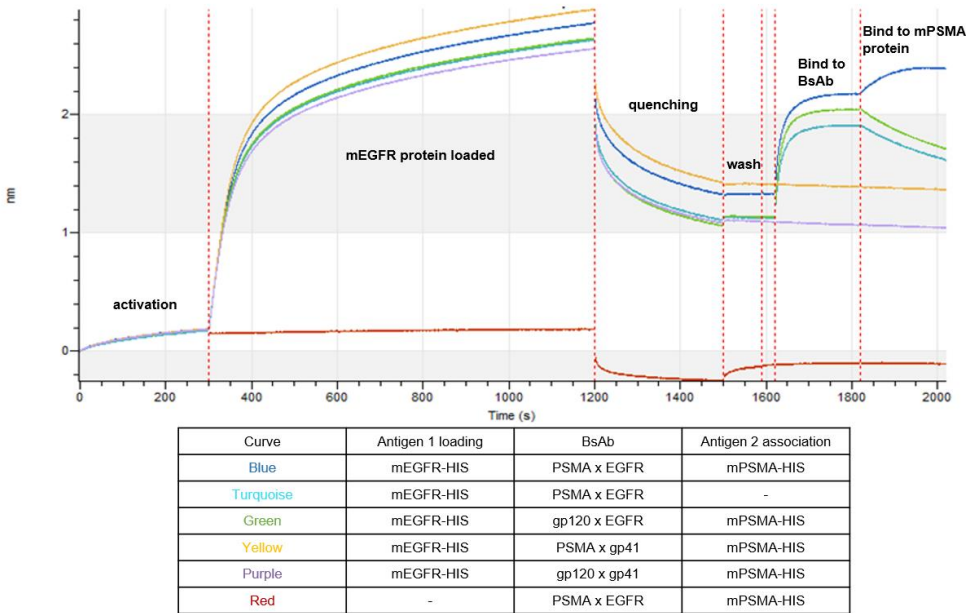
TFGQGTKLERKRADAAPTVSIFPPSSEQLTSGGASVVCFLNNFYPKDI
NVKWKIDGSERQNGVLNSWTDQDSKDSTYSMSSTLTLTKDEYERHNS
YTCEATHKTSTSPIVKSFNRNEC

DB.2H10(anti-gp41).mi2a.T370K.K409R

MAVLGLLFCLVTFPSCVLSEVQLVESGGGLVQPGGSLRLSCAASGSIS
SVDVMSWYRQAPGKQRELVAFITDRGRTNYKVSVKGRFTISRDN SKN
MVY LQMNSLKPEDTADYLCRAESRTSWSSPSPLDVWGRGTQVTVSS
EPKIPQPQPKPQPQPQPQPQPKPQKPCPPCKCPAPNLLGGPSVFIFPPK
IKDVLMI SLSPMVT CVVVDVSEDDPDVQISWVFN NVEVLTAQTQTHRE
DYNSTLRVVSALPIQH QDWMSGKEFKCKVNNKALPAPIERTISKPKGS
VRAPQVYVLPPEEEMTKKQVTLTCMVKDFMPEDIYVEWTNNGKTEL
NYKNTEPVLDS DGSYFMYSRLRVEKKNWVERNSYSCSVVHEGLHNH
HTTKSFSRTPGK



Supplementary Fig 1. SEC-HPLC profiles of (A) DB.PSMA x EGFR, (B) CP.PSMA x EGFR and (C) KIH.PSMA x EGFR.



Supplementary Fig 2. Raw data binding kinetics of BsAbs to AR2G-sensor bound antigen 1 (mEGFR-His), and soluble antigen 2 (mPSMA-His) as measured by BLI on an Octet machine.

References

Atwell, S., Ridgway, J.B.B., Wells, J.A., Carter, P., Jul. 1997. Stable heterodimers from remodeling the domain interface of a homodimer using a phage display library¹¹ Edited by P.E.Wright. *J. Mol. Biol.* 270 (1), 26–35. <https://doi.org/10.1006/jmbi.1997.1116>.

Bluemel, C., et al., Aug. 2010. Epitope distance to the target cell membrane and antigen size determine the potency of T cell-mediated lysis by BiTE antibodies specific for a large melanoma surface antigen. *Cancer Immunol. Immunother.* 59 (8), 1197–1209. <https://doi.org/10.1007/s00262-010-0844-y>.

Bönisch, M., et al., Sep. 2017. Novel CH1:CL interfaces that enhance correct light chain pairing in heterodimeric bispecific antibodies. *Protein Eng. Des. Sel.* 30 (9), 685–696. <https://doi.org/10.1093/protein/gzx044>.

Brinkmann, U., Kontermann, R.E., Feb. 2017. The making of bispecific antibodies. *mAbs* 9 (2), 182–212. <https://doi.org/10.1080/19420862.2016.1268307>.

Burton, D.R., et al., Nov. 1994. Efficient neutralization of primary isolates of HIV-1 by a recombinant human monoclonal antibody. *Science* 266 (5187), 1024–1027. <https://doi.org/10.1126/science.7973652>.

Chailyan, A., Marcatili, P., Tramontano, A., 2011. The association of heavy and light chain variable domains in antibodies: implications for antigen specificity. *FEBS J.* 278 (16), 2858–2866. <https://doi.org/10.1111/j.1742-4658.2011.08207.x>.

Davis, J.H., et al., Apr. 2010. SEEDbodies: fusion proteins based on strand-exchange engineered domain (SEED) CH3 heterodimers in an fc analogue platform for asymmetric binders or immunofusions and bispecific antibodies. *Protein Eng. Des. Sel.* 23 (4), 195–202. <https://doi.org/10.1093/protein/gzp094>.

Garber, K., Nov. 2014. Bispecific antibodies rise again. *Nat. Rev. Drug Discov.* 13 (11), 799–801. <https://doi.org/10.1038/nrd4478>.

Grilo, A.L., Mantalaris, A., Jan. 2019. The increasingly human and profitable monoclonal antibody market. *Trends Biotechnol.* 37 (1), 9–16. <https://doi.org/10.1016/j.tibtech.2018.05.014>.

Gunasekaran, K., et al., Jun. 2010. Enhancing antibody fc heterodimer formation through electrostatic steering effects APPLICATIONS TO BISPECIFIC MOLECULES AND MONOVALENT IgG. *J. Biol. Chem.* 285 (25), 19637–19646. <https://doi.org/10.1074/jbc.M110.117382>.

Ha, J.-H., Kim, J.-E., Kim, Y.-S., 2016. Immunoglobulin fc heterodimer platform technology: from design to applications in therapeutic antibodies and proteins. *Front. Immunol.* 7. <https://doi.org/10.3389/fimmu.2016.00394>.

Herold, E.M., et al., Sep. 2017. Determinants of the assembly and function of antibody variable domains. *Sci. Rep.* 7 (1), 1–17. <https://doi.org/10.1038/s41598-017-12519-9>.

Hulsik, D.L., et al., 2013. A gp41 MPER-specific llama VHH requires a hydrophobic CDR3 for neutralization but not for antigen recognition. *PLoS Pathog.* 9 (3), e1003202. <https://doi.org/10.1371/journal.ppat.1003202>.

Igawa, T., et al., Aug. 2010. VH/VL interface engineering to promote selective expression and inhibit conformational isomerization of thrombopoietin receptor agonist singlechain diabody. *Protein Eng. Des. Sel.* 23 (8), 667–677. <https://doi.org/10.1093/protein/gzq034>.

Jackman, J., et al., Jul. 2010. Development of a two-part strategy to identify a therapeutic human Bispecific antibody that inhibits IgE receptor Signaling. *J. Biol. Chem.* 285 (27), 20850–20859. <https://doi.org/10.1074/jbc.M110.113910>.

Krah, S., et al., Apr. 2017. Generation of human bispecific common light chain antibodies by combining animal immunization and yeast display. *Protein Eng. Des. Sel.* 30 (4), 291–301. <https://doi.org/10.1093/protein/gzw077>.

Labrijn, A.F., et al., 2013. Efficient generation of stable bispecific IgG1 by controlled fab-arm exchange. *Proc. Natl. Acad. Sci.* 110 (13), 5145–5150. <https://doi.org/10.1073/pnas.1220145110>.

Labrijn, A.F., et al., 2017. Efficient generation of Bispecific murine antibodies for preclinical investigations in syngeneic rodent models. *Sci. Rep.* 7 (1), 1–14. <https://doi.org/10.1038/s41598-017-02823-9>.

Laszlo, G.S., et al., Jan. 2014. Cellular determinants for preclinical activity of a novel CD33/CD3 bispecific T-cell engager (BiTE) antibody, AMG 330, against human AML. *Blood* 123 (4), 554–561. <https://doi.org/10.1182/blood-2013-09-527044>.

Lewis, S.M., et al., Feb. 2014. Generation of bispecific IgG antibodies by structure-based design of an orthogonal fab interface. *Nat. Biotechnol.* 32 (2), 191–198. <https://doi.org/10.1038/nbt.2797>.

Lopez-Albaitero, A., et al., 2017. Overcoming resistance to HER2-targeted therapy with a novel HER2/CD3 bispecific antibody. *Oncolmunology* 6 (3), e1267891. <https://doi.org/10.1080/2162402X.2016.1267891>.

Masuda, K., Sakamoto, K., Kojima, M., Aburatani, T., Ueda, T., Ueda, H., 2006. The role of interface framework residues in determining antibody VH/VL interaction strength and antigen-binding affinity. *FEBS J.* 273 (10), 2184–2194. <https://doi.org/10.1111/j.1742-4658.2006.05232.x>.

Mazor, Y., et al., 2015a. Insights into the molecular basis of a bispecific antibody's target selectivity. *mAbs* 7 (3), 461–469. <https://doi.org/10.1080/19420862.2015.1022695>.

Mazor, Y., et al., 2015b. Improving target cell specificity using a novel monovalent bispecific IgG design. *mAbs* 7 (2), 377–389. <https://doi.org/10.1080/19420862.2015.1007816>.

Mazor, Y., et al., Jan. 2017. Enhanced tumor-targeting selectivity by modulating bispecific antibody binding affinity and format valence. *Sci. Rep.* 7 (1), 1–11. <https://doi.org/10.1038/srep40098>.

Merchant, A.M., et al., Jul. 1998. An efficient route to human bispecific IgG. *Nat. Biotechnol.* 16 (7), 677–681. <https://doi.org/10.1038/nbt0798-677>.

Moore, G.L., et al., Nov. 2011. A novel bispecific antibody format enables simultaneous bivalent and monovalent co-engagement of distinct target antigens. *mAbs* 3 (6), 546–557. <https://doi.org/10.4161/mabs.3.6.18123>.

Moores, S.L., et al., Jul. 2016. A novel Bispecific antibody targeting EGFR and cMet is effective against EGFR inhibitor-resistant lung Tumors. *Cancer Res.* 76 (13), 3942–3953. <https://doi.org/10.1158/0008-5472.CAN-15-2833>.

Nisonoff, A., Wissler, F.C., Lipman, L.N., Dec. 1960. Properties of the major component of a peptic digest of rabbit antibody. *Science* 132 (3441), 1770–1771. <https://doi.org/10.1126/science.132.3441.1770>.

Oberst, M.D., et al., Nov. 2014. CEA/CD3 bispecific antibody MEDI-565/AMG 211 activation of T cells and subsequent killing of human tumors is independent of mutations commonly found in colorectal adenocarcinomas. *mAbs* 6 (6), 1571–1584. <https://doi.org/10.4161/19420862.2014.975660>.

Schaefer, G., et al., Oct. 2011. A two-in-one antibody against HER3 and EGFR has superior inhibitory activity compared with Monospecific antibodies. *Cancer Cell* 20 (4), 472–486. <https://doi.org/10.1016/j.ccr.2011.09.003>.

Staerz, U.D., Kanagawa, O., Bevan, M.J., Apr. 1985. Hybrid antibodies can target sites for attack by T cells. *Nature* 314 (6012), 628–631. <https://doi.org/10.1038/314628a0>.

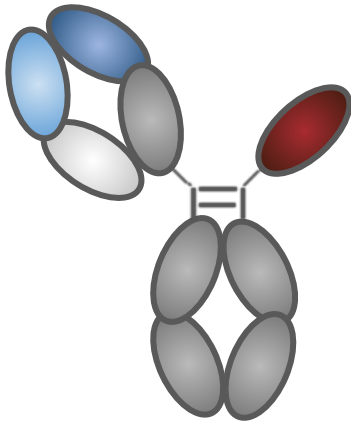
Urh, M., Simpson, D., Zhao, K., 2009. Chapter 26 affinity chromatography: General methods. In: Burgess, R.R., Deutscher, M.P. (Eds.), *Methods in*

Enzymology. 463. Academic Press, pp. 417–438.

Wranik, B.J., Christensen, E.L., Schaefer, G., Jackman, J.K., Vendel, A.C., Eaton, D., Dec. 2012. LUZ-Y, a novel platform for the mammalian cell production of full-length IgG-bispecific antibodies. *J. Biol. Chem.* 287 (52), 43331–43339. <https://doi.org/10.1074/jbc.M112.397869>.

Zaiss, D.M.W., et al., Feb. 2013. Amphiregulin enhances regulatory T cell-suppressive function via the epidermal growth factor receptor. *Immunity* 38 (2), 275–284. <https://doi.org/10.1016/j.immuni.2012.09.023>.

4



Shortened Hinge Design of Fab x sdAb-Fc Bispecific Antibodies Enhances Redirected T-Cell Killing of Tumor Cells

Shuyu Huang^{1,2,†}, Aina Segués^{1,2,†}, Martin Waterfall¹, David Wright¹, Charlotte Vayssiere¹, Sander M. J. van Duijnhoven³, Andrea van Elsas⁴, Alice J. A. M. Sijts² and Dietmar M. Zaiss^{1,5,6,7,*}

¹ Institute of Immunology and Infection Research, School of Biological Sciences, University of Edinburgh, Edinburgh EH9 3FL, UK

² Faculty of Veterinary Medicine, Department of Infectious Diseases and Immunology, Utrecht University, 3584 CS Utrecht, The Netherlands

³ ImmunoPrecise Antibodies Ltd., 5349 AB Oss, The Netherlands

⁴ Third Rock Ventures, San Francisco, CA 94158, USA

⁵ Department of Immune Medicine, University Regensburg, 93053 Regensburg, Germany

⁶ Institute of Clinical Chemistry and Laboratory Medicine, University Hospital Regensburg, 93053 Regensburg, Germany

⁷ Institute of Pathology, University Regensburg, 93053 Regensburg, Germany

* Correspondence: dietmar.zaiss@ukr.de

† These authors contributed equally to this work.

Biomolecules. 2022; 12(10):1331.

Contribution statement: Shuyu Huang conceived of the presented idea. Shuyu Huang performed the experiments and analyzed the data. All authors provided critical feedback and helped shape the research, analysis and manuscript.

Abstract

T cell engager (TCE) antibodies have emerged as promising cancer therapeutics that link cytotoxic T-cells to tumor cells by simultaneously binding to CD3E on T-cells and to a tumor associated antigen (TAA) expressed by tumor cells. We previously reported a novel bispecific format, the IgG-like Fab x sdAb-Fc (also known as half-IG_VH-h-CH2-CH3), combining a conventional antigen-binding fragment (Fab) with a single domain antibody (sdAb). Here, we evaluated this Fab x sdAb-Fc format as a T-cell redirecting bispecific antibody (TbsAbs) by targeting mEGFR on tumor cells and mCD3E on T cells. We focused our attention specifically on the hinge design of the sdAb arm of the bispecific antibody. Our data show that a TbsAb with a shorter hinge of 23 amino acids (TbsAb.short) showed a significantly better T cell redirected tumor cell elimination than the TbsAb with a longer, classical antibody hinge of 39 amino acids (TbsAb.long). Moreover, the TbsAb.short form mediated better T cell-tumor cell aggregation and increased CD69 and CD25 expression levels on T cells more than the TbsAb.long form. Taken together, our results indicate that already minor changes in the hinge design of TbsAbs can have significant impact on the anti-tumor activity of TbsAbs and may provide a new means to improve their potency.

Keywords: bispecific antibody; cancer immunotherapy; mCD3E; mEGFR; hinge

1. Introduction

T-cell engager antibodies (TCEs) redirect cytotoxic T-cells to tumor cells by simultaneously binding to a component of the TCR complex (commonly CD3E) and a tumor associated antigen (TAA) on tumor cells [1]. Due to the clinical success of the bispecific T-cell engager (BiTE) blinatumomab, approved by the FDA in 2014 [2,3], the majority of bispecific antibodies (BsAbs) in clinical development are currently TCEs [4]. TCEs can further be classified into two broad classes according to their formats: IgG-like or fragment-based TCEs. Currently, the IgG-like T cell redirecting bispecific antibodies (TbsAbs) being the most widely used form, largely due to their longer in vivo serum half-life due to the presence of an Fc region [5].

Although the concept of BsAbs has a long history, due to challenges in BsAb manufacturing, they only began to stimulate the interest of pharmaceutical companies in the past decade. The production of IgG-like BsAbs requires the correct assembly of antibody's light and heavy chain fragments. A random assembly of four distinctive polypeptide chains may result in 16 combinations [6]. Therefore, in order to manufacture IgG-like BsAb that can reliably be assembled, it is required to ensure the selective formation of the heterodimerized heavy chains (HCs) and the proper pairing of the light chains of each arm with the cognate HC [7]. Multiple recombinant technologies have been developed to ensure the correct formation of IgG-like bispecific antibodies. In our previous study, we developed a novel Fab x sdAb-Fc format which combined a single domain antibody (sdAb) with a conventional antigen-binding fragment (Fab) [8]. Both arms were linked to an Fc domain optimized for heavy-heavy chain heterodimerization by the introduction of matched amino acid mutations, thus ensuring both correct heavy-chain and heavy-light chain assembly [8]. However, the hinge between sdAb and Fc can be designed in various ways, dependent on different applications. Previous studies demonstrated a direct role of the distance between TAA and CD3E binding sites of TbsAbs on T-cell mediated tumor cell lysis [9,10]. In these applications, the authors modulated their format using various approaches with the common objective of shortening the distance between the two arms of TbsAbs which resulted in improved tumor cell lysis [11–14]. Additional studies looked at the correlation between the length of effector/target cell synapse distance and T-cell mediated tumor killing by alternative strategies, such as tumor antigen epitope distance to the cancer cell membrane or the overall size of the antigen, which can increase the distance between the effector and target cell [9]. Thereby, it has

become apparent that TbsAbs that bind to membrane-distal epitopes extend the intermembrane spacing resulting in decreased tumor killing compared to TbsAbs that bind membrane-proximal epitopes [15–19]. Additionally, the size of the targeted antigen can also effectively increase the distance within the synapse between the T-cell and target cell and has been shown to affect TbsAb potency [15,16]. In particular, it was noticed that the IgG hinge region in different IgG subclasses was a major modulator of antibody function. IgG3 molecules have an extended hinge region of 62 amino acids. This long hinge provides superior flexibility and leads to improved phagocytosis. In contrast, other IgG molecules have shorter and less flexible hinge regions, which was associated with improved antibody-dependent cellular cytotoxicity [20]. These findings suggested that the size of the hinge between the heavy chain and the Fab arm may determine the flexibility of the antibody and therefore the cytotoxic effector functions of it. Therefore, we hypothesized that TbsAbs in the Fab x sdAb-Fc format may benefit from a short hinge design.

To address this hypothesis, we constructed and evaluated TbsAbs targeting mouse EGFR and mouse CD3E with two different hinge region lengths connecting the mEGFR binding domain and its cognate constant region. The longer hinge TbsAb (TbsAb.long) format was designed to mimic the distance between two binding sites of conventional IgG format TbsAb, while the shorter hinge TbsAb (TbsAb.short) was designed to minimize the distance between two binding sites. Our results demonstrated that the efficiency of T cell redirected tumor cell killing directly correlated with the proximity of mEGFR and mCD3E binding regions in Fab x sdAb-Fc TbsAbs.

2. Results

2.1. Designing and Preparation of mCD3E x mEGFR TbsAbs with Different Hinges

In order to avoid potential heavy-light chain mispairing during BsAb expression, we previously suggested a novel Fab x sdAb-Fc bispecific antibody format [8]. To further investigate this novel antibody format, we designed and expressed TbsAbs, using a mCD3E Fab-Fc combined with an mEGFR sdAb-Fc with two different hinges. The design of the shorter hinge (23 amino acids in total) was based on the natural mouse IgG2a hinge sequence, with the exception of an Arginine residue at position 3 which we replaced with a lysine residue in order to stabilize the sdAb [21]. The longer hinge (39 amino acids in total) was designed as a chimer hinge based on a

combination between a mouse IgG2a hinge and a part of the llama hinge. This resulted in 16 additional amino acids compared with the shorter hinge and mimicked the length of an entire CH1 domain (starts at the end of the hinge and ends with VDKKI, approximately 32.6 Å, Figure S2) [22], in this way, extending the length of the sdAb arm to a similar length of a conventional Fab (Figure 1A).

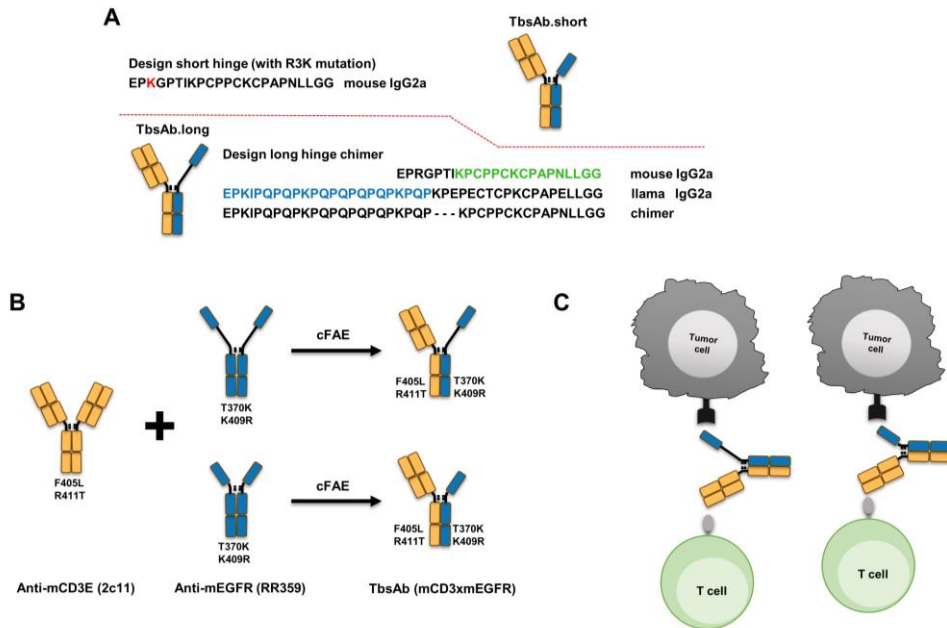


Figure 1. Preparation of Fab x sdAb-Fc TbsAbs with different hinge designs. (A) Schematic diagrams of two types of Fab x sdAb-Fc TbsAbs: TbsAb.long, TbsAb.short. (B) Schematic illustration of mCD3E x mEGFR TbsAbs generated by the duobody platform. (C) Schematic diagrams of tumor cell eliminated by mCD3E x mEGFR TbsAbs.

To abrogate Fc-FcR mediated effector functions without affecting affinity, LALAPG mutations were introduced to each parental antibody (anti-mCD3E, clone 2c11; anti-mEGFR, clone RR359) [23]. The mCD3E x mEGFR TbsAb with a long hinge (TbsAb.long) and mCD3E x mEGFR TbsAb with a short hinge (TbsAb.short) were then constructed by performing controlled Fab-arm exchange (cFAE) based on the duobody platform (Figure 1B,C).

The purity of each expressed TbsAb was analyzed by size-exclusion chromatography (SEC) and sodium dodecyl sulfate–polyacrylamide gel electrophoresis (SDS-PAGE). The monomericity of each parental antibody was >97% (HcAb.RR359.long), >97% (HcAb.RR359.short), and >98%

(2c11), respectively (Figure S1). Following cFAE, a single peak was observed in the resulting SEC for each TbsAb and monomericity evaluated was $\geq 96\%$ (TbsAb.long) and $\geq 99\%$ (TbsAb.short), respectively (Figure 2A). Under non-reducing SDS-PAGE conditions, the desired TbsAbs showed a predominant band with an MW of ~ 125 kDa, whereas parental antibodies showed predominant bands with an MW of ~ 95 kDa or ~ 165 kDa, respectively (Figure 2B). For TbsAb.long and TbsAb.short, additional minor bands were detected at the same size as of parental antibodies, which indicated minor contamination of the parental mEGFR HcAb and mCD3E mAb in the TbsAb. The purity of TbsAb.long and TbsAb.short were evaluated as $\sim 80.7\%$ and 82.8% , respectively. Under reducing conditions, one band for mEGFR HcAb, two bands for mCD3E mAb and three bands for TbsAbs were detected, as expected (Figure 2C). The bands just below 63 kDa detected in TbsAbs and mCD3E mAb represent the heavy chain of the mCD3E mAb, while the MW bands just above 48 kDa which are detected in mEGFR HcAb and TbsAbs represent the heavy chain of the mEGFR HcAb. The bands at ~ 35 kDa detected in TbsAbs and mCD3E mAb represent the light chain of the mCD3E mAb. Taken together, these results demonstrate the successful generation of TbsAbs with long and short hinges.

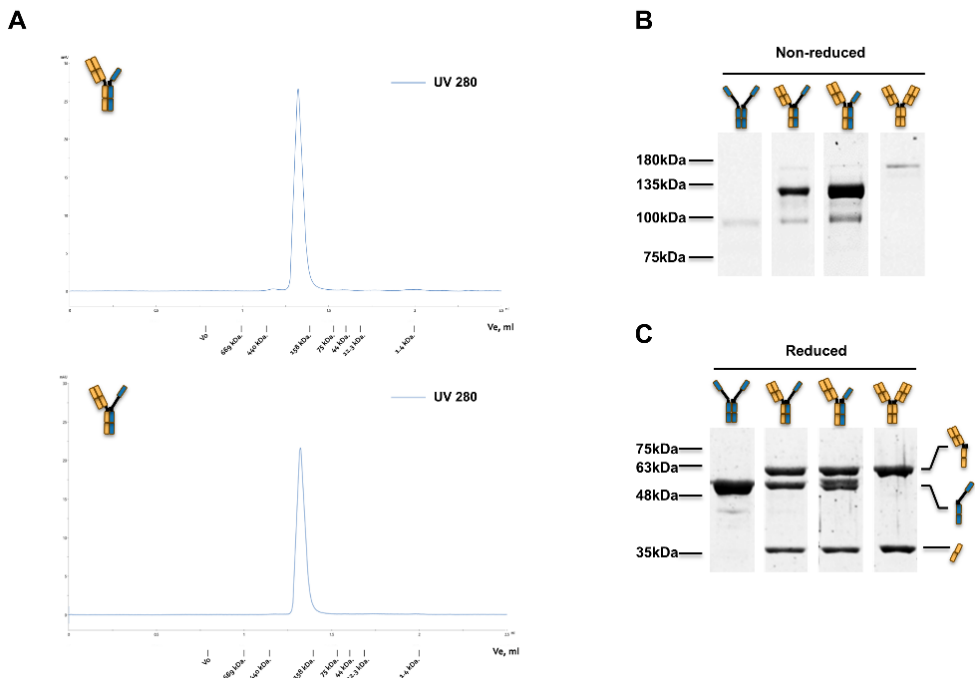


Figure 2. Analysis of the expressed mCD3E \times mEGFR TbsAbs. (A) Size

exclusion chromatography (SEC) analysis of TbsAb.long and TbsAb.short proteins. Ten μL of each respective sample (TbsAb.long and TbsAb.short), at 0.5 mg/mL were eluted by DPBS buffer at a flow rate of $50 \mu\text{L}\cdot\text{min}^{-1}$. (B, C) SDS-PAGE analysis of TbsAb.long and TbsAb.short proteins under non-reducing and reducing conditions, respectively.

2.2. Generation of TbsAb Negative Control Antibody

In order to express an appropriate negative control TbsAb [24], we disrupted the binding ability of the mEGFR arm of the TbsAb to mEGFR through site-directed mutagenesis. We started out by evaluating the structure of mEGFR sdAb (RR359) using Colab-Fold (Figures 3A and S3) [25]. By aligning the sequence of mEGFR sdAb to the PDB database, the molecule with PDB ID 5IMMB was found to be the most similar sdAb to mEGFR sdAb, which facilitated the identification of CDR1,2,3 of mEGFR sdAb (Figure 3B). Given that the CDR3 of the mEGFR sdAb differs most from 5IMMB, we considered it was very likely the region that determined the antibody specificity. Consequently, we performed targeted mutagenesis on this region. Based on the computational analysis of the interactions between sdAb and mEGFR protein by using Discovery Studio software, several amino acids (e.g., Y101, D105, D107, L110, H115 etc.) appeared to be critical for antigen binding. A set of HcAbs containing site-specific mutations were expressed and subsequently affinity to mEGFR recombinant protein was measured by biolayer interferometry using Octet (Figure S4). The HcAbs with Y101S, D105A or H115K mutation showed no detectable binding to mEGFR protein based on the Octet results (Figure 3C). Considering the mEGFR recombinant protein might differ in structure from the natural mEGFR, the binding activity of the HcAbs with either Y101S, D105A or H115K mutation were further examined by FACS, using a CHO cell line overexpressing the mEGFR. No binding of the HcAb with D105A mutation in CDR3 was confirmed with CHO/mEGFR cells (Figure 3D). This version of HcAb was subsequently incorporated into a mCD3E \times mEGFR TbsAb by cFAE and used as negative control bispecific antibody (TbsAb.con). The expressed TbsAb.con showed similar purity to the other TbsAbs (Figure S5) and retained its binding capacity to mCD3E (Figure 3E).

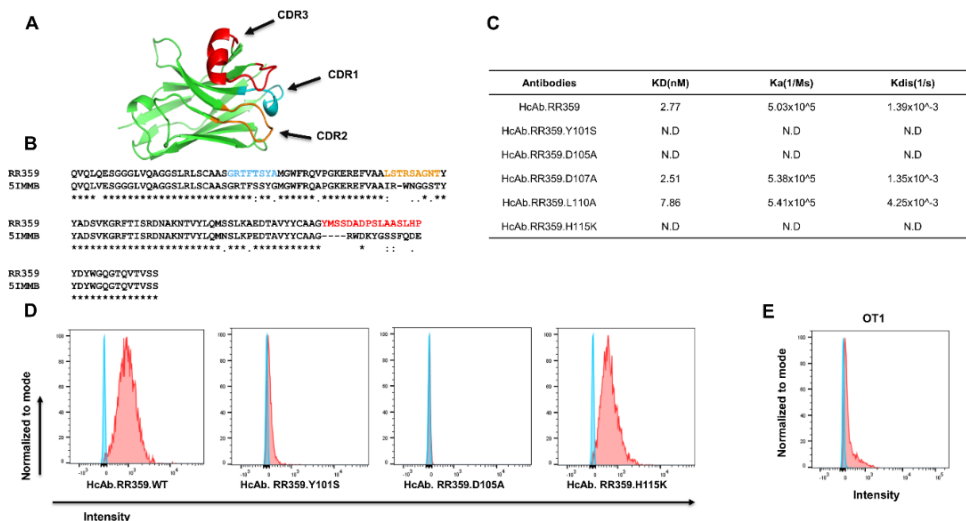


Figure 3. Generation of bispecific negative control antibody by CDR3 mutagenesis. (A) Structure of anti-mEGFR sdAb (RR359) predicted by ColabFold. (B) The sequence of anti-mEGFR sdAb (RR359) aligned to sdAb (51IMMB). The sequence of CDR1 (blue), CDR2 (orange), CDR3 (red) was indicated. (D) mEGFR HcAbs to CHO/mEGFR cell line. (E) TbsAb.con (mCD3E x mEGFR.D105A) binds to OT-1 cells detected by flow cytometry. N.D, not detectable. The “*” (asterisk) indicates positions with conserved residues. The “:” (colon) indicates conservation between groups of amino acids with similar properties. The “.” (period) indicates amino acids with weakly similar properties.

2.3. mCD3E x mEGFR TbsAb.short Molecule Mediated Enhanced T Cell Redirected Killing In Vitro

To investigate the capacity of the purified TbsAb for mEGFR+ cell killing, Lactate dehydrogenase (LDH) release cytotoxicity assays were performed. As target cells in the cytotoxicity assays, different mEGFR+ cell lines were used. In order to determine mEGFR expression level on target cells, ID8, CHO/mEGFR, and CHO/K1 were stained with RR359 and antibody binding was measured by FACS (Figure 4A). In order to generate an mEGFR-deficient control cell line, CRISPR/Cas9 was performed to disrupt the mEGFR gene on ID8 cells (Figure 4A). As effector T cells, OT-1s were derived from the spleens of OT-1 x Rag1^{-/-} mice. OT-1 CD8 T-cells were derived from a C57BL/6 mouse strain, transgenic for a T-cell receptor (TCR) which recognizes an immunodominant ovalbumin-derived epitope. These T-cells can be activated with their cognate antigen, the ovalbumin-derived



peptide SIINFEKL. Following a 48 h incubation with the SIINFEKL peptide, activated OT-1s and target cells were mixed and incubated with each TbsAb for 24 h. At the concentration of 0.02688 nM (0.0032 µg/mL) of each group, significantly more and bigger T cell clumps were observed in the TbsAb.short-treated group compared to TbsAb.long and TbsAb.con treated groups, which suggested stronger proliferation (T-cell blast) of T cells induced by the TbsAb.short form than by the other two TbsAbs (Figure 4B,C). Furthermore, the LDH release assay showed higher LDH release in the presence of the TbsAb.short molecules, suggesting that the TbsAb.short form induced better T-cell mediated cytotoxicity towards ID8 and CHO/mEGFR cells than the TbsAb.long form. The TbsAb.con form appeared not to induce any specific cell lysis. In addition, mEGFR negative cell lines, ID8/mEGFR^{-/-} and CHO.K1, showed no specific cell lysis induced in the presence of either the TbsAb.long, the TbsAb.short or the TbsAb.con form (Figure 4D).

To corroborate these findings, an alternative approach was used to measure tumor cell killing. To this end, ID8 cells and ID8 mEGFR^{-/-} cells were labeled by eFluo 450 or eFluo 670, respectively, and incubated with OT-1 cells at a concentration of 0.02688 nM (0.0032 µg/mL) for each TbsAb or PBS for 24 h. OT-1 cells were carefully washed off by PBS and adherent ID8 cells were then harvested using trypsin detachment. Flow cytometry was performed to detect live ID8 and ID8 mEGFR^{-/-} cells (Figure 4E). As shown in Figure 4F, the TbsAb.short form depleted mEGFR-expressing ID8 cells significantly better than the TbsAb.long form (Figure 4F).

Taken together, using two different approaches, these data strongly suggest that mCD3E × mEGFR TbsAb.short molecules mediate better T cell redirected killing than the TbsAb.long form.

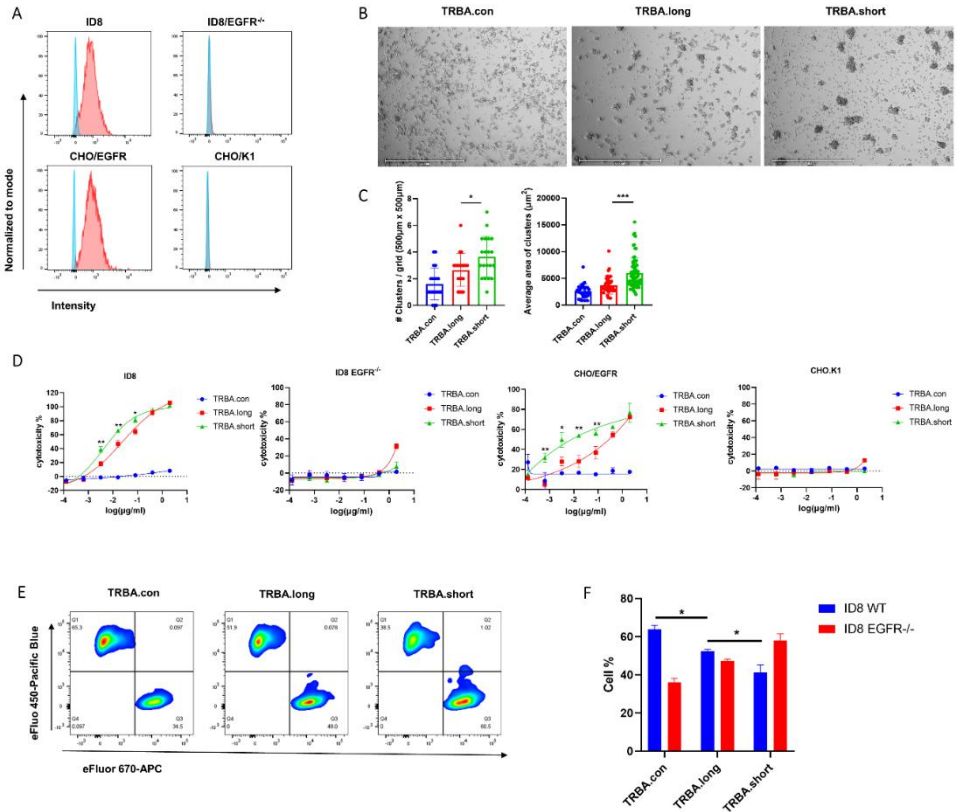


Figure 4. The TbsAb.short form mediates superior T cell mediated cytotoxic. (A) Expression of mEGFR on ID8, ID8/mEGFR^{-/-}, CHO/mEGFR and CHO/K1 cell lines were measured by flow cytometry. (B) OT-1 T cell blasts with CHO/mEGFR cells in the presence of 0.02688 nM (0.0032 μg/mL) of either mCD3E x mEGFR TbsAb.long or TbsAb.short at an E: T ratio of 5:1 following 24 h incubation. Images were obtained under 4 × magnification, and scale bars 650 μm. (C) Quantified number of T cell blasts per grid and average area per T cell blasts by EVOS analysis software. (D) In vitro cytotoxicity assay of mCD3E x mEGFR TbsAbs using LDH release assay. Curves were fitted using a four-parameter logistic fitting with GraphPad Prism 8. (E) In vitro cytotoxicity assay of mCD3E x mEGFR TbsAbs (0.02688 nM, equal to 0.0032 μg/mL) using FACS. (F). Data points represent the mean of three samples; error bars, SD. *: p < 0.05; **: p < 0.01; ***: p < 0.001.

2.4. mCD3E x mEGFR TbsAb.short Mediated Enhanced Cell-Cell

Association In Vitro

To investigate the underlying mechanisms, which may lead to the improved redirected T cell killing observed with the mCD3E × mEGFR TbsAb.short molecules, we evaluated the ability of the different TbsAbs to induce ID8/OT-1 cell association. Non-activated, naïve OT-1 cells and ID8 cells were used for association and cell aggregation, as measured by FACS. ID8 and OT-1 cells were stained with two different cell-staining dyes and subsequently mixed and incubated with TbsAb.long, TbsAb.short or TbsAb.con. The flow cytometry results showed that a clear cell–cell association was observed with both TbsAb.long and TbsAb.short molecules, but not with the TbsAb.con control construct (Figure 5A,B). Furthermore, the TbsAb.short molecules could induce more cell aggregates than the TbsAb.long form (up to ~8% of the total cell population in the presence of TbsAb.short molecules compared to ~4% of the cell aggregates in the presence of the TbsAb.long molecules). Such an enhanced level of cell–cell association mediated by TbsAb.short molecules was observed consistently across a range of concentrations of the bispecific antibodies. As expected, the TbsAb.con molecule did not induce the cell–cell association of ID8 and OT-1 cells at any concentration tested (Figure 5B). Taken together, these data show that the TbsAb.short form has a higher capacity to form cell aggregates than the TbsAb.long form. Compared to ~30% cell aggregates we reported in our previous study and ~5–17% cell aggregates that others have typically reported [8,18], the relatively lower percentage of cell aggregates induced in our experiments might be for several reasons. So far, we have not yet followed up on these, nevertheless, several aspects such as the expression level of antigens, the affinity of antibodies used or the geometry of the specific antigens could all influence the efficiency with which such TbsAb molecules can link two different cell populations.

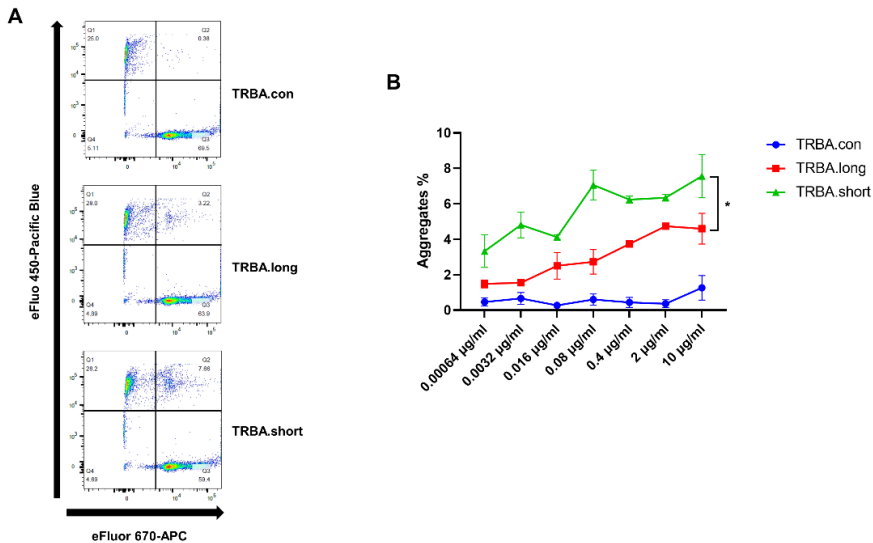


Figure 5. The TbsAb.short form shows better cell aggregate formation than the TbsAb.long form. OT-1 cells were labeled with eFluor 670 dye, and ID8 cells were labeled with the eFluor 450 dye. Cells were incubated for 30 min at room temperature with TbsAb.con, TbsAb.long or TbsAb.short molecules at 0.672 nM (0.08 µg/mL). The OT-1-ID8 cell-cell association was determined using cytometry and quantified as the percentage of eFluor 450 and eFluor 670 double positive cells in upper right quadrant. (B) The experiment was repeated using increasing concentrations for each the molecules. Each experimental point was set up in duplicate and the mean SD was plotted. 0.05.

2.5. mCD3E × mEGFR TbsAb.short Mediated Enhanced T Cell Activation In Vitro

To investigate to what extent either form of the mCD3E × mEGFR TbsAb could T cell activation, splenocytes were mixed with ID8 cells in the presence or absence of the different TbsAb forms and the expression levels of the early activation marker CD69 and of the late activation marker CD25 were determined by flow cytometry on CD4⁺ CD8⁺ T cells after 24 h of in vitro incubation. Our data show that in the presence of cells, the expression levels of activation marker CD69 and CD25 were considerably by the TbsAb.long form as well as by the TbsAb.short form. However, in comparison to the TbsAb.long form, the TbsAb.short form activated a

significantly higher fraction of CD4 T cells (Figure 6A,F). Furthermore, on a single cell level, the TbsAb.short form activated a significantly higher expression levels of CD69 and CD25 per cell (Figure 6D,I). For CD8 T cells, both TbsAb forms activated a similar fraction of CD8 T-cells (Figure 6B,G), but the TbsAb.short form induced significantly higher expression levels of CD69 and CD25 than the TbsAb.long form (Figure 6E,J). Gating strategy is shown in Figure S6. These data strongly suggest that while both TbsAb can induce T cell activation, the TbsAb with the shorter hinge induced a stronger T cell activation than the TbsAb with the longer hinge.

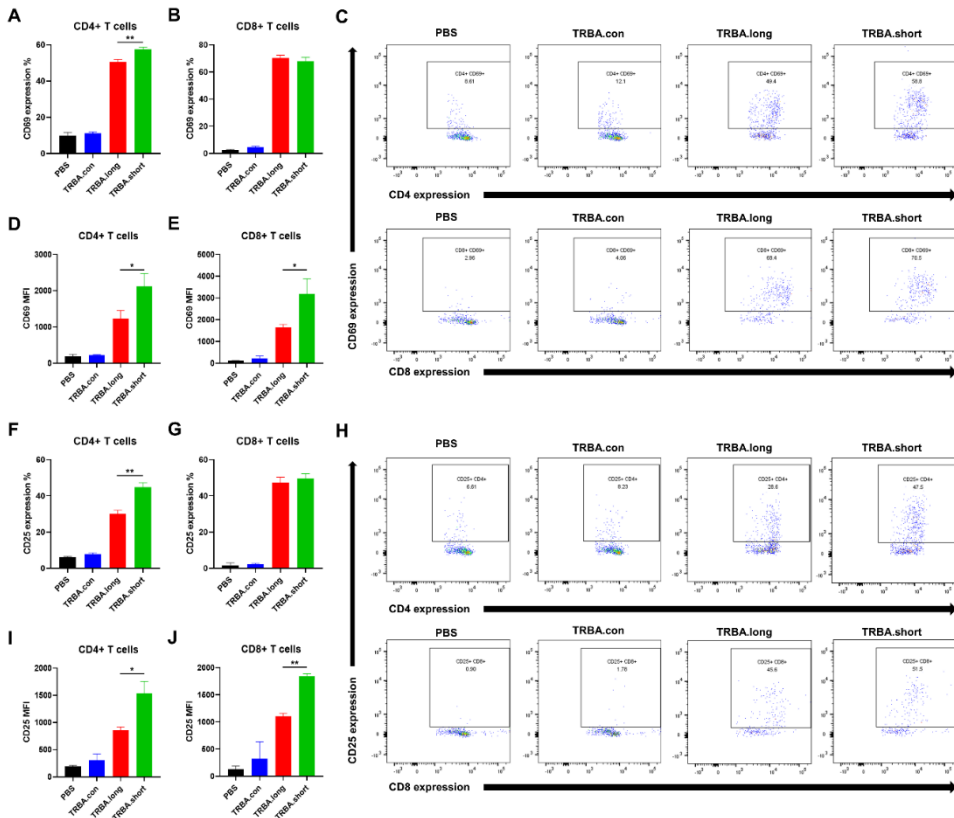


Figure 6. The TbsAb.short form induces superior T cell activation. (A–E) The expression level of CD69 on CD4+ and CD8+ T cells was detected after incubating with each TbsAb for 24 h (E:T = 5:1). (F–J) The expression level of CD25 on CD4+ and CD8+ T cells was detected after incubating with each TbsAb for 24 h (E:T = 5:1). *: $p < 0.05$; **: $p < 0.01$.

3. Discussion

Several different factors have been described that can affect the potency of bispecific T-cell engagers. These include the copy number of the targeted antigen, the size of the antigen, and the distance of the target epitope to the membrane, as well as antibody formats with different sizes, valences, and geometries [9,10]. In this study, we focused on modulating the distance between T cells and tumor cells, by modulating the hinge region between the heavy chain backbone of the antibody molecule and the Fab arm. To this end, two mCD3E × mEGFR bispecific antibodies with different hinge designs in the Fab x sdAb-Fc format were generated; one with a shorter hinge and one with a longer hinge design. As our results show, the TbsAb.short molecule exhibited significantly greater potency than the TbsAb.long molecule in T-cell redirected killing (Figure 4D). Furthermore, the TbsAb.short form linked T cells to mEGFR-expressing tumor cells more efficiently than the TbsAb.long form by forming more T cell-tumor cell aggregates. In addition, as measured by CD69 and CD25 expression, T cells appeared to be more strongly activated by the TbsAb.short than by the TbsAb.long format.

Since the same antigen recognition specificities were used, the enhancement observed with the TbsAb.short molecule was presumably due to the hinge difference in the molecules. Such a finding is consistent with previous studies. Bluemel and colleagues designed TbsAbs to target different epitopes on human melanoma chondroitin sulfate proteoglycan (hMCSP) and found that the distance of the binding domain to the target cell membrane had a significant impact on the potency of T cell redirecting bispecific antibodies [16]. Additionally, several more recent studies, targeting other TAAs such as FcRH5, ROR1, and CD3E, further confirmed that targeting membrane-proximal epitopes, which also shortened the distance between T cells and tumor cells, could improve the *in vitro* potency of their antibody constructs to facilitate T cell mediated target cell lysis [15,19,26]. In yet another study, TbsAbs in conventional IgG2 format were compared to a Diabody-Fc (DbFc) format in *in vitro* tumor cell cytotoxicity assays. The DbFc format shortened the distance between antigen-binding arms and turned out to be more potent [27]. With TbsAbs in all these cases, also in the one we have described here, several factors may contribute to the enhanced tumor elimination potency by using a short hinge format. For instance, we found that the TbsAb.short molecule induced significantly more T cell-tumor cell aggregation than the TbsAb.long molecule (Figure 5). Such improved aggregation could facilitate the T cell mediated attack of tumor

cells. It has been reported that immunological synapse formation requires an optimal distance between T cells and tumor cells [10]. This optimal distance might be influenced by the geometric configurations of the different antibody constructs. In line with such an assumption, it was reported previously, that targeting membrane-proximal epitope by TbsAbs could facilitate efficient T cell synapse formation leading to enhanced tumor cell elimination [15]. Based on this finding, one could argue that possibly by forming tight immunological synapses the TbsAb.short form might be more potent in T cell redirected tumor cell elimination than the TbsAb.long form. Alternatively, efficient T cell-tumor cell engagement might form multiple TbsAbs mediated connections at the immune synapse. In such a situation, the property of individual TbsAbs, such as the flexibility of the binding sites, could be an important factor in forming efficient T cell-tumor cell aggregation [14,15]. In line with such an assumption, it has been reported by Kapelskia et al. that the different flexibility shown in the hinge region of human IgG subclasses (IgG1 > IgG4 > IgG2, IgG1 being the most flexible) significantly impacted the T cell redirected tumor cell elimination [28]. Compared to the TbsAb.long molecule, the TbsAb.short molecule has a shorter and relatively rigid hinge, which results in a relatively fixed distance and orientation between the two binding domains. Consequently, given the same specific concentration of each TbsAb, the binding arm of randomly free-floating TbsAb.long molecules would require more time to adjust the preferable orientation to bridging T cells and tumor cells than the more rigid TbsAb.short molecules. In addition, due to the dynamic and reversible binding property of TbsAbs, once the T cell-tumor cell aggregation has been formed, TbsAb.short could keep the distance between T cells and tumor cells shorter. This might facilitate other free TbsAb.short molecules to support and further enhance this originally brief interaction between T cells and tumor cells; consequently, resulting in a tighter T cell-tumor cell aggregation than the TbsAb.long molecule might be able to establish. In line with such an assumption, the TbsAb.short construct induced in comparison to the TbsAb.long construct increased CD69 and CD25 expression on T cells, suggesting a more extensive activation of the T cells. T cell activation is generally considered to be sensitive to consistent TCR signaling, which is triggered by constant antigen/receptor interaction [29]. Therefore, the higher expression level of CD69 and CD25 could be assumed to be a direct result of a tighter T cell: tumor cell aggregation induced and maintained by the TbsAb.short molecule.

In summary, we investigated the potential application of the Fab x sdAb-Fc bispecific format for T-cell mediated tumor cell killing. We demonstrated that a TbsAb with a shorter distance between the two arms allows for a tighter bridging between the tumor cells and the effector T cells, subsequently leading to a more robust T cell activation and in turn greater tumor cell killing. Instead of comparing different bispecific formats [14,30–36], here, we demonstrated that by already changing a dozen of the amino acids in the hinge region in the same bispecific format could induce a substantial impact on its cytotoxic activity. So far, our data have been limited to mouse antibody constructs. However, the hinge length of human antibodies differs from that of mouse antibodies. Therefore, additional research might be needed to apply our findings to human antibody constructs. Nonetheless, our data strongly suggest that the development of human Fab x sdAb-Fc TbsAb for the treatment of cancers could potentially benefit from a shortened hinge design. Therefore, our data indicate that the modulation of the ‘hinge region length’ parameter could potentially also be applied to other IgG-like TbsAb formats in order to optimize their efficacy.

4. Materials and Methods

4.1. Cell Lines

CHO.K1 and CHO/mEGFR cell lines were described in our previous study [8]. Mouse ovarian cancer surface epithelial cell line (ID8) was kindly provided by Professor Rose Zamoyska, the cells were cultured in IMDM (ThermoFisher Scientific, UK #I3390-500ML) supplemented with 10% FBS (Gibco, UK #10500-064), 1% L-glutamine (ThermoFisher Scientific, UK #25030-081), 0.1% 2-mercaptoethanol (Sigma-Aldrich) in 10-cm-Petri dishes and incubated at 37 °C. ID8/mEGFR^{-/-} cell line was generated by CRISP/Cas9 gene-editing system. Cloning was performed using Truecut V2 cas9 (ThermoFisher Scientific). ID8 cells were transfected with CRISPR plasmid-containing gRNA for mEGFR-KO by electroporation (1600V, 10ms, 3 pulses) using the InvitrogenTM NeonTM Transfection System (ThermoFisher Scientific). TRACR RNA was obtained from Integrated DNA technologies and the gRNA sequence is 50 CCTCATTGCCCTCAACACCG 30. The transfected cells were cultured with IMDM (ThermoFisher Scientific, UK #I3390-500ML) for 4 days before sorting. Cells were stained with HcAb anti-mouse EGFR (clone RR359), followed by anti-mouse IgG2a-PE (1:100). Using the BD FACSAriaTM II sorter, the mEGFR⁻ ID8 population was bulk-

sorted based on mEGFR expression. Sorted ID8 clones without mEGFR expression were isolated and expanded.

OT-1 cells were derived from spleens of OT-1 Rag1^{-/-} (C57BL/6) mice. Spleens were gently dissociated mechanically through a 70 µm filter. The suspension was then centrifuged at 300g at 4°C for 5 min, the supernatant discarded, and RBC lysis buffer (Sigma-Aldrich, UK #R7757-100ML) was added. The suspension was incubated for 5 min at room temperature, cells were then centrifuged again and the pellet was resuspended in IMDM. Cells were counted and cultured in IMDM (ThermoFisher Scientific, UK #I3390-500ML) supplemented with 10% FBS (Gibco, UK #10500-064), 1% L-glutamine (ThermoFisher Scientific, UK #25030-081), 0.1% 2-mercaptoethanol (Sigma-Aldrich, USA #M6250) in 10 cm petri dishes and incubated at 37°C.

4.2. Designation and Construction of Expression Vectors for Bispecific Antibodies

By using the established duobody platform, we designed IgG2a-mCD3E x mEGFR TbsAbs in a Fab x sdAb-Fc format previously developed by Huang et al. with two different hinge lengths. These comprised (i) the variable light chain (VL) and variable heavy chain (VH) domains of 2c11, an anti-mCD3E monoclonal antibody, (ii) VH domain of anti-mEGFR single domain antibody RR359, and (iii) a mouse IgG2a Fc module with duobody mutations for heterodimerization.

The anti-mEGFR sdAb (RR359) was described previously and the amino acid sequence of anti-mCD3E (2c11) was obtained from the IMGT database [8,37]. The amino acid mutations introduced to each vector to allow heavy-heavy chain heterodimerization are depicted in Figure 3C. T370K and K409R point mutations were introduced to the CH3 region of heavy chain only anti-mEGFR antibody RR359. F405L and R411T point mutations were introduced to the CH3 region of the conventional anti-mCD3E antibody 2c11. In addition, L234A, L235A, and P329G (LALA-PG) mutations were introduced to the Fc domain of each 2c11 and RR359 sequence to silence their Fc-mediated effector functions. The amino acid sequences of the expressed constructs are shown in supplementary Table S1. The parental mAb expression vectors were constructed by de novo synthesis (GeneArt, ThermoFisher Scientific).

Two different hinge constructs were produced by introducing different linkers in the parental anti-mEGFR plasmids. For the short hinge design, a

full mouse IgG2a linker was introduced (EPKGPTIKPCPPCKCPAPNLLGG) between the sdAb part and the Fc part of RR359 antibody. For the long hinge design, a camelid/mouse chimeric linker (EPKIPQPQPKPQPQPQPQPKPQPKPCPPCKCPAPNLLGG) was introduced between the sdAb part and Fc domain of the RR359 antibody (Figure 1). The expression vectors of these antibodies were constructed by de novo synthesis (GeneArt, ThermoFisher Scientific Scientific).

4.3. Generation of Bispecific Antibodies

FreeStyle™ 293-F cells (Invitrogen, UK # R79007) were grown in FreeStyle 293 Expression medium (Invitrogen, UK #12338-018). Each relevant heavy and light chain expression vector was co-transfected into FreeStyle™ 293-F cells (Invitrogen, UK # R79007), using 293fectin™ reagent (Invitrogen, UK #12347-019) according to the manufacturer's recommended conditions. At 7-days post-transfection, the antibodies were purified by protein A affinity chromatography (Peptide Synthetics), dialyzed overnight to PBS (Gibco, UK #D8537-500ML), and filter-sterilized over 0.22- μ m filters. Antibody concentration was calculated based on the Beer-Lambert Law, $A = \epsilon \times b \times c$, (A is the A280 absorbance, b is the path length, c is the analyte concentration, and ϵ is the wavelength-dependent molar absorptivity coefficient with units of $M^{-1} \text{ cm}^{-1}$). A280 absorbance was measured by spectrophotometry using a Nanodrop ND-1000 system (ThermoFisher Scientific). Equimolar amounts of relevant parental antibodies were mixed and incubated with 2-mercaptoethylamine (2-MEA; Sigma, Switzerland #30078-25G) at a final concentration of 1 mg/mL total antibody in PBS (Gibco, UK #D8537-500ML). The final concentration of 2-MEA was 75 mM. The mixtures were incubated for 5 h at 31 °C. The mixtures were then buffer-exchanged against PBS using Slide-A-Lyzer cassettes (ThermoFisher Scientific, USA #66380) to remove 2-MEA. Samples were stored overnight at 4 °C to allow for the re-oxidation of the disulfide bonds. Bispecific antibody concentration was calculated as previously described. The purity of TbsAbs was evaluated by SDS-PAGE in reducing and non-reducing conditions.

4.4. Generation of Control TbsAb by Mutagenesis

The three-dimensional structure model of mEGFR sdAb was predicted by ColabFold, which combines a protein homolog search MMseqs2 with AlphaFold2(<https://colab.research.google.com/github/sokrypton/ColabFold/>

blob/main/AlphaFold2.ipynb, accessed on 1 June 2021). The mutations were introduced into the mEGFR binding CDR3 of the RR359.short antibody sequence by site-directed mutagenesis by PCR. mEGFR-His recombinant protein (R&D systems) was diluted to 50 mM in 10 mM acetate pH 5.0 (ForteBio, USA #18-1069) and loaded on NHS/EDC activated AR2G biosensors (ForteBio, USA #18-5088). HcAb.mEGFR antibodies with different mutations were diluted to 20 $\mu\text{g}/\text{mL}$ in 10x kinetic buffer (ForteBio, USA #18-1092) and associated to mEGFR-His protein and 10 x kinetic buffer was used as negative control. Binding kinetics were measured by the Octet system according to the manufacturer's instructions (ForteBio). Data was analyzed using data analysis software HT V10.0 (ForteBio). Signal of negative control was subtracted in the BLI experiment. cFAE was performed as described above, using parental antibodies HcAb.mEGFR with short hinge and D105A mutation and mCD3E mAb to generate the TbsAb.con.

4.5. Size-Exclusion Chromatography (HP-SEC)

Aggregation and degradation of TbsAbs were quantified by SEC. Ten μL of each respective sample (TbsAb.long and TbsAb.short), at 0.5 mg/mL were loaded (20 μL load volume) onto a calibrated Superdex-200 Increase 3.2/300 GL (Cytiva, UK #28990946) size exclusion column pre-equilibrated in PBS, pH 7.4, at 8 C and run with a flow rate of 50 $\mu\text{L} \cdot \text{min}^{-1}$ on an ÄKTA PURE Micro™ LC system (Cytiva, UK # 29302479). Elution was monitored at 220 nm, 256 nm, and 280 nm, with 2.5 s integration. The concentration of protein in respective peaks was calculated using the peak analysis software (with a morphological baseline with a skim value of 7.0) provided with the instrument (UNICORN v7.7™; Cytiva) and the relative purity was calculated as a percentage of all integrated peaks.

4.6. In Vitro Cytotoxicity Assays

Naïve OT-1 cells (enriched from spleens of OT-1 Rag1^{-/-} mice) were activated by exposure to ovalbumin peptide SIINFEKL (2 ng/mL, Peptide Synthetics) for 48 h. LDH method: Target cells were seeded in IMDM (ThermoFisher Scientific, UK #I3390-500ML) with 10% FBS (ThermoFisher Scientific, UK #10500-064) at a density of 1×10^4 cells/well on a 96-well flat-bottom cell culture plate. Five-fold serial gradient dilution of either TbsAb.long, TbsAb.short, or TbsAb.con was performed in a complete medium, starting with a 16.8 nM (2 $\mu\text{g}/\text{mL}$) concentration and incubated for 0.5 h. Samples were added to corresponding wells at a final volume of 150

Enhanced T-Cell killing of tumor cells by shortened hinge design

μL. Subsequently, in IMDM with 10% inactivated FBS medium, OT-1 cells were adjusted to 5×10^4 cells/well added into the plate at an effector cell: tumor cell (E:T) ratio of 5:1. The cytotoxicity assay was detected after plates were incubated at 37 °C for 24 h from supernatant samples using CytoTox96® Non-Radioactive LDH Kit (Promega, USA #G1781). The cytotoxicity percentages were calculated following the manufacturer's instructions as shown here:

$$\text{Cytotoxicity \%} = \frac{\text{signal (Experimental)} - \text{Effector spontaneous}}{\text{signal (Target maximum)} - \text{signal(target spontaneous)}} \times 100\%$$

Flow cytometry method: ID8 cells and ID8 mEGFR^{-/-} cells were labeled by eFluo 450 or eFluor 670, respectively. ID8 cells and ID8 mEGFR^{-/-} were seeded in IMDM (ThermoFisher Scientific, UK #I3390-500ML) with 10% FBS (ThermoFisher Scientific, UK #10500-064) at a density of 2×10^4 cells/well on a 96-well flat-bottom cell culture plate. Five-fold serial gradient dilution of either TbsAb.long, TbsAb.short, or TbsAb.con was performed in a complete medium, starting with a 16.8 nM (2 μg/mL) concentration and incubated for 0.5 h. PBS treated samples were used as negative control. Samples were added to corresponding wells at a final volume of 150 μL. Subsequently, in IMDM with 10% inactivated FBS medium, OT-1 cells were adjusted to 1×10^5 cells/well added into the plate at an effector cell: tumor cell (E:T) ratio of 5:1. The OT-1 cells were washed off by PBS after 24 h incubation. Remaining attached ID8 and ID8 mEGFR^{-/-} cells were detected by flow cytometry. The ID8 lysis percentages were calculated following the formula as shown here:

$$\text{ID8 lysis \%} = \left[1 - \frac{\text{number of Pacific blue positive cells(TRBA treated)}}{\text{number of Pacific blue positive cells(PBS treated)}} \right] \times 100\%$$

All tests were repeated in triplicates and linear or nonlinear regression analysis to fit dose-response curves were assayed with GraphPad Prism Version 8.0.

4.7. Microscopy

Ovalbumin peptide SIINFEKL activated OT-1s were incubated with CHO/mEGFR cells in the presence of TbsAb.con, TbsAb.long or TbsAb.short respectively for 24 h. Images of activated OT-1s were taken

with an EVOS M7000 microscope under 4 x magnification. T cell blasts analysis was performed using EVOS analysis software to count the number and calculate the area of T cell blasts in each group. T cell blasts in randomly selected 20 grids (500 μm x 500 μm) of each photo were counted and calculated for analyzing.

4.8. Cell-Cell Association Assays

OT-1 cells were labelled with fixable viability dye eFluor 670 (eBiosciences, USA #65-0840-85) as effector cells and ID8 cells were labelled with fixable viability dye eFluor 450 (eBiosciences, USA #65-0842-85) as target cells, according to the manufacturer's instructions. Mixtures of 5×10^4 cells of each labelled cell line were incubated together at 4 °C for 45 min in a 96-round bottom plate, with 5-fold serially diluted TbsAb.long, TbsAb.short, or TbsAb.con in FACS buffer (PBS supplemented with 1% BSA + 1% EDTA, Gibco), starting with an 84 nM (10 $\mu\text{g}/\text{mL}$) concentration. All tests were repeated in duplicates. Cells were then washed in FACS buffer and resuspended in 200 μL for analysis on a FACSCanto II flow cytometer (BD Biosciences). Data were analyzed using FlowJo v.10.8.0 software (BD Biosciences), and GraphPad Prism Version 9.0 software. Ten thousand events were collected.

4.9. T Cell Activation Assays

Freshly isolated splenocytes from the WT C57BL/6 mice (1×10^5 cells/mL) were treated with either TbsAb.long, TbsAb.short or TbsAb.con at 3.36 nM (0.4 $\mu\text{g}/\text{mL}$) and incubated with ID8 target cells (2×10^4 cells/mL) in 96-well plates for 18 h. The splenocytes were collected and stained with CD8-APC (eBioscience, USA #17-0081-83), CD4-Pacific blue (eBioscience, USA, #57004282) and CD69-PE (PharMingen, USA #553237)/CD25-PE (PharMingen, USA #09985B). Cells were counted by flow cytometry on a FACSCanto II system (BD Biosciences) and data were analyzed with FlowJo v.10.8.0 software (BD Biosciences). Percentage of PE positive cells and mean fluorescence intensities (MFI) were used for statistical analysis using GraphPad Prism version 9.0 software.

4.10. Statistical Analysis

Statistical analyses were performed using Prism software version 9.0 (GraphPad). P values were determined for comparisons between TbsAb.long and TbsAb.short-mediated T-cell cytotoxicity by paired T-test

and T-cell activation by unpaired t-test. p values for comparisons between TbsAb.long and TbsAb.short-mediated cell-cell association were determined by 2-way ANOVA test. For all statistical tests, results with a p value <0.05 were considered significant. *: p < 0.05; **: p < 0.01; ***: p < 0.001.

Supplementary Materials: The following supporting information can be downloaded at: <https://www.mdpi.com/article/10.3390/biom12101331/s1>, Figure S1: Monomericity of each parental antibody (RR359.long, RR359.short and 2c11) analyzed by size-exclusion chromatography (SEC); Figure S2: Length of antibody CH1 evaluated by Discovery Studio; Figure S3: Prediction quality judged by visualizing multiple sequence alignments (MSA) depth and showing the AlphaFold2 confidence measures; Figure S4: Raw data binding kinetics of HcAb.RR359 with different mutations to AR2G-sensor bound mEGFR-His protein as measured by BLI on an Octet machine; Figure S5: Purity of TbsAb.con evaluated by SDS-Page at non-reducing condition; Figure S6: The gating strategy for the T-cells shown in Figure 6; Table S1: The amino acid sequences of the expressed constructs.

Author Contributions: S.H., A.S. and C.V. prepared BsAb samples. S.H. and A.S. performed the experiments with support by D.W. M.W. helped with the analysis of flow cytometry data. S.H. and C.V. drafted the manuscript. S.M.J.v.D. designed BsAb constructs. D.M.Z., A.J.A.M.S., S.M.J.v.D., and A.v.E. designed and discussed the study. All authors have read and agreed to the published version of the manuscript.

Funding: This research was funded by the European Union, Horizon 2020 research and innovation programme under the Marie Skłodowska-Curie Innovative Training Networks [grant number 765394, 2018]. Further support came from the Edinburgh Protein Production Facility (EPPF) and the Centre Core Grants (092076 and 203149) to the Wellcome Centre for Cell Biology at the University of Edinburgh.

Conflicts of Interest: The authors declare no conflict of interest.

Supplementary

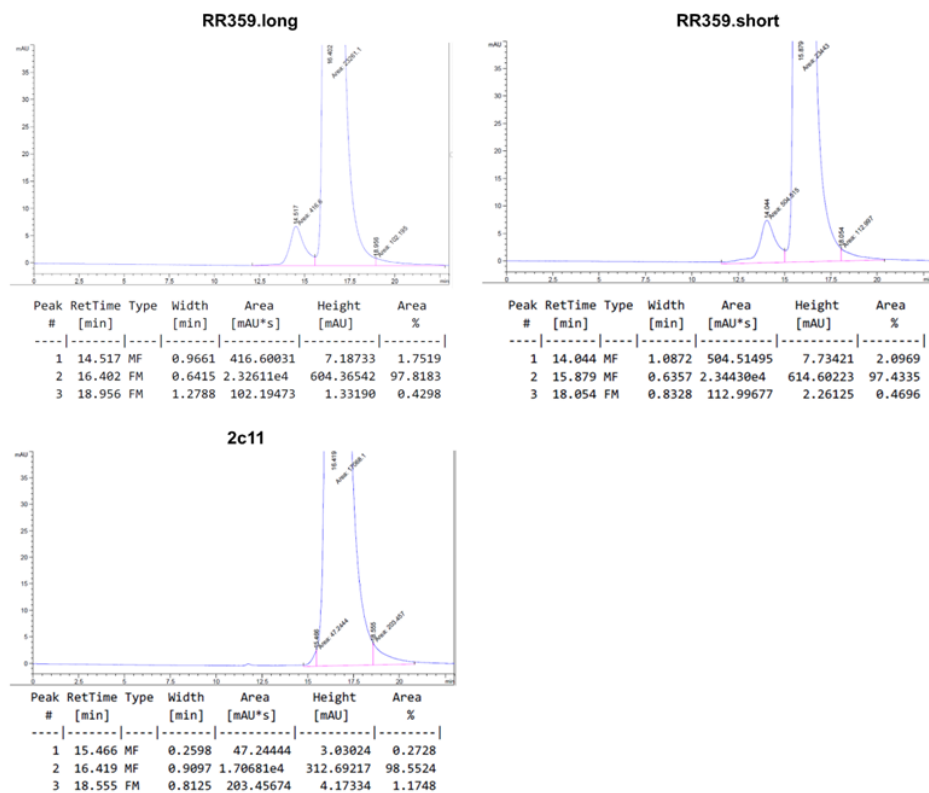


Figure S1. Monomericity of each parental antibody (RR359.long, RR359.short and 2c11) analyzed by size-exclusion chromatography (SEC).

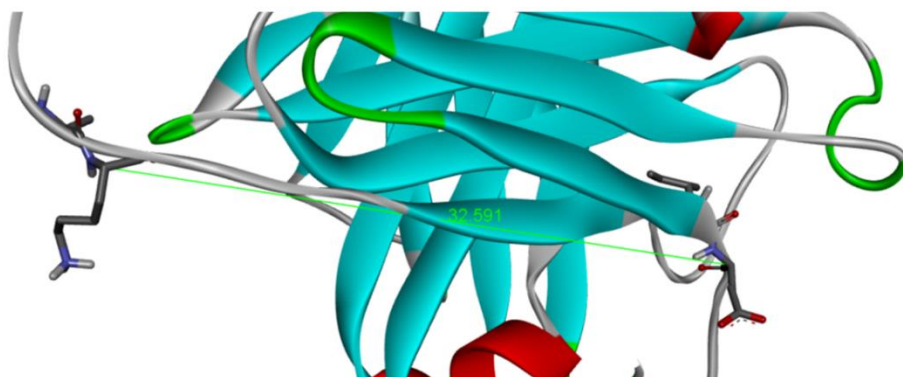


Figure S2. Length of antibody CH1 evaluated by Discovery Studio (used

PDB ID 3R06 as template).

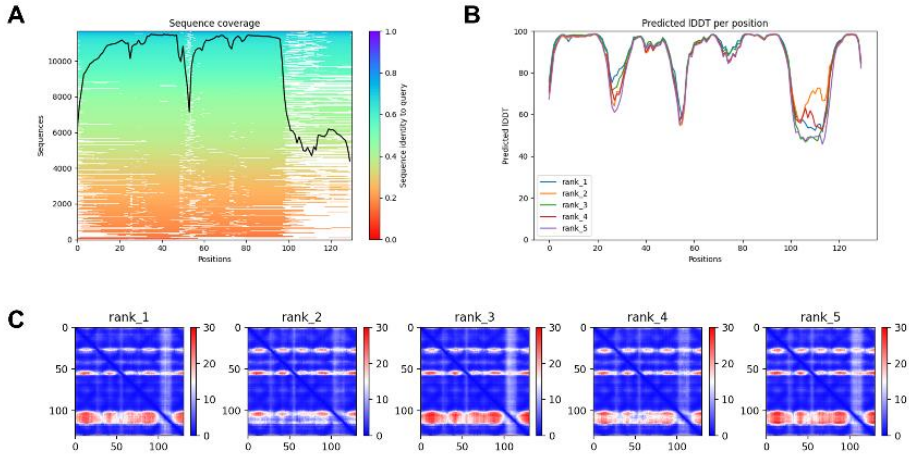


Figure S3. Prediction quality judged by visualizing multiple sequence alignments (MSA) depth and showing the AlphaFold2 confidence measures. (A) Multiple se-quence alignments. Number of sequences per position, the higher the better. (B) Pre-dicted local distance difference test (IDDT) per position. Model confidence (out of 100) at each position. The higher the better. (C) Predicted alignment error (PAE). A useful metric to assess how confident the model is about the interface. The lower the better. Rank 1 structure was used in this study.

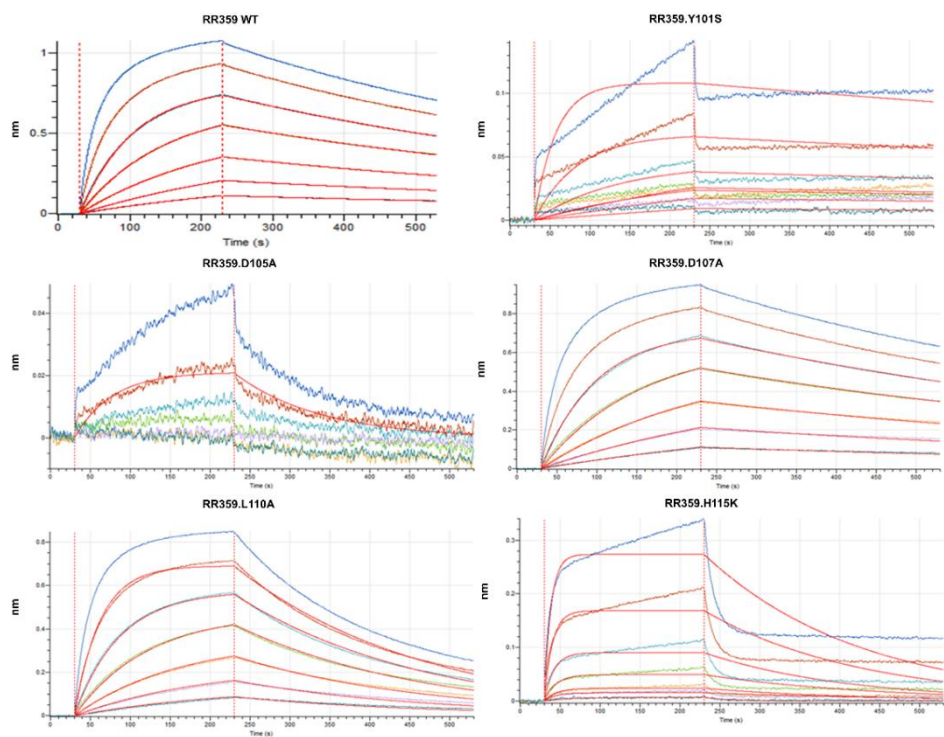


Figure S4. Raw data binding kinetics of HcAb.RR359 with different mutations to AR2G-sensor bound mEGFR-His protein as measured by BLI on an Octet machine.

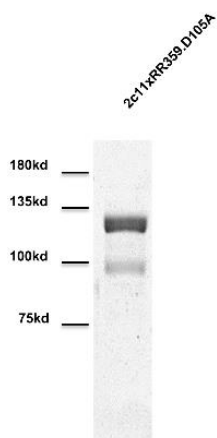


Figure S5. Purity of TbsAb.con evaluated by SDS-Page at non-reducing condition.

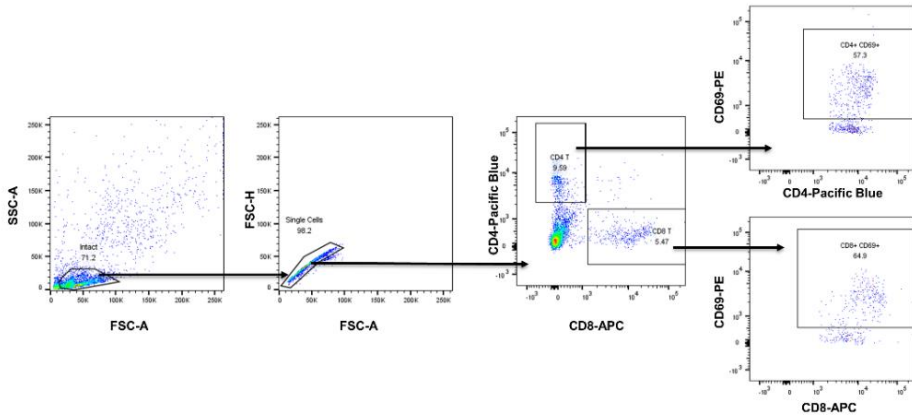


Figure S6. The gating strategy for the T-cells shown in Figure 6.

Supplementary Table 1.

RR359(anti-EGFR)-long-migg2a.LALAPG.T370K.K409R
QVQLQESGGGLVQAGGSLRLSCAASGRTFTSYAMGWFRQVPGKERE FVAALSTRSAGNTYYADSVKGRFTISRDNANKNTVYVLQMSSLKAEDTA VYYCAAGYMSSDADPSLAASLHPYDYWGQGTQVTVSSEPKIPQPQP KPQPQPQPQPKPQPKPCPPCKCPAPNAAGGPSVFIFPPKIKDVLMLISL SPMVT CVVVDVSEDDPDVQISWVFNNEVLTAQTQTHREDYNSTLR VVSALPIQHQDWMSGKEFKCKVNNKALGAPIERTISKPKGSVRAPQV YVLPPEEEMTKKQVTLT CMVKDFMPEDIYVEWTNNGKTELNYKNT EPVLDS DGSYFMYSRLRVEKKNWVERNSYSCSVVHEGLHNHHTTKS FSRTPGK
RR359(anti-EGFR)-sh-migg2a.LALAPG.T370K.K409R
QVQLQESGGGLVQAGGSLRLSCAASGRTFTSYAMGWFRQVPGKERE FVAALSTRSAGNTYYADSVKGRFTISRDNANKNTVYVLQMSSLKAEDTA VYYCAAGYMSSDADPSLAASLHPYDYWGQGTQVTVSSEPKGPTIKPC PPCKCPAPNAAGGPSVFIFPPKIKDVLMLISLSPMVT CVVVDVSEDDPD VQISWVFNNEVLTAQTQTHREDYNSTLRVVSALPIQHQDWMSGKE FKCKVNNKALGAPIERTISKPKGSVRAPQVYVLPPEEEMTKKQVTLT CMVKDFMPEDIYVEWTNNGKTELNYKNTEPVLDS DGSYFMYSRLRV EKKNWVERNSYSCSVVHEGLHNHHTTKSFSRTPGK
RR359(anti-EGFR)-sh-migg2a.D105A.LALAPG.T370K.K409R
QVQLQESGGGLVQAGGSLRLSCAASGRTFTSYAMGWFRQVPGKERE FVAALSTRSAGNTYYADSVKGRFTISRDNANKNTVYVLQMSSLKAEDTA VYYCAAGYMSSAADPSLAASLHPYDYWGQGTQVTVSSEPKGPTIKPC PPCKCPAPNAAGGPSVFIFPPKIKDVLMLISLSPMVT CVVVDVSEDDPD VQISWVFNNEVLTAQTQTHREDYNSTLRVVSALPIQHQDWMSGKE FKCKVNNKALGAPIERTISKPKGSVRAPQVYVLPPEEEMTKKQVTLT CMVKDFMPEDIYVEWTNNGKTELNYKNTEPVLDS DGSYFMYSRLRV EKKNWVERNSYSCSVVHEGLHNHHTTKSFSRTPGK
2c11(anti-CD3)-migg2a.LALAPG.F405L.R411T
EVQLVESGGGLVQPGLSLKLSCEASGFTFSGYGMHWVRQAPGRGLES VAYITSSINIKYADAVKGRFTVSRDNANKNLLFLQMNILKSEDTAMYY CARFDWDKNYWGQGTMTVTVSSAKTTAPSVYPLAPVCGDITGSSVTL GCLVKGYFPEPVTLTWNSGSLSSGVHTFPAVLQSDLYTLSSSVTVTSST WPSQSITCNVAHPASSTKVDKIEPRGPTIKPCPPCKCPAPNAAGGPS VFIFPPKIKDVLMLISLSPMVT CVVVDVSEDDPDVQISWVFNNEVLTA QTQTHREDYNSTLRVVSALPIQHQDWMSGKEFKCKVNNKALGAPIE

RTISKPKGSVRAPQVYVLPPEEEMTKKQVTLTCMVTDMPEDIYVE
WTNNGKTELNYKNTEPVLDSG SYLMYSKLTVEKKNWVERNSYSCS
VVHEGLHNHHTTKSFSRTPGK

2c11(anti-CD3), light chain

DIQMTQSPSSLPASLGDRVTINCQASQDISNYLNWYQQKPGKAPKLLI
YYTNKLADGVPSRFSGSGSGRDSSFTISSLESEDIGSYQCQQYYNYPWT
FGPGTKLEIKRADAAPTVSIFPPSEQLTSGGASVVCFLNMFYPKDINV
KWKIDGSRQNGVLNSWTDQDSKDYMSSTLTLTKDEYERHNSYT
CEATHKTSTSPIVKSFNREK

References

1. Blanco, B.; Compte, M.; Lykkemark, S.; Sanz, L.; Alvarez-Vallina, L. T Cell-Redirecting Strategies to 'STAb' Tumors: Beyond CARs and Bispecific Antibodies. *Trends Immunol.* 2019, 40, 243–257.
2. Seimetz, D.; Lindhofer, H.; Bokemeyer, C. Development and Approval of the Trifunctional Antibody Catumaxomab (Anti-EpCAManti-CD3) as a Targeted Cancer Immunotherapy. *Cancer Treat. Rev.* 2010, 36, 458–467.
3. Przepiorka, D.; Ko, C.-W.; Deisseroth, A.; Yancey, C.L.; Candau-Chacon, R.; Chiu, H.-J.; Gehrke, B.J.; Gomez-Broughton, C.; Kane, R.C.; Kirshner, S.; et al. FDA Approval: Blinatumomab. *Clin. Cancer Res.* 2015, 21, 4035–4039.
4. Huang, S.; van Duijnhoven, S.M.J.; Sijts, A.J.A.M.; van Elsas, A. Bispecific Antibodies Targeting Dual Tumor-Associated Antigens in Cancer Therapy. *J. Cancer Res. Clin. Oncol.* 2020, 146, 3111–3122.
5. Strohl, W.R.; Naso, M. Bispecific T-Cell Redirection versus Chimeric Antigen Receptor (CAR)-T Cells as Approaches to Kill Cancer Cells. *Antibodies* 2019, 8, 41.
6. Wang, Q.; Chen, Y.; Park, J.; Liu, X.; Hu, Y.; Wang, T.; McFarland, K.; Betenbaugh, M.J. Design and Production of Bispecific Antibodies. *Antibodies* 2019, 8, 43.
7. Schaefer, W.; Regula, J.T.; Böhner, M.; Schanzer, J.; Croasdale, R.; Dürr, H.; Gassner, C.; Georges, G.; Kettenberger, H.; Imhof-Jung, S.; et al. Immunoglobulin Domain Crossover as a Generic Approach for the Production of Bispecific IgG Antibodies. *Proc. Natl. Acad. Sci. USA* 2011, 108, 11187–11192.
8. Huang, S.; Segués, A.; Hulsik, D.L.; Zaiss, D.M.; Sijts, A.J.A.M.; van Duijnhoven, S.M.J.; van Elsas, A. A Novel Efficient Bispecific Antibody Format, Combining a Conventional Antigen-Binding Fragment with a Single Domain Antibody, Avoids Potential Heavy-Light Chain Mis-Pairing. *J. Immunol. Methods* 2020, 483, 112811.
9. Ellerman, D. Bispecific T-Cell Engagers: Towards Understanding Variables Influencing the in Vitro Potency and Tumor Selectivity and Their Modulation to Enhance Their Efficacy and Safety. *Methods* 2019, 154, 102–117.
10. Dickopf, S.; Georges, G.J.; Brinkmann, U. Format and Geometries Matter: Structure-Based Design Defines the Functionality of Bispecific Antibodies. *Comput. Struct. Biotechnol. J.* 2020, 18, 1221–1227.

11. Klein, D.; Jacobs, S.; Sheri, M.; Anderson, M.; Attar, R.; Barnakov, A.; Brosnan, K.; Bushey, B.; Chevalier, K.; Chin, D.; et al. Abstract LB-312: Bispecific Centyrin Simultaneously Targeting EGFR and c-Met Demonstrates Improved Activity Compared to the Mixture of Single Agents. *Cancer Res.* 2013, 73, LB-312.
12. Wuellner, U.; Klupsch, K.; Buller, F.; Attinger-Toller, I.; Santimaria, R.; Zbinden, I.; Henne, P.; Grabulovski, D.; Bertschinger, J.; Brack, S. Bispecific CD3/HER2 Targeting FynomAb Induces Redirected T Cell-Mediated Cytolysis with High Potency and Enhanced Tumor Selectivity. *Antibodies* 2015, 4, 426–440.
13. Santich, B.H.; Park, J.A.; Tran, H.; Guo, H.-F.; Huse, M.; Cheung, N.-K.V. Interdomain Spacing and Spatial Configuration Drive the Potency of IgG-[L]-ScFv T Cell Bispecific Antibodies. *Sci. Transl. Med.* 2020, 12, eaax1315.
14. Moore, P.A.; Zhang, W.; Rainey, G.J.; Burke, S.; Li, H.; Huang, L.; Gorlatov, S.; Veri, M.C.; Aggarwal, S.; Yang, Y.; et al. Application of Dual Affinity Retargeting Molecules to Achieve Optimal Redirected T-Cell Killing of B-Cell Lymphoma. *Blood* 2011, 117, 4542–4551.
15. Li, J.; Stagg, N.J.; Johnston, J.; Harris, M.J.; Menzies, S.A.; DiCara, D.; Clark, V.; Hristopoulos, M.; Cook, R.; Slaga, D.; et al. Membrane-Proximal Epitope Facilitates Efficient T Cell Synapse Formation by Anti-FcRH5/CD3 and Is a Requirement for Myeloma Cell Killing. *Cancer Cell* 2017, 31, 383–395.
16. Bluemel, C.; Hausmann, S.; Fluhr, P.; Sriskandarajah, M.; Stallcup, W.B.; Baeuerle, P.A.; Kufer, P. Epitope Distance to the Target Cell Membrane and Antigen Size Determine the Potency of T Cell-Mediated Lysis by BiTE Antibodies Specific for a Large Melanoma Surface Antigen. *Cancer Immunol. Immunother.* 2010, 59, 1197–1209.
17. James, S.E.; Greenberg, P.D.; Jensen, M.C.; Lin, Y.; Wang, J.; Till, B.G.; Raubitschek, A.A.; Forman, S.J.; Press, O.W. Antigen Sensitivity of CD22-Specific Chimeric TCR Is Modulated by Target Epitope Distance from the Cell Membrane. *J. Immunol.* 2008, 180, 7028–7038.
18. Root, A.R.; Cao, W.; Li, B.; LaPan, P.; Meade, C.; Sanford, J.; Jin, M.; O'Sullivan, C.; Cummins, E.; Lambert, M.; et al. Development of PF-06671008, a Highly Potent Anti-P-Cadherin/Anti-CD3 Bispecific DART Molecule with Extended Half-Life for the Treatment of Cancer. *Antibodies* 2016, 5, 6.
19. Qi, J.; Li, X.; Peng, H.; Cook, E.M.; Dadashian, E.L.; Wiestner, A.; Park, H.; Rader, C. Potent and Selective Antitumor Activity of a T Cell-Engaging Bispecific Antibody Targeting a Membrane-Proximal Epitope of ROR1. *Proc.*

Natl. Acad. Sci. USA 2018, 115, E5467–E5476.

20. Chu, T.H.; Patz, E.F.; Ackerman, M.E. Coming Together at the Hinges: Therapeutic Prospects of IgG3. *mAbs* 2021, 13, 1882028.

21. Wang, F.; Tsai, J.C.; Davis, J.H.; Chau, B.; Dong, J.; West, S.M.; Hogan, J.M.; Wheeler, M.L.; Bee, C.; Morishige, W.; et al. Design and Characterization of Mouse IgG1 and IgG2a Bispecific Antibodies for Use in Syngeneic Models. *mAbs* 2019, 12, 1685350.

22. Griffin, L.M.; Snowden, J.R.; Lawson, A.D.G.; Wernery, U.; Kinne, J.; Baker, T.S. Analysis of Heavy and Light Chain Sequences of Conventional Camelid Antibodies from *Camelus Dromedarius* and *Camelus Bactrianus* Species. *J. Immunol. Methods* 2014, 405, 35–46.

23. Bailey, M.J.; Duehr, J.; Dulin, H.; Broecker, F.; Brown, J.A.; Arumemi, F.O.; Bermúdez González, M.C.; Leyva-Grado, V.H.; Evans, M.J.; Simon, V.; et al. Human Antibodies Targeting Zika Virus NS1 Provide Protection against Disease in a Mouse Model. *Nat. Commun.* 2018, 9, 4560.

24. Choi, B.D.; Gedeon, P.C.; Kuan, C.-T.; Sanchez-Perez, L.; Archer, G.E.; Bigner, D.D.; Sampson, J.H. Rational Design and Generation of Recombinant Control Reagents for Bispecific Antibodies through CDR Mutagenesis. *J. Immunol. Methods* 2013, 395, 14–20.

25. Mirdita, M.; Schütze, K.; Moriwaki, Y.; Heo, L.; Ovchinnikov, S.; Steinegger, M. ColabFold: Making Protein Folding Accessible to All. *Nat. Methods* 2022, 19, 679–682.

26. Nair-Gupta, P.; Diem, M.; Reeves, D.; Wang, W.; Schulingkamp, R.; Sproesser, K.; Mattson, B.; Heidrich, B.; Mendonça, M.; Joseph, J.; et al. A Novel C2 Domain Binding CD33CD3 Bispecific Antibody with Potent T-Cell Redirection Activity against Acute Myeloid Leukemia. *Blood Adv.* 2020, 4, 906–919.

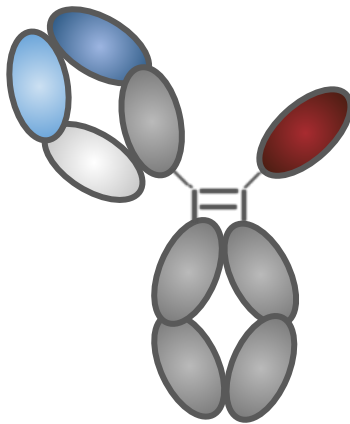
27. Chen, W.; Yang, F.; Wang, C.; Narula, J.; Pascua, E.; Ni, I.; Ding, S.; Deng, X.; Chu, M.L.-H.; Pham, A.; et al. One Size Does Not Fit All: Navigating the Multi-Dimensional Space to Optimize T-Cell Engaging Protein Therapeutics. *mAbs* 2021, 13, 1871171.

28. Kapelski, S.; Cleiren, E.; Attar, R.M.; Philippar, U.; Häslar, J.; Chiu, M.L. Influence of the Bispecific Antibody IgG Subclass on T Cell Redirection. *mAbs* 2019, 11, 1012–1024.

29. Aleksic, M.; Dushek, O.; Zhang, H.; Shenderov, E.; Chen, J.-L.; Cerundolo, V.; Coombs, D.; van der Merwe, P.A. Dependence of T Cell Antigen Recognition on T Cell Receptor-Peptide MHC Confinement Time. *Immunity* 2010, 32, 163–174.

30. Ellwanger, K.; Reusch, U.; Fucek, I.; Knackmuss, S.; Weichel, M.; Gantke, T.; Molkenhain, V.; Zhukovsky, E.A.; Tesar, M.; Treder, M. Highly Specific and Effective Targeting of EGFRvIII-Positive Tumors with TandAb Antibodies. *Front. Oncol.* 2017, 7, 100.
31. Kipriyanov, S.M.; Moldenhauer, G.; Schuhmacher, J.; Cochlovius, B.; Von der Lieth, C.-W.; Matys, E.R.; Little, M. Bispecific Tandem Diabody for Tumor Therapy with Improved Antigen Binding and Pharmacokinetics. Edited by J. Karn. *J. Mol. Biol.* 1999, 293, 41–56.
32. Hoseini, S.S.; Guo, H.; Wu, Z.; Hatano, M.N.; Cheung, N.-K.V. A Potent Tetravalent T-Cell-Engaging Bispecific Antibody against CD3 in Acute Myeloid Leukemia. *Blood Adv.* 2018, 2, 1250–1258.
33. Harwood, S.L.; Alvarez-Cienfuegos, A.; Nuñez-Prado, N.; Compte, M.; Hernández-Pérez, S.; Merino, N.; Bonet, J.; Navarro, R.; Van Bergen en Henegouwen, P.M.P.; Lykkemark, S.; et al. ATTACK, a Novel Bispecific T Cell-Recruiting Antibody with Trivalent EGFR Binding and Monovalent CD3 Binding for Cancer Immunotherapy. *Oncol Immunology* 2018, 7, e1377874.
34. Kipriyanov, S.M.; Moldenhauer, G.; Strauss, G.; Little, M. Bispecific CD3 CD19 Diabody for T Cell-Mediated Lysis of Malignant Human B Cells. *Int. J. Cancer* 1998, 77, 763–772.
35. Feldmann, A.; Stamova, S.; Bippes, C.C.; Bartsch, H.; Wehner, R.; Schmitz, M.; Temme, A.; Cartellieri, M.; Bachmann, M. Retargeting of T Cells to Prostate Stem Cell Antigen Expressing Tumor Cells: Comparison of Different Antibody Formats. *Prostate* 2011, 71, 998–1011.
36. Durben, M.; Schmiedel, D.; Hofmann, M.; Vogt, F.; Nübling, T.; Pyz, E.; Bühring, H.-J.; Rammensee, H.-G.; Salih, H.R.; Große-Hovest, L.; et al. Characterization of a Bispecific FLT3 X CD3 Antibody in an Improved, Recombinant Format for the Treatment of Leukemia. *Mol. Ther.* 2015, 23, 648–655.
37. Zaiss, D.M.W.; van Loosdregt, J.; Gorlani, A.; Bekker, C.P.J.; Gröne, A.; Sibilia, M.; van Bergen en Henegouwen, P.M.P.; Roovers, R.C.; Coffey, P.J.; Sijts, A.J.A.M. Amphiregulin Enhances Regulatory T Cell-Suppressive Function via the Epidermal Growth Factor Receptor. *Immunity* 2013, 38, 275–284.

5



In a therapeutic setting, mouse IgG2a isotype is superior to mIgG1 or mIgE in controlling tumor growth

Natasa Vukovic^{1†}, Aina Segués^{1,2,†}, Shuyu Huang^{1,2,†}, Martin Waterfall¹, Alice J.A.M. Sijts², Dietmar M. Zaiss^{1,3,4,5*}

¹ Institute of Immunology and Infection Research, School of Biological Sciences, University of Edinburgh, Edinburgh, United Kingdom;

² Faculty of Veterinary Medicine, Department of Infectious Diseases and Immunology, Utrecht University, Utrecht, The Netherlands;

³ Department of Immune Medicine, University Regensburg, Regensburg, Germany;

⁴ Institute of Clinical Chemistry and Laboratory Medicine, University Hospital Regensburg, Regensburg, Germany;

⁵ Institute of Pathology, University Regensburg, Regensburg, Germany

† Authors contributed equally.

* Correspondence: e-mail address: dietmar.zaiss@ukr.de (D.M.Z)

Cancer Research Communications (2023) 3 (1): 109–118.

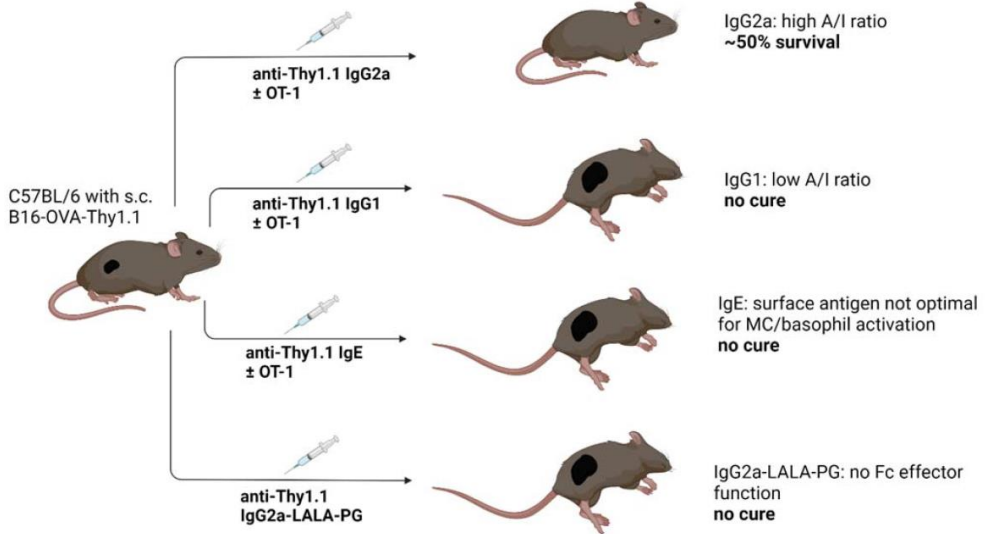
Contribution statement: Shuyu Huang designed the study together with other authors. Shuyu Huang helped the expression and purification of antibodies. Shuyu Huang contributed to the implementation of in vivo studies, to the analysis of the results.

Abstract

In the last decades, antibody based tumor therapy has fundamentally improved the efficacy of treatment for cancer patients. Currently, almost all tumor-antigen targeting antibodies approved for clinical application are of IgG1 Fc-isotype. Similarly, the mouse homolog mIgG2a is the most commonly used in tumor mouse models. However, in mice the efficacy of antibody based tumor therapy is largely restricted to a prophylactic application. Direct isotype comparison studies in mice in a therapeutic setting are scarce. In this study, we assessed the efficacy of mouse tumor targeting antibodies of different isotypes in a therapeutic setting using a highly systematic approach. To this end, we engineered and expressed antibodies of the same specificity but different isotypes, targeting the artificial tumor antigen CD90.1 / Thy1.1 expressed by B16 melanoma cells. Our experiments revealed that in a therapeutic setting mIgG2a was superior to both mIgE and mIgG1 in controlling tumor growth. Furthermore, the observed mIgG2a antitumor effect was entirely Fc-mediated as the protection was lost when antibodies with a Fc silenced mIgG2a isotype (LALA-PG mutations) was used. These data confirm mIgG2a superiority in a therapeutic tumour model.

Keywords: antibody isotype, tumor, igg2a, LALA-PG, therapeutic setting

Graphical Abstract



Introduction

Monoclonal antibodies (mAbs) are among the fastest-growing class of drugs, with more than 100 mAbs with marketing approval since 1986¹. Most of them belong to cancer therapeutics², where their introduction critically contributed to better outcomes and increased survival for different types of cancer. However, many patients are still unresponsive to such tumor-targeting antibody therapy, underlying the need for further optimisation of antibody-based approaches.

Most of the mAbs used in cancer therapy target tumor antigens which are, to varying extent, involved in tumor survival, growth and invasiveness. Interfering with tumor cell signalling pathways can induce tumor cell death on its own (e.g. anti-HER2, anti-EGFR)^{3,4}. However, despite the fact that almost all currently approved monoclonal antibodies have an IgG1 isotype, it has become increasingly apparent that Fc-mediated activation of the immune system substantially contributes to tumor cell destruction and the efficacy of treatment^{4,5}. With their Fc tail, antibodies can engage the complement system and different effector cells such as natural killer cells and macrophages, mediating antibody-dependent cell-mediated cytotoxicity (ADCC), antibody-dependent cell-mediated phagocytosis (ADCP) and complement-dependent cytotoxicity (CDC) against tumor cells^{5,6}. Since different antibody isotypes bind to different FcRs on immune cells and differ in their potential to activate the complement system, they can induce diverse immune responses. Thus, the downstream effector function is determined by antibody isotype.

For murine IgG antibodies, it has been established that mIgG2a offers superior activity to mIgG1, mostly due to differential affinity for activating and inhibitory FcRs, also defined as activating-to-inhibitory (A/I) ratio. Similar to human IgG1, mIgG2a has high A/I ratio reflecting its high affinity for activating FcRs and low affinity for the inhibitory one. In contrast, mIgG1 shows very low A/I ratio⁷. Thus, mIgG2a has been dominantly used as the most active antibody isotype in mouse tumor models, based on the seminal publication by Nimmerjahn et al⁸. Here, the tumor-targeting mIgG2a showed superior tumor control to mIgG1 in B16 lung metastasis model. However, the antibody treatment in this study was prophylactic, as it started on the same day when the tumor cells were injected. On the other hand, the same antibody typically failed to control the tumor growth in a therapeutic setting once the tumors are established⁹.

Therefore, the aim of this study was to compare the *in vivo* efficacy of

tumor-targeting antibodies of different isotypes in a therapeutic setting. To this end, we followed a similar approach as in the prophylactic setting⁸ and compared the therapeutic efficacy of one monoclonal antibody targeting Thy1.1 with either a mIgG2a, mIgG1 or mIgE isotype. Our results show that mIgG2a was superior to both mIgE and mIgG1 in controlling tumor growth in a therapeutic setting. Furthermore, the observed mIgG2a anti-tumor effect was entirely Fc-mediated as the protection was lost when a Fc-silenced mIgG2a isotype (via LALA-PG mutations) was used.

Materials and methods

Antibody design, production and purification

Amino acid sequences of all anti-Thy1.1 antibodies are provided in **supplementary table 1**. The design and production of murine anti-Thy1.1 IgG1 and IgE has been done as described before¹⁰. In short, the starting point was OX7 hybridoma (anti-Thy1.1 IgG1) which was sequenced in order to obtain heavy and light chain variable domain sequences (VH, VL). Next, we designed chimeric anti-Thy1.1 mIgE and mIgG1 heavy chains by combining the VH with the known sequences of the constant domains of murine IgE or IgG1 (CHs). Just between VH and CH domains, a unique restriction site (AfeI) was introduced, allowing us to change the isotypes by cloning. The IgG2a HC and the IgG2a HC featuring silencing LALA-PG mutations were cloned using standard cloning techniques from plasmids available in house (anti-Siglec and anti-TNFR2, respectively) into the pcDNA3.1(+) encoding for anti-Thy1.1_VH (Fig.1 A, B). Correct clones were confirmed by Sanger sequencing (GENEWIZ). The plasmid encoding for the anti-Thy1.1 light chain was de novo synthesized (GeneArt).

Anti-Thy1.1 IgG2a and anti-Thy1.1 IgG2a-LALA-PG were produced in ExpiCHO-S™ cells and FreeStyle293 cells, respectively, as described before¹⁰. Purification was done with MabSelect SuRe LX resin. Anti-Thy1.1 IgG2a had to be polished with preparative size-exclusion chromatography (SEC) (data not shown). Preparative SEC and the quality control consisting of UPLC-SEC, CE-SDS and SDS-PAGE were performed as described previously¹⁰.

Thy1.1 plasmids

Full-length Thy1.1 was cloned from pCR4-Blunt-TOPO into pcDNA3.1(+) with EcoRI and Apal two-step digestion, using a standard

cloning procedure. In short, digested bands of interest were excized from the gel and extracted with Qiagen Gel Extraction Kit, according to manufacturer's protocol. Dephosphorylation of the vector and subsequent ligation were done with Rapid DNA Dephos & Ligation Kit (Roche) in 1:3 vector:insert molar ratio. DH5 α competent cells were transformed with the ligation reaction and plated on LBampicillin plates. Colonies were picked, expanded and submitted to plasmid isolation with MidiPrep Kit (GenElute HP, Sigma). The correct clone was confirmed by Sanger sequencing with T7 promoter and BGH-R universal primers (Macrogen).

GPI anchor of Thy1 was replaced with MHC-1 transmembrane domain in the following way. Thy1.1 propeptide, which is removed when GPI is attached to Cys130 in the endoplasmic reticulum, was replaced with a part of MHC-1 molecule (Uniprot ID P01900) consisting of the connecting peptide, transmembrane domain and cytoplasmic region. pcDNA3.1(+)_Thy1.1-MHC-1 plasmid was de novo synthesized (Biomatik). Thy1.1-MHC-1 was cloned into a pSG5 vector using standard cloning techniques described above with EcoRI and BglII restriction enzymes in two-step digestion. The correct clone was confirmed by Sanger sequencing (University of Dundee). The amino acid sequence of the designed construct is given in **supplementary table 2**.

Cell culture

The B16-OVA cells with intracellular OVA were a kind gift from Ton Schumacher (The Netherlands Cancer Institute)¹¹. They were cultured in IMDM medium (Gibco) supplemented with 10% heat-inactivated Fetal Bovine Serum (Gibco), 1% penicillin/streptomycin (Gibco), 2mM L-glutamine (Gibco) and 50 μ M 2-mercaptoethanol (Gibco) (IMDM complete). CHO.K1 cells (ATCC) were cultured in DMEM/F12 medium (Gibco) supplemented with 5% New Born Calf Serum (Biowest) and 1% penicillin/streptomycin (Gibco).

Generation of B16-OVA-Thy1.1 stable cell line

The cells were co-transfected with 1.5 μ g of pSG5-Thy1.1-MHC-1 plasmid and 0.5 μ g of pLXSP plasmid coding for puromycin resistance with FuGENE HD reagent (Promega) in 6:1 FuGENE: DNA ratio. Briefly, the DNA was diluted in OptiMEM medium, after which FuGENE HD was added, and the mixture was incubated for 10 min at room temperature. The transfection mixture was added dropwise to the cells at 80% confluency. 24 h after transfection, 3 μ g/mL of puromycin was added to the culture medium, and

the cells were grown under puromycin pressure for 10-14 days. Selected cells were stained with 2 µg/mL of PE anti-Thy1.1 antibody (OX7 clone, Biolegend #202524) and single-cell sorted into 96-well plates containing the selection medium with puromycin. Thy1.1 expression was regularly monitored by flow cytometry with the antibody mentioned above on FACSCanto. Positive clones were expanded and the one showing stable Thy1.1 expression even after puromycin retrieval was selected for the in vivo study.

Thy1.1 transient transfection and cell ELISA

An amount of 24 µg of pcDNA3.1(+)-Thy1.1 plasmid was transfected into CHO.K1 cells (10 mm Petri dish, 80% confluent) using the lipofectamine 2000 reagent (Invitrogen) according to the manufacturer's recommendation. The following day, cells were plated into a 96-well plate (5×10^5 cells/well). Two days after transfection, an antibody binding ELISA was performed. The cell supernatant was discarded, and either anti-Thy1.1 IgE, IgG2a or IgG1 were added in serial dilutions. After incubation at room temperature for 1 h, goat anti-mouse IgE-HRP conjugate (Southern Biotech, 1:4000) or goat anti-mouse IgG Fc-HRP (Jackson Immuno Research 1:5000) in 1:1 1% BSA PBS/PBST were added for 45 min at room temperature. Immunoreactivity was visualized with TMB Stabilized Chromogen (Invitrogen). Reactions were stopped after 15 min with 0.5M H₂SO₄, and absorbances were read at 450 nm and 620 nm. All samples were tested in duplicate.

OT-1 activation

Fresh spleens from OT-1 mice were used for splenocyte isolation. The spleens were mashed through a 70 µm cell strainer, after which the Red Blood Cell Lysing Buffer (Hybri-Max, Sigma) was used to remove any erythrocytes. The splenocytes were plated at the density of 0.5 million cells/ml in 12-well plates (1ml/well). They were cultured in IMDM medium (Gibco) supplemented with 10% heat-inactivated Fetal Bovine Serum (Gibco), 1% penicillin/streptomycin (Gibco), 2mM L-glutamine (Gibco), 50 µM 2-mercaptoethanol (Gibco) and 2 µg/mL OVA peptide (SIINFEKL). 48h later (day 2), the cells were subcultured 1:2. On day 3, the activated OT-1 cells were washed with PBS and injected intravenously via tail. OT-1 activation was confirmed by flow cytometry based on CD8 (BD Biosciences) and CD25 (Biolegend) expression using FACS analysis. Consistently we found that about 90% of the cells injected were fully activated OT-1 (CD8+ CD25+) (**Supplementary Fig. 3A**).

Mice

OT-1 mice were maintained in the animal facility at the University of Edinburgh. Age-matched, 6–10-week-old female mice on a C57BL/6 background were purchased from Charles River. Experiments were carried out under the project license PPL: PP7488818. All animal experiments were approved by The University of Edinburgh.

Tumor rejection studies

5×10^5 B16-OVA-Thy1.1-MHC-1 cells were subcutaneously injected into the right flank. Antibody treatment consisted of either 200 μg anti-Thy1.1 IgG2a or 200 μg anti-Thy1.1 Ig1 or 10 μg anti-Thy1.1 IgE (all in house produced as described above). IgGs were administered intraperitoneally, whereas IgE was administered intravenously. The antibodies were injected on days 7, 13, 17 and 24. Some mice received the adoptive cell transfer of 2.5×10^5 activated OT-1 cells in PBS intravenously on day 13. The tumor size was measured regularly with a caliper. The mice were sacrificed when the tumors reached 10 mm in diameter or at the first sign of ulceration or if significant weight loss was observed ($> 20\%$ of initial weight). Tumor volume was calculated by the modified ellipsoidal formula: $V = \frac{1}{2} (\text{Length} \times \text{Width}^2)$.

Complement-dependent cytotoxicity (CDC) assay

B16 and B16.Thy1.1 cells were detached with 2mM EDTA (Gibco) and were pre-stained with eF450 and eF670 (eBioscience) respectively, following manufacturers' instructions. The stained cells were then mixed in 1:1 ratio in 96-well round bottom plate (5×10^5 cells per well). Cells were washed three times with FACS buffer (1% FBS in PBS) at 400g for 3min at 4°C and incubated with indicated antibodies at 50 $\mu\text{g}/\text{ml}$ (50 μl per well) for 30min at 4°C in the dark. Next, the cells were washed three times and were incubated with pre-warmed Rabbit Complement (RC) (Cedarlane) diluted 1:8 in IMDM complete media (50 μl of RC/well). The cells were incubated for 1 hour at 37°C, after which DNase (Promega) (1 U/ μl) diluted in FACS buffer was added and the cells were washed three times. Finally, the cells were resuspended in 150 μl FACS buffer with 1 mg/ml Propidium iodide (PI) (Sigma Aldrich). 100 μl of the stained cells were analysed on a FACS LSRFortessa (BD) using the software program BD FACSDiva. Further analysis was performed with FlowJo and shown results plotted in GraphPad.

Generation of NK cells

Spleens from Rag1 KO mice were homogenized and submitted to red blood cell lysis using the RBC lysis buffer (Sigma Aldrich). The splenocytes were seeded at 2×10^6 cells/ml in 24-wells plates with RPMI (Sigma) supplemented with 10% heat-inactivated Fetal Bovine Serum (Gibco), 1% penicillin/streptomycin (Gibco), 2mM L-glutamine (Gibco), 50 μ M 2-mercaptoethanol (Gibco), 20 ng/ml of IL-2 (BD Pharmingen) and 20 ng/ml of IL-15 (Peprotech). Cells were used at day 5 when ~95% of intact cell population was identified as NK cells based on the expression of NKp46 (eBioscience) and NK1.1 (eBioscience) and lack of expression of CD3 (BD Pharmingen) by flow cytometry (CD3- NKp46+ NK1.1+) using FACS LSRFortessa (BD).

Antibody-dependent cell cytotoxicity (ADCC) assay

B16 and B16.Thy1.1 target cells were detached with 2mM EDTA (Gibco) and added to 96-well round bottom plates at 1×10^4 cells/well. The indicated anti-Thy1.1 antibodies were added at 10 μ g/ml per well in FACS buffer and incubated for 30min at 4°C, followed by two washing steps with FACS buffer at 400g for 3min at 4°C. The effector NK cells were then added in pre-warmed media at 3-fold decreasing concentrations starting at 9:1 effector:target ratio. The cells were centrifuged at 400g for 2min to concentrate them at the bottom of the wells and ADCC assay was run for 4 hours at 37°C. After 4 hours of incubation, the cells were centrifuged at 300g for 5min, and the supernatant was used to assess the cell toxicity with CytoTox 96® Non-Radioactive Cytotoxicity Assay LDH cytotoxicity Assay kit (Promega) following manufacturer's instructions. The LDH activity of medium alone was subtracted from the LDH activity of test conditions to obtain the corrected values. These corrected values were then used to calculate the percentage of cellular cytotoxicity using the following formula: percentage specific lysis = $\frac{(E+T+mAb)-(E+T)}{T \max lysis - T} \times 100$, where E are the effector cells, T are the target cells and Tmax the lysed target cells alone.

Statistical analysis

Statistical analysis was performed in GraphPad Prism software. Survival was evaluated with the Mantel-Cox test. P-values of ≤ 0.05 were considered statistically significant. ns = $P > 0.05$, * = $P \leq 0.05$. CDC assay was evaluated by one-way ANOVA applied to subtracted values (no RC – with RC) of each condition. ADCC assay was evaluated by multiple t-test at each specific ratio. Indicated * mean the significant difference between B16-OVA-

Thy1.1 IgG1 and IgG2a versus all the other conditions.

Results

Expression of anti-Thy1.1 antibodies with different Fc-isotypes

In order to compare the therapeutic capacity of antibodies with the same specificity but different isotypes, we repeated an approach used by Nimmerjahn et al. 8 and expressed antibodies with the same specificity but different isotypes (**Fig. 1A**). For our study, we chose an antibody, which recognises CD90.1 / Thy1.1, a congenic marker often used for immunological studies. This antibody binds to thymocytes expressing Thy1.1, which is expressed by some mouse lines, such as AKR mice, but does not bind to Thy1.2, which is expressed by other mouse lines, such as C57BL/6. To this end, we sequenced the heavy and light chain variable domain sequences (VH, VL) of the OX7 hybridoma (anti-Thy1.1). OX7 expresses antibodies with an IgG1 isotype and is known to lack cell depleting activity once injected into mice. We therefore designed chimeric anti-Thy1.1 mIgG2a heavy chains by combining the VH with the known sequences of the constant domains of murine IgG2a (CHs). In addition, we expressed antibodies with the same anti-Thy1.1 specificity but an IgE isotype. This was mainly due to the fact that it has been reported that in some preclinical models, IgE antibodies have been shown to exhibit superior tumor control in comparison to their IgG homologs ^{12,13}.

The anti-Thy1.1 antibodies with different Fc-isotypes were expressed *in vitro* and purified using MabSelect SuRe LX resin. Preparative size-exclusion chromatography (SEC) and quality control consisting of ultra-performance liquid chromatography (UPLC)-SEC, capillary electrophoresis sodium dodecyl sulphate (CE-SDS) and SDS-PAGE were performed. Size-exclusion ultra-performance liquid chromatography (SE-UPLC) showed that all three antibodies (anti-Thy1.1 IgG1, IgG2a and IgE) reached monomericity levels of >95% (**Supplementary Fig. 1A**). Next, the purity was tested by CE-SDS. Since CE-SDS was not optimized for IgE, we also included SDS-PAGE to confirm the correct molecular weights and purity of IgE. The analysis under non-reducing conditions confirmed the expected molecular weights and indicated that a high purity (>90%) was reached in all samples (**Supplementary Fig. 1B (left) and C**). Furthermore, only heavy chain (HC) and light chain (LC) were observed under reducing conditions,

confirming the correct sample composition (**Supplementary Fig. 1B (right) and C**).

Taken together, the produced antibodies complied with high-quality standards regarding monomericity and purity. In addition, we confirmed that the antigen binding was preserved in binding ELISA with Thy1.1 expressing CHO cells (**Fig. 1B**). Importantly, no difference in binding was observed between different isotypes.

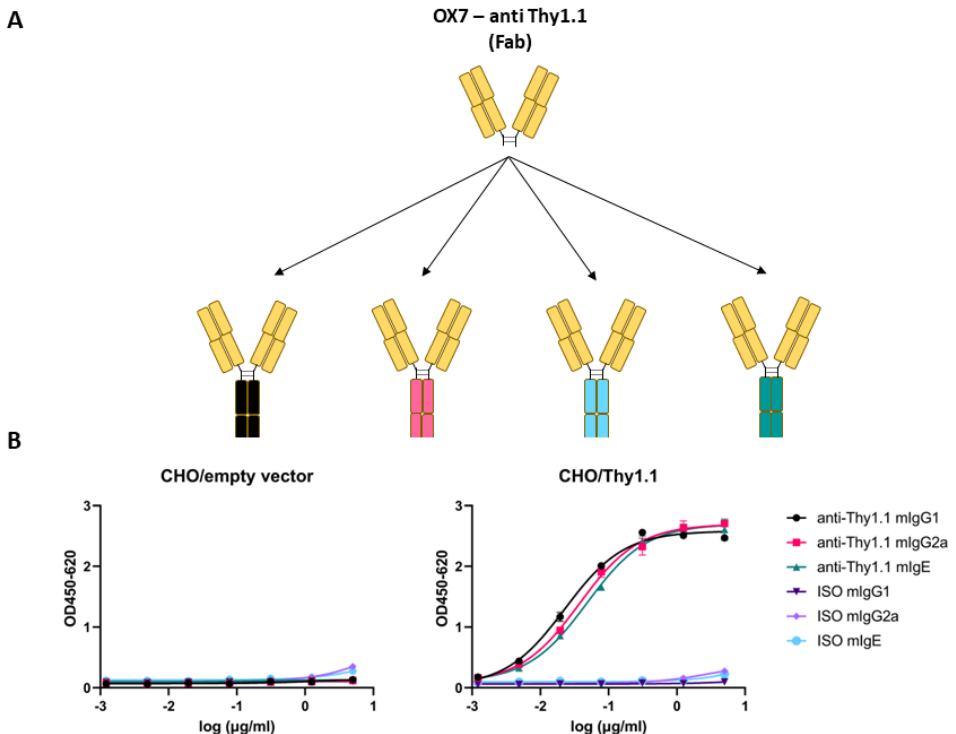


Figure 1. Panel of the different OX-7 antibodies targeting Thy1.1 used. (A) Schematic summary of the different isotypes of OX7 antibodies used. Fab (Fragment antigen-binding). (B) Cell binding ELISA of anti-Thy1.1 antibodies. The binding of anti-Thy1.1 IgG1, IgG2a and IgE was tested on CHO cells transiently transfected with an empty vector (left) or Thy1.1 (right). Isotype controls were used for each antibody isotype. Mean + SD of duplicates is shown.

Stable Thy1.1 expression by B16-OVA cells

CD90 (Thy1) is a glycoposphatidylinositol (GPI) anchored cell surface protein, and it is, therefore, susceptible to the cleavage of GPI anchor by

Phospholipase-C¹⁴ (**Fig. 2A**). To overcome a possible loss of expression, as it has been reported before¹⁵, we replaced the GPI anchor of Thy1.1 with a murine MHC-1 transmembrane domain (**Fig. 2B**). Transfected B16-OVA cells were tested for their expression stability for about five weeks. B16-OVA-Thy1.1 clone showed no changes in Thy1.1 expression even after removal of puromycin used for selection, confirming stable expression by this clone (**Fig. 2C-E**). The replacement of the Thy1.1 transmembrane domain did not affect the binding capacity of anti-Thy1.1 antibodies, as Thy1.1-MHC-1 expression levels were measured using the same anti-Thy1.1 antibody clone (OX7).

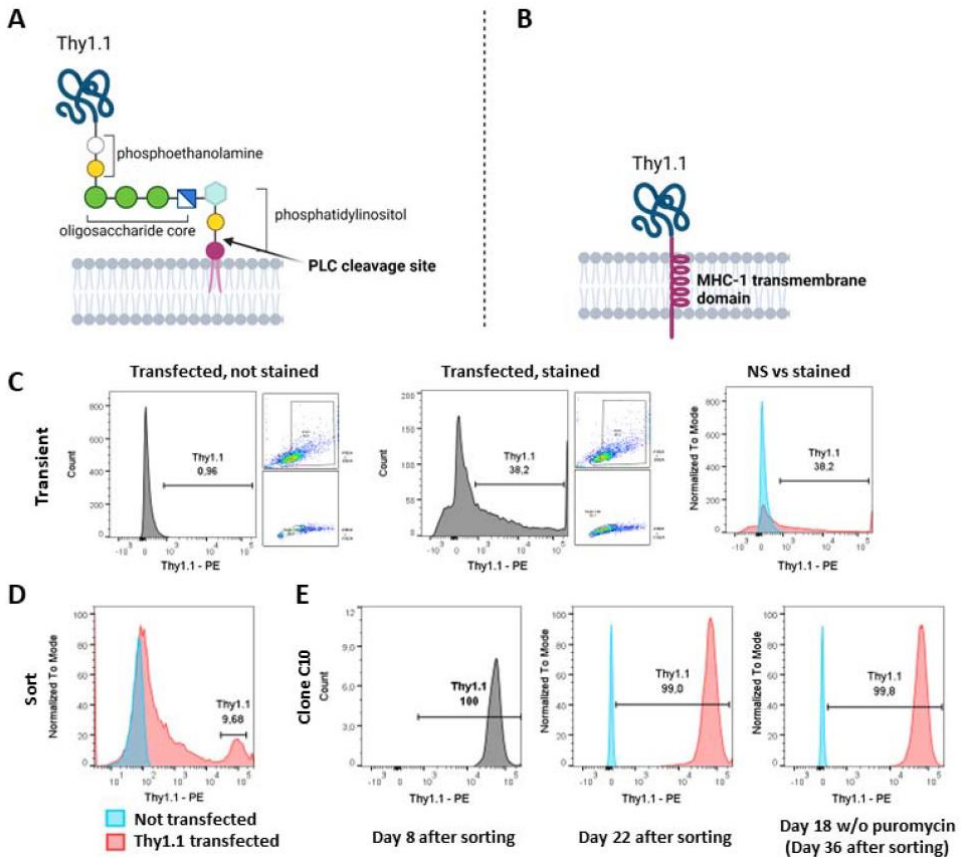


Figure 2. Thy1.1-MHC-1 expression on B16-OVA cell. B16-OVA cells were co-transfected with pSG5-Thy1.1-MHC-1 and pLXSP, selection agent (puromycin) was added 24h after transfection and single-cell sorting was performed after at least 10 days of growing the cells in the selection medium. Thy1.1 expression was regularly tested by FACS. Schematic representation of (A) Thy1.1 with its GPI anchor and (B) the designed construct in which

the GPI anchor has been replaced with MHC-1 transmembrane domain. (C-E) FACS analysis of Thy1.1 expression on B16-OVA cells after transfection with pSG5-Thy1.1_MHC-1. (C) Transient expression 24h after transfection. (D) Expression at single-cell sorting. (E) Expression on the selected clone on the indicated days.

Different CDC and ADCC profiles for IgG2a, IgG1 and IgE antibodies

To assess the capacity of the different antibodies to induce complement-mediated CDC and NK cell-mediated ADCC, *in vitro* cytotoxicity assays were performed. In order to detect on-target CDC killing, we mixed B16-OVA-Thy1.1 target cells with B16-OVA control cells in 1:1 ratio and tested how the ratio changes after antibody-mediated complement activation. As expected, only IgG2a significantly reduced the ratio (**Fig. 3A-B**), suggesting that only the IgG2a isotype successfully mediated CDC against target cells. Furthermore, as a control, the introduction of the Fc silencing LALA-PG mutations into IgG2 isotype abrogated the complement mediated activity (**Fig 3B**). In parallel, different antibody isotypes were evaluated in an ADCC assay where NK cells were used as effector cell population (**supplementary figure 2**). Here, both IgG2a and IgG1 showed high cytotoxicity towards B16-OVA-Thy1.1 cells (**Fig 3C**), whereas IgE and IgG2a-LALA-PG did not induce NK cell-mediated cell killing. Finally, no cytotoxicity was observed with B16-OVA control cells not expressing Thy1.1 antigen with any of the tested isotypes.

Taken together, these data show that the expressed antibodies retained their described effector function. Although our data showed the highest complement-mediated activity for IgG2a, the ADCC effect was similar for both IgG2a and IgG1. This is to be expected as NK cells were used as effector cells in the ADCC assay. NK cells only express FcγRIII^{16,17}, which shows similar binding profiles for IgG1 and IgG2a¹⁸. Nonetheless, IgG2a presents higher affinity for the activating FcγRIV, which is absent on NK cells, but present on macrophages. Therefore, *in vivo*, where macrophages may also contribute as effector cells, superior effector function of IgG2a expressing antibodies could be postulated¹⁹⁻²¹.

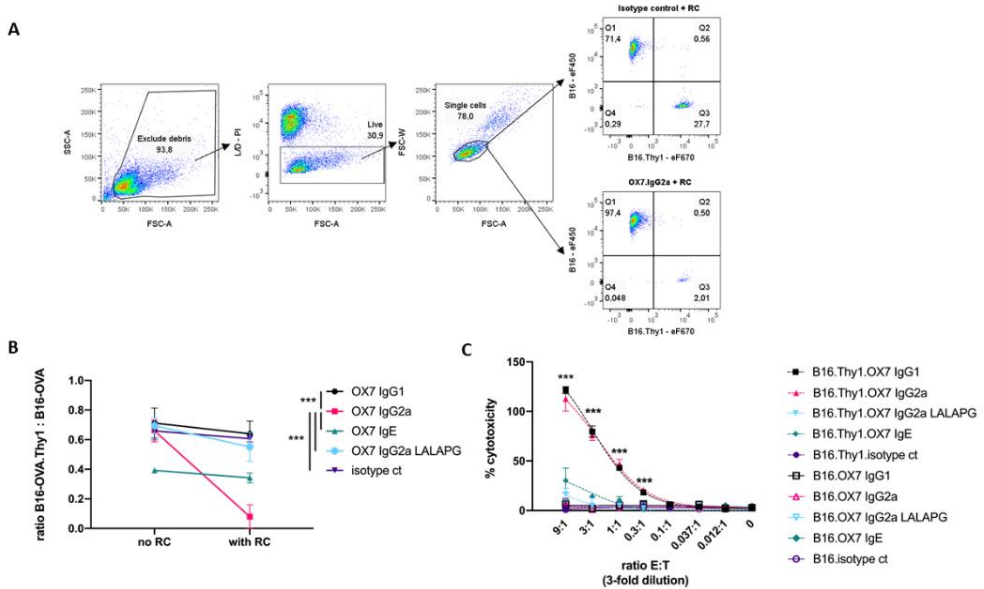


Figure 3. CDC and ADCC profiles of anti-Thy1.1 IgG1, IgG2a, IgE and IgG2a-LALA-PG. (A) Representative plots used to calculate B16.Thy1:B16 ratio. First, B16 cells were gated based on FSC-A / SSC-A properties. Next, Live cells were based on FSC-A/ PI staining. Live cells were gated for single cells based FSC-A / FSC-W. Target cells B16.Thy1 are found in Q3 as eF670+ and B16 are found as Q1 as eF450+. Data representative from samples incubated isotype control or OX7.IgG2a and with RC. (B) B16-OVA-Thy1.1 target cells and B16-OVA control cells were previously stained, then co-incubated with 50 µg/mL of anti-Thy1.1 antibodies at 4 °C for 30 min and finally incubated with RC for 1h at 37°C. Cells were analyzed by FACS and B16-OVA-Thy1.1/B16-OVA ratio was calculated. (C) B16-OVA-Thy1.1 target cells and B16-OVA control cells were incubated independently with 10 µg/mL of anti-Thy1.1 antibodies and then co-incubated at various effector-to-target ratios with NK cells for 4 h at 37°C. CytoTox 96® Non-Radioactive Cytotoxicity Assay LDH cytotoxicity Assay kit was used to assess cytotoxic effect mediated by the antibodies. Mean ± SD of triplicates is shown of a representative biological replicate out of n=3 biological replicates. (Statistics: CDC assay - one-way ANOVA on subtracted values (no RC – with RC); ADCC assay – multiple t-test, ***P < 0.001).

IgG2a antibodies show superior therapeutic tumor control to their IgG1 and IgE homologues

To test the therapeutic capacity of different antibody isotypes to control

tumor growth in a syngeneic mouse model, C57BL/6 mice were subcutaneously injected with B16-OVA-Thy1.1 cells and treated with either anti-Thy1.1 IgG2a, IgG1 or IgE antibodies, starting on day 7 after tumor cells transfer (**Fig. 4A**). Similar to the prophylactic setting, in this therapeutic setting antibody treatment with an IgG2a isotype showed superior tumor growth control compared with antibodies with an IgG1 or IgE isotype (**Fig. 3B-C**). Whereas all IgG1 (10/10) or IgE (12/12) treated animals reached the human defined endpoint by day 49, 50% (6/12) of IgG2a antibody treated mice showed very small or no tumor growth at all, at day 60. Median survival was 24 days for IgG1 and 26 days for IgE, compared to 48 days for IgG2a (**Fig. 3D**).

To confirm that the superior tumor control is mediated via the IgG2a interaction with the immune system, we introduced LALA-PG mutations in the constant domain of the IgG2a heavy chain. LALA-PG mutations have been shown to significantly reduce the binding of both human and murine IgG antibodies to Fc γ receptors²². In the case of mIgG2a, the binding to Fc γ RI, II and IV is completely interrupted, while the binding to Fc γ RIII is reduced more than 50-fold. In addition, LALA-PG mutants show decreased C1q binding and C3 fixation in murine serum and, consequently, lose the capacity to mediate complement mediated cell lysis. When we compared the anti-Thy1.1 IgG2a and IgG2a-LALA-PG in vivo, we observed a complete loss of efficacy with the Fc-silenced antibody (**Fig. 5**). Whereas IgG2a survival rate was around 50% at day 60, all mice treated with IgG2a-LALA-PG reached the endpoint by day 39 (**Fig. 5B**). Median survival was 42 days for IgG2a compared to 25,5 days for IgG2a-LALAPG and 27 days for the untreated group (**Fig. 5C**). These results clearly show that the observed anti-tumor effect of the anti-Thy1.1 IgG2a antibody was Fc mediated and isotype dependent.

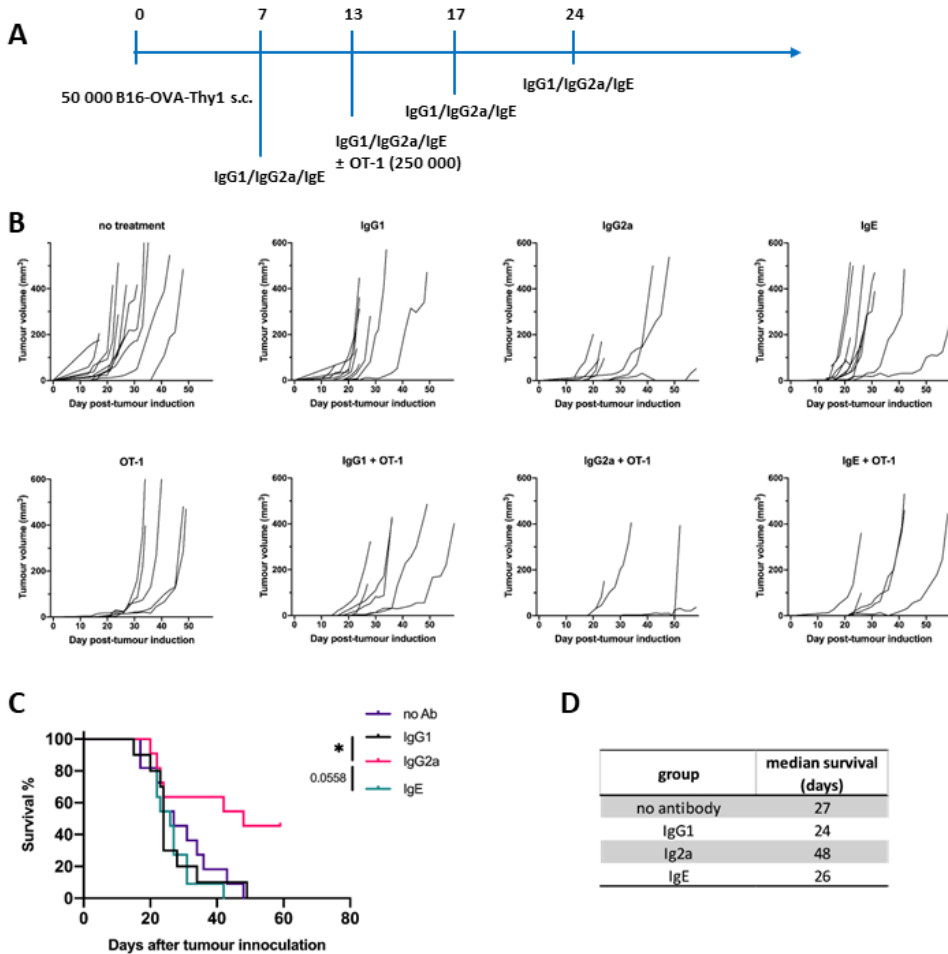


Figure 4. Superior tumor growth control of anti-Thy1.1 IgG2a *in vivo*. C57BL/6 mice were subcutaneously injected with 50 000 B16-OVA-Thy1.1 cells in the flank and were treated with anti-Thy1.1 IgG1, IgG2a or IgE antibodies. (A) Experimental scheme of the antibody isotype comparison in the B16-OVA-Thy1.1 model. (B) Tumor growth curves. (C) Survival analysis. (D) Median survival in days. Statistical significance was calculated with the Mantel-Cox test. * = $P \leq 0.05$ B, C and D: $n=10-12$, combined data of two independent experiments.

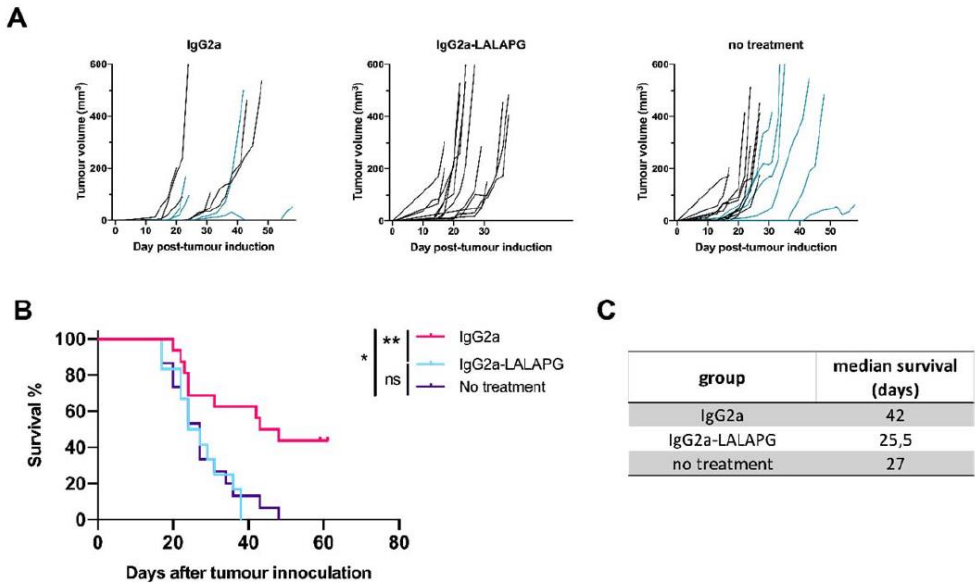


Figure 5. *In vivo* tumor control is lost when IgG2a Fc tail is silenced. C57BL/6 mice were subcutaneously injected with 50 000 B16-OVA-Thy1.1 cells in the flank and were treated with anti-Thy1.1 IgG2a (active) or anti-Thy1.1 IgG2a-LALA-PG (Fc silent) antibody. (A) Tumor growth curves. (B) Survival analysis. (C) Median survival in days. Combined data of three independent experiments are shown (n=12-16). Green lines in Fig. 5A are indicative of data from figure 4 in IgG2a and control group. Statistical significance was calculated with the Mantel-Cox test. (*P < 0.1, **P < 0.01).

Antibody treatment is not synergising with T-cell based adoptive cell transfer (ACT)

In addition, the antibodies were also tested in combination with the adoptive cell transfer of activated OT-1 cells. B16-OVA tumors are characterized by an immune-suppressive tumor microenvironment dominated by T regulatory cells (Tregs). It has been shown that depletion of intratumoral Tregs offers tumor protection when combined with the GVAX vaccine due to enhanced activation of CD8+ T cells^{23,24}. These data suggest that, in this setup, OT-1 efficacy can be inversely correlated with Treg function. With the B16-OVA cell line that we used, OT-1 monotherapy is usually ineffective when given after day seven post tumor implantation. Therefore, we injected the OT-1 cells at a later stage of tumor development when they can no longer control the tumor growth due to an established immune-suppressive tumor microenvironment. This allowed us to test

whether our antibodies attenuate this immune-suppressive tumour microenvironment (TME) and may rescue OT-1 efficacy. Nonetheless, our results show that OT-1 treated mice had similar outcomes to those that did not receive OT-1 adoptive cell transfer (**Supplementary Fig. 4A**). These data suggest that none of the IgG2a, IgG1, or IgE treatments synergized with ACT treatment.

Discussion

In mice, the efficacy of antibody-based treatments is largely restricted to a prophylactic application, but lack efficacy in a therapeutic setting, once the tumour has been established. In this study, we directly compared the therapeutic activity of murine IgG2a, IgG1 and IgE antibodies of the same specificity, targeting a surface tumor antigen (Thy1.1). Wild type mice bearing syngeneic B16-OVA-Thy1.1 tumors were used for this purpose. Our results show that in this setting antibodies with an IgG2a isotype offer superior tumor control in comparison to antibodies with an IgG1 or IgE isotype. The observed effect was entirely Fc-mediated as it was completely lost using IgG2a featuring Fc silencing LALA-PG mutations.

IgG2a is known as the most active IgG subclass in mice due to its high A/I ratio. Nevertheless, direct comparisons of different antibody isotypes of the same specificity in cancer settings are still scarce, although the first mechanistic basis for different activity of IgG subclasses was provided in 2005⁸. By using the B16-F10 lung metastasis model and a prophylactic treatment with TA99 antibody of different IgG subclasses (targeting Trp1 expressed on B16-F10 cells), the authors showed in that study that IgG2a offers superior tumor control to IgG1, IgG2b and IgG3⁸. However, these TA99 antibodies lack activity in therapeutic setting⁹. Furthermore, Dahan et al. showed that an anti-PD-L1 IgG2a antibody is superior to IgG1 in MC38 and B16-OVA tumor models²⁵. However, PD-L1 expression is not restricted to tumor cells and has a substantial influence on local immune responses within tumors, making it challenging to extrapolate these results to exclusively tumor antigen-targeting mAbs.

Here, we sought to further our understanding of the therapeutic capacity of IgG2a expressing antibodies. To this end, we focused our study exclusively on therapeutic setting and started antibody-based treatment on day 7 after tumor cell injection. Furthermore, we focused our study on an artificially and well-characterized model antigen exclusively presented by

tumor cells. For this purpose, Thy1.1 was chosen as a target antigen. As wild type C57BL/6 mice express only Thy1.2, the anti-Thy1.1 antibody treatment would be tumor-selective. Furthermore, in contrast to other model tumour antigens, Thy1.1 has not functional importance for the tumor cell as such. Therefore, the anti-tumor effect observed is solely due to Fc-mediated effects, making it an ideal model system for comparing the therapeutic efficacy of different antibody isotypes.

In addition, we also included antibodies expressing the IgE isotype in this study. In multiple preclinical studies, antibodies with the IgE isotype have been shown to mediate superior anti-tumor effects in comparison to antibodies expressing commonly used IgG isotypes^{12,13,26}. However, these studies have not addressed the potential outcome of IgE-mediated activation of mast cells (MCs) and basophils on tumor development. Since IgE can induce extremely potent immune reactions through these cell types, diverting them against tumor cells could have therapeutic benefits. Mice represent a good model for addressing this question, as their FcεRI expression is limited to MCs and basophils²⁷. Nonetheless, our results show that IgE treatment did not have any effect on tumor growth, as the growth curves and survival rate of IgE antibody treated mice were not significantly different compared to untreated mice. A similar approach has been recently used by a group at Massachusetts Institute of Technology (MIT) that showed that IgE targeting a surface tumor antigen could not successfully control the tumor growth in B16-OVA and MC-38 models in C57BL/6 wild type mice²⁸. In many studied types of tumor, mast cells have been detected to be located mainly in the peritumoral space and less so in the intra-tumoral²⁹. Therefore, a lack of effect as we observed it with IgE based antibody treatment could potentially be explained by a poor presence of IgE effector populations within B16-OVA tumors. Thus, targeting a surface tumor antigen with an IgE antibody may not be optimal for MC/basophil activation. Such limitations could potentially be overcome by using soluble tumor antigens, as they may have a higher probability of reaching MCs at the tumor edges. In line with such an assumption, our data may suggest that a tumor resident cell surface antigen, such as Thy1.1 we used in our model system, might not be an optimal IgE target for inducing MC and basophil activation at the site of solid tumors. Therefore, in order to perform a proper comparison between the therapeutic capacity of antibodies with an IgG2a and an IgE isotype, studies using mice with a humanised expression pattern of the IgεR^{12,13,26} appear warranted.

Finally, we combined antibody treatment with OT-1 adoptive cell transfer, which, as monotherapy, is usually not effective in rejecting already established B16-OVA tumors due to the immune-suppressive TME of the tumor¹¹. To our knowledge, such combination therapies consisting of tumor-targeting antibodies and adoptively transferred CTLs have not been previously tested. However, they could potentially have a beneficial effect, if the antibody treatment could attenuate the immune-suppressive state of the TME. We were particularly interested, if IgE could mediate such an effect by inducing the Treg suppression via histamine released from degranulating MCs³⁰. Nonetheless, none of the tested antibody isotypes was able to improve the efficacy of OT-1 treatment, not even treatment with the IgG2a antibody which showed substantial efficacy in monotherapy. Such findings indicate that the immune-suppressive tumor microenvironment within the transferred B16 tumours may not have been substantially altered by the antibody treatment.

Nonetheless, one should keep in mind that such a lack of response as we have observed it in our study might not necessarily be generalisable. We purposely chose the well-established B16 melanoma model system for our study, as it allowed us to keep all other factors stable, but selectively manipulate exactly one variable, i.e. the isotype of the heavy chain of the used antibodies. However, using such a highly artificial model system also has its limitations, as other tumour models might potentially be more susceptible to antibody mediated shifts in the TME. B16 melanoma, for instance, are not particularly susceptible to PD-1 targeted antibody treatment, while the colon carcinoma cell line MC38 is highly responsive to such treatment. Therefore, it might be worthwhile to investigate susceptibilities of different tumour models to ACT in combination with therapeutic antibody treatment in future studies. Furthermore, it appears necessary to aim for a better understanding of how such combined treatment might influence immune cell influx. Due to technical limitations, we could not assess such differences following the treatment with different antibodies in this study. However, there has been substantial progress in the field of highly sensitive techniques that might allow to explore this aspect in future studies. As mentioned before, in particular with respect to IgE antibodies such studies might be able to open entire novel fields of research and, potentially, therapeutic treatment opportunities. Alternatively, synergisms between tumour targeting antibody treatment and regulatory T-cell (Treg) depleting antibodies might want to be explored in more detail. In

the B16 melanoma model system, it has been shown that targeting intra-tumoral Tregs, using CTLA-4 antibodies, offers tumor protection when combined with CD8 T-cell inducing vaccination^{23,24}. Therefore, at this stage, it remains tempting to speculate that in future experiments a combination of Treg-depleting or TGF β -neutralising antibody treatments with tumor antigen targeting antibodies may show synergistic effects in reverting an immunosuppressive TME and, hence, in enhancing the efficacy of treatment.

Therefore, in conclusion, while this study provides in vivo evidence that tumor antigen-targeting IgG2a is superior to its IgG1 and IgE homologs in controlling the tumor growth in a therapeutic setting in wild type C57BL/6 mice, future studies may have to dissect how these different isotypes influence immune cell influx into tumors and gauge their capacity to influence the immunosuppressive micro-environment within tumors.

Declaration of competing interest

None.

Acknowledgements

This work was supported by the European Union's Horizon 2020 research and innovation programme under the Marie Skłodowska-Curie grant agreement [grant numbers 765394, 2018]. We thank Nicola Logan (University of Edinburgh) for her technical assistance in animal experiments. We are grateful to Aduro Biotech Europe team, especially Andrea van Elsas and Sander van Duijnhoven, for their support in antibody production and quality control.

Declaration of competing interest

None.

Supplementary data

Supplementary Table 1. Amino acid sequences of anti-Thy1.1 antibodies. Signal peptides are highlighted in grey, and LALA-PG mutations in cyan.

Anti-Thy1.1 IgG2a HC
MAVLGLLFCCLVTFPSCVLSEIQLQQSGPELMKPGASVKISCKASGYSFTSYMDW VKQSHGKNLEWIGYIDPFNGDTSYNQKFKDKATLTVDKSSSTAYMHLSSLTSEDS AVYYCARGIYYGYGGYFDYWGQGTTLTVSSAKTTAPSVYPLAPVCGDTTGSSVTL GCLVKGYFPEPVTLTWNSGSLSSGVHTFPAVLQSDLYTLSSSVTVTSSTWPSQSIT CNVAHPASSTKVDKKIEPRGPTIKCPPCKCPAPNLLGGPSVFIFPPKIKDVLMI SLSPIVTCVVDVSEDDPDVQISWVFNNEVHTAQTQTHREDYNSTLRVVSALPIQH QDWMSGKEFKCKVNNKDLPAPIERTISKPKGSVRAPQVYVLPPEEEMTKKQVTL TCMVTDMPEDIYVEWTNNGKTELNYKNTEPVLDSDGSYFMYSKLRVEKKNWV ERNYSYSCSVVHEGLHNHHTTKSFSRTPGK
Anti-Thy1.1 IgG2a LALA-PG HC
MAVLGLLFCCLVTFPSCVLSEIQLQQSGPELMKPGASVKISCKASGYSFTSYMDW VKQSHGKNLEWIGYIDPFNGDTSYNQKFKDKATLTVDKSSSTAYMHLSSLTSEDS AVYYCARGIYYGYGGYFDYWGQGTTLTVSSAKTTAPSVYPLAPVCGDTTGSSVTL GCLVKGYFPEPVTLTWNSGSLSSGVHTFPAVLQSDLYTLSSSVTVTSSTWPSQSIT CNVAHPASSTKVDKKIEPRGPTIKCPPCKCPAPNAAAGGPSVFIFPPKIKDVLMI SLSPIVTCVVDVSEDDPDVQISWVFNNEVHTAQTQTHREDYNSTLRVVSALPIQ HQDWMSGKEFKCKVNNKDLGAPIERTISKPKGSVRAPQVYVLPPEEEMTKKQV TLTCMVTDMPEDIYVEWTNNGKTELNYKNTEPVLDSDGSYFMYSKLRVEKKNW VERNSYSCSVVHEGLHNHHTTKSFSRTPGK
Anti-Thy1.1 IgG1 HC
MAVLGLLFCCLVTFPSCVLSEIQLQQSGPELMKPGASVKISCKASGYSFTSYMDW VKQSHGKNLEWIGYIDPFNGDTSYNQKFKDKATLTVDKSSSTAYMHLSSLTSEDS AVYYCARGIYYGYGGYFDYWGQGTTLTVSSAKTTAPSVYPLAPGSAQAQTNSMVT LGCLVKGYFPEPVTVTWNSGSLSSGVHTFPAVLQSDLYTLSSSVTVPSSTWPSETV TCNVAHPASSTKVDKKIVPRDCGCKPCICTVPEVSSVFIFPPKPKDVLITITLTPKVTC VVVDISKDDPEVQFSWFVDDVEVHTAQTQPREEQFNSTFRSVSELPIMHQDWL NGKEFKCRVNSAAFPAPIEKTISKTKGRPKAPQVYTIPPPKEQMAKDKVSLTCMIT DFFPEDITVEWQWNGQPAENYKNTQPIMDTDGSYFVYSKLVNQSNWEAGNT FTCSVLHEGLHNHHTTEKSLSHSPGK
Anti-Thy1.1 IgE HC
MAVLGLLFCCLVTFPSCVLSEIQLQQSGPELMKPGASVKISCKASGYSFTSYMDW

VKQSHGKNLEWIGYIDPFNGDTSYNQFKDKATLTVDKSSSTAYMHLSSLTSEDS
 AVYYCARGIYYGYGGYFDYWGQGTTLTVSSASIRNPQLYPLKPKCGTASMTLGLCL
 VKDYFPNPVTVTWYSDSLNMSTVNFALGSELKVTTSQVTSWGKSAKNFTCHVT
 HPPSFNESRILVRPVNITEPTLELLHSSCDPNAFHSTIQLYCFIYGHILNDVSVSWL
 MDDREITDTLAQTVLIKEEGKLASTCSKLNITEQQWWMSESTFTCKVTSQGVLYLA
 HTRRCPDHEPRGVITYLIPPSPLDLYQNGAPKLTCLVVDLESEKNVNVNTWNQEKK
 TSVSASQWYTKHHNNATTSITSILPVVAKDWIEGYGYQCIVDHPDFPKPIVRSITKT
 PGQRSAPEVYVFPPEEESDKRTLTLCLIQNFFPEDISVQWLGDGKLISNSQHSTTT
 PLKSNQSNQGFFIFSRLEVAKTLWTQRKQFTCQVIHEALQKPRKLEKTISTSLGNTS
 LRPS

Anti-Thy1.1 LC

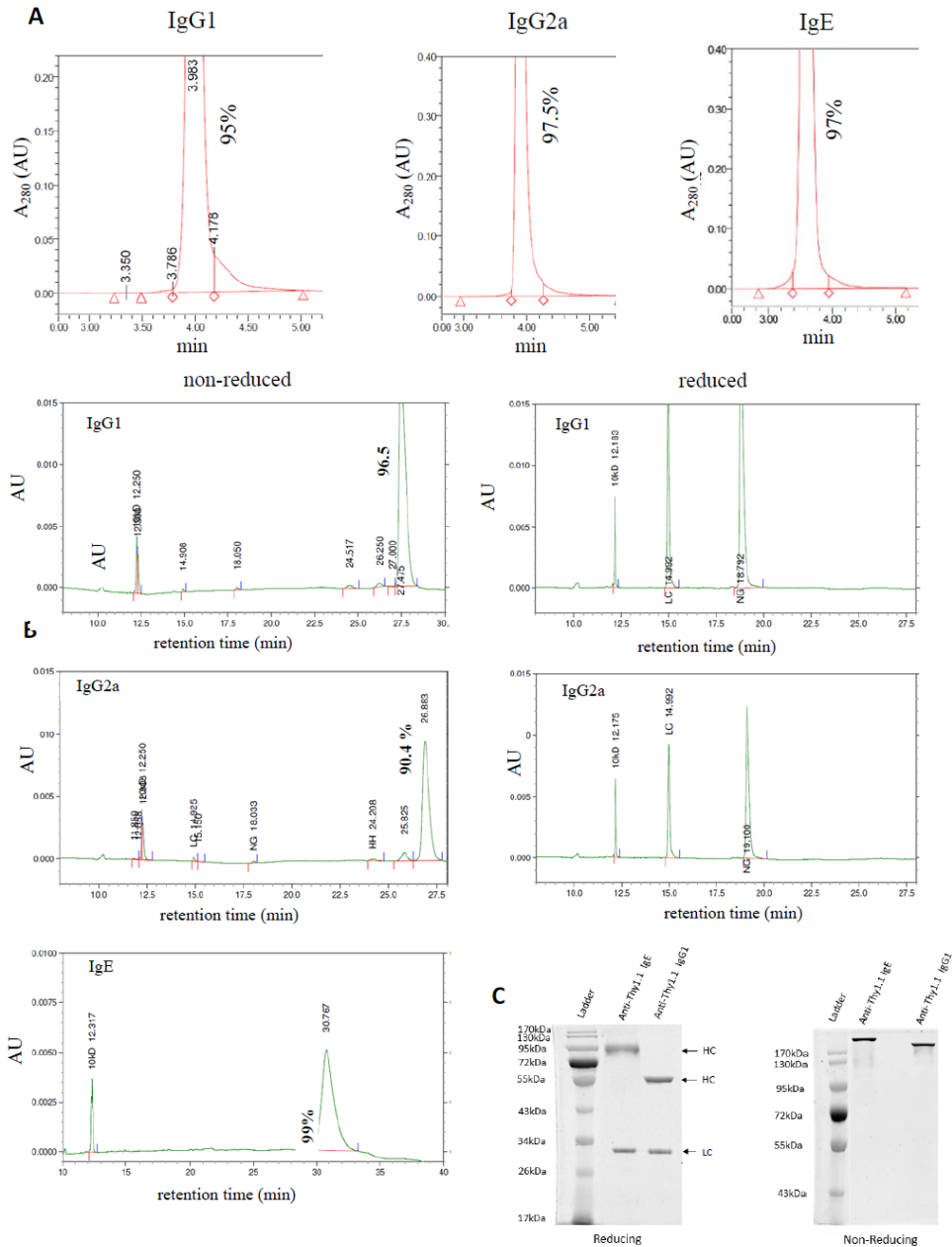
MSVLTQVLALLLWLTGARCDIVLTQSPASLAVSLGQRATISCRASDSVDSFGNSF
 MHWFQQKPGQPPKLLIYRASTPESGIPARFSGSGSRTDFLTISPVEADDVATYYC
 QQSIEDPFTFGGGTKLEIKRADAAPTVSIFPPSSEQLTSGGASVVCFLNNFYPKDIN
 VKWKIDGSERQNGVLNSWTDQDSKSTYSMSSTLTLTKDEYERHNSYTCEATHK
 TSTSPIVKSFNRENC

Supplementary Table 2. Amino acid sequence of designed Thy1.1-MHC-1 construct

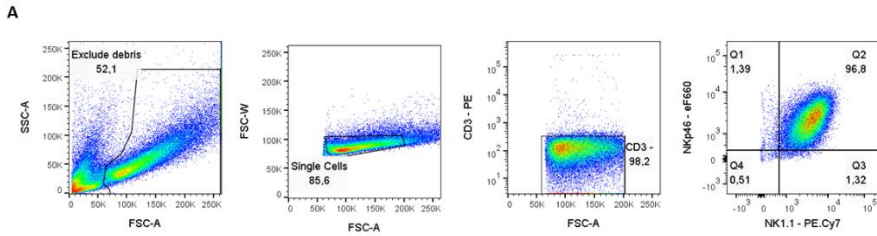
Thy1.1-MHC-1

MNPVISITLLLSVLQMSRGRVISLTAQLVNQNLRLDCRHENNTNLPIQHEFSLTR
 EKKKHVLSGTLGVPEHTYRSRVNLFSDRFIKVLTLANFTTKDEGDYMCCLRVSQGN
 PTSSNKTINVIRDKLVKCGKEPPSSTKTNTVIIAVPVVLGAVVILGAVMAFVMKRR
 RNTGGKGGDYALAPGSQSSDMSLPDCKV

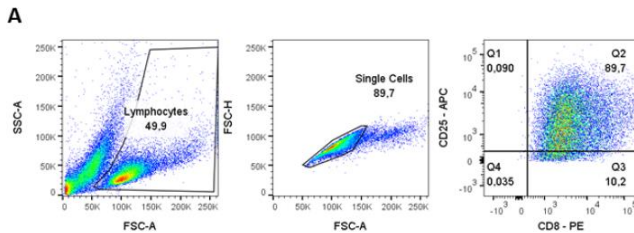
Legend: Signal peptide – Thy1.1 without its propeptide – connecting peptide – transmembrane domain of MHC-1 – cytoplasmic domain of MHC-1



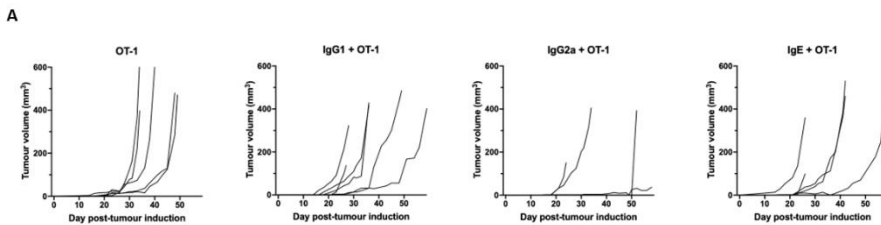
Supplementary Figure 1. Quality control of anti-Thy1.1 antibodies. (A) Monomericity was evaluated with UPLC-SEC, monomer percentage is shown; (B) CE-SDS under non-reducing conditions and purity percentage (left) and under reducing conditions (right); (C) SDS-PAGE was used for IgE evaluation as a complementary method, since CE-SDS was not optimised for IgE. The data for IgE has been previously published ¹⁰.



Supplementary Figure 2. Flow cytometry data used for ADCC. (A) Characterization of NK population at day 5 derived from ex vivo material. Gating was done on unstained splenocytes at day 5 and its respective fluorescence-minus-one sample. First, NK cells were gated based on FSC-A / SSC-A properties. Next, single cells were gated based FSC-A / FSC-W. NK population were gated as CD3 negative. Next to the CD3- population, NK population are found at NKp46+ NK1.1+ gate.



Supplementary Figure 3. Confirmation of OT-1 cells activation by flow cytometry. (A) Characterization of OT-1 cells at day 3 before injection. Gating was done based on FSC-A / SSC-A properties. Next, single cells were gated based FSC-A / FSC-H. OT-1 cells were gated as CD8 positive and activated cells as CD25 positive. CD8 and CD25 quadrants based on non-stained sample.



Supplementary Figure 4. No synergistic effect is achieved combining anti-thy1.1 antibodies with adoptive cell transfer of activated OT-1s. C57BL/6 mice were subcutaneously injected with 50 000 B16-OVA-Thy1.1 cells in the flank and were treated with anti-Thy1.1 IgG1, IgG2a or IgE antibodies. Mice received the combination treatment consisting

Chapter 5

of anti-Thy1.1 antibodies and adoptive cell transfer of activated OT-1 cells.

(A) Tumor growth curves. n=5-6, the experiment was done once.

References

1. Antibody therapeutics approved or in regulatory review in the EU or US. The Antibody Society. Accessed April 4, 2022. <https://www.antibodysociety.org/resources/approved-antibodies/>
2. Grilo AL, Mantalaris A. The Increasingly Human and Profitable Monoclonal Antibody Market. *Trends in Biotechnology*. 2019;37(1):9-16. doi:10.1016/j.tibtech.2018.05.014
3. Hudis CA. Trastuzumab — Mechanism of Action and Use in Clinical Practice. *New England Journal of Medicine*. 2007;357(1):39-51. doi:10.1056/NEJMr043186
4. Weiner GJ. Monoclonal antibody mechanisms of action in cancer. *Immunol Res*. 2007;39(1):271-278. doi:10.1007/s12026-007-0073-4
5. Chenoweth AM, Wines BD, Anania JC, Mark Hogarth P. Harnessing the immune system via FcγR function in immune therapy: A pathway to next - gen mAbs. *Immunol Cell Biol*. Published online March 11, 2020:imcb.12326. doi:10.1111/imcb.12326
6. Bordron A, Bagacean C, Tempescul A, et al. Complement System: a Neglected Pathway in Immunotherapy. *Clinic Rev Allerg Immunol*. 2020;58(2):155-171. doi:10.1007/s12016-019-08741-0
7. Vukovic N, van Elsas A, Verbeek JS, Zaiss DMW. Isotype selection for antibody-based cancer therapy. *Clin Exp Immunol*. Published online November 5, 2020. doi:10.1111/cei.13545
8. Nimmerjahn F. Divergent Immunoglobulin G Subclass Activity Through Selective Fc Receptor Binding. *Science*. 2005;310(5753):1510-1512. doi:10.1126/science.1118948
9. Ly LV, Sluijter M, Burg SH van der, Jager MJ, Hall T van. Effective Cooperation of Monoclonal Antibody and Peptide Vaccine for the Treatment of Mouse Melanoma. *The Journal of Immunology*. 2013;190(1):489-496. doi:10.4049/jimmunol.1200135
10. Vukovic N, Harraou S, van Duijnhoven SMJ, Zaiss DM, van Elsas A. Purification of murine immunoglobulin E (IgE) by thiophilic interaction chromatography (TIC). *J Immunol Methods*. 2021;489:112914. doi:10.1016/j.jim.2020.112914
11. de Witte MA, Coccoris M, Wolkers MC, et al. Targeting self-antigens through allogeneic TCR gene transfer. *Blood*. 2006;108(3):870-877. doi:10.1182/blood-2005-08-009357

12. Pellizzari G, Bax HJ, Josephs DH, et al. Harnessing Therapeutic IgE Antibodies to Re-educate Macrophages against Cancer. *Trends in Molecular Medicine*. 2020;26(6):615-626. doi:10.1016/j.molmed.2020.03.002
13. Daniels-Wells TR, Helguera G, Leuchter RK, et al. A novel IgE antibody targeting the prostate-specific antigen as a potential prostate cancer therapy. *BMC Cancer*. 2013;13:195. doi:10.1186/1471-2407-13-195
14. Bütikofer P, Malherbe T, Boschung M, Roditi I. GPI-anchored proteins: now you see 'em, now you don't. *The FASEB Journal*. 2001;15(2):545-548. doi:10.1096/fj.00-0415hyp
15. Ferris ST, Durai V, Wu R, et al. cDC1 prime and are licensed by CD4+ T cells to induce anti-tumour immunity. *Nature*. 2020;584(7822):624-629. doi:10.1038/s41586-020-2611-3
16. Mandelboim O, Malik P, Davis DM, Jo CH, Boyson JE, Strominger JL. Human CD16 as a lysis receptor mediating direct natural killer cell cytotoxicity. *Proc Natl Acad Sci U S A*. 1999;96(10):5640-5644. doi:10.1073/pnas.96.10.5640
17. Bryceson YT, March ME, Ljunggren HG, Long EO. Synergy among receptors on resting NK cells for the activation of natural cytotoxicity and cytokine secretion. *Blood*. 2006;107(1):159-166. doi:10.1182/blood-2005-04-1351
18. Dekkers G, Bentlage AEH, Stegmann TC, et al. Affinity of human IgG subclasses to mouse Fc gamma receptors. *MAbs*. 2017;9(5):767-773. doi:10.1080/19420862.2017.1323159
19. Uccellini MB, Aslam S, Liu STH, Alam F, García-Sastre A. Development of a Macrophage-Based ADCC Assay. *Vaccines*. 2021;9(6):660. doi:10.3390/vaccines9060660
20. Beum PV, Lindorfer MA, Taylor RP. Within Peripheral Blood Mononuclear Cells, Antibody-Dependent Cellular Cytotoxicity of Rituximab-Opsonized Daudi cells Is Promoted by NK Cells and Inhibited by Monocytes due to Shaving. *The Journal of Immunology*. 2008;181(4):2916-2924. doi:10.4049/jimmunol.181.4.2916
21. Beum PV, Kennedy AD, Williams ME, Lindorfer MA, Taylor RP. The Shaving Reaction: Rituximab/CD20 Complexes Are Removed from Mantle Cell Lymphoma and Chronic Lymphocytic Leukemia Cells by THP-1 Monocytes. *The Journal of Immunology*. 2006;176(4):2600-2609. doi:10.4049/jimmunol.176.4.2600
22. Lo M, Kim HS, Tong RK, et al. Effector-attenuating Substitutions That Maintain Antibody Stability and Reduce Toxicity in Mice. *Journal of Biological*

Chemistry. 2017;292(9):3900-3908. doi:10.1074/jbc.M116.767749

23. van Elsas A, Hurwitz AA, Allison JP. Combination Immunotherapy of B16 Melanoma Using Anti-Cytotoxic T Lymphocyte-Associated Antigen 4 (Ctla-4) and Granulocyte/Macrophage Colony-Stimulating Factor (Gm-Csf)-Producing Vaccines Induces Rejection of Subcutaneous and Metastatic Tumors Accompanied by Autoimmune Depigmentation. *J Exp Med*. 1999;190(3):355-366.

24. Simpson TR, Li F, Montalvo-Ortiz W, et al. Fc-dependent depletion of tumor-infiltrating regulatory T cells co-defines the efficacy of anti-CTLA-4 therapy against melanoma. *J Exp Med*. 2013;210(9):1695-1710. doi:10.1084/jem.20130579

25. Dahan R, Segal E, Engelhardt J, Selby M, Korman AJ, Ravetch JV. FcγRs Modulate the Anti-tumor Activity of Antibodies Targeting the PD-1/PD-L1 Axis. *Cancer Cell*. 2015;28(3):285-295. doi:10.1016/j.ccell.2015.08.004

26. Gould HJ, Mackay GA, Karagiannis SN, et al. Comparison of IgE and IgG antibody-dependent cytotoxicity in vitro and in a SCID mouse xenograft model of ovarian carcinoma. *Eur J Immunol*. 1999;29(11):3527-3537. doi:10.1002/(SICI)1521-4141(199911)29:11<3527::AID-IMMU3527>3.0.CO;2-5

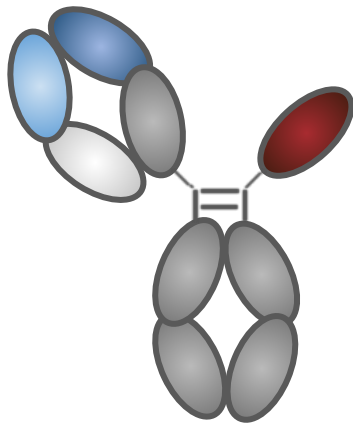
27. Leoh LS, Daniels-Wells TR, Penichet ML. IgE Immunotherapy Against Cancer. In: Lafaille JJ, Curotto de Lafaille MA, eds. *IgE Antibodies: Generation and Function*. Vol 388. Springer International Publishing; 2015:109-149. doi:10.1007/978-3-319-13725-4_6

28. Adrienne Marie Rothschilds. *Engineering Protein-Based Modulators of Allergic, Temporal, and Checkpoint Blockade Anti-Cancer Immunity*. Massachusetts Institute of Technology; 2019. <https://dspace.mit.edu/handle/1721.1/123064>

29. Carlini MJ, Dalurzo MCL, Lastiri JM, et al. Mast cell phenotypes and microvessels in non-small cell lung cancer and its prognostic significance. *Hum Pathol*. 2010;41(5):697-705. doi:10.1016/j.humpath.2009.04.029

30. de Vries VC, Wasiuk A, Bennett KA, et al. Mast cell degranulation breaks peripheral tolerance. *Am J Transplant*. 2009;9(10). doi:10.1111/j.1600-6143.2009.02755.x

6



General discussion

Over the past 30 years, monoclonal antibody (mAb) treatments have become significant to medical care [1]. Over this period, numerous important scientific and technological advancements have aided the discovery and development of mAb-based therapies. Hybridoma and phage display technology were two developments crucial to the production and identification of antibodies that were recognized with Nobel awards in 1984 and 2018 respectively [2,3]. Since then, organizations all across the world have used these technologies for antibody research and development [4,5]. As of June 30th, 2022, according to Antibody Therapies Database (Umabs-DB, <https://umabs.com>), 162 antibody therapies had received approval from at least one regulatory agency worldwide. 122 of these therapies have been approved in the US, 114 in Europe, 82 in Japan, and 73 in China [6]. Moreover, recently, to overcome the limitations of mAb therapy, bispecific antibodies (BsAbs) presenting advantages over the mAbs have become increasingly of interest [7]. The potential advantages of BsAbs include an improved selectivity towards tumors, modulation of two functional pathways in the tumor, thus avoiding resistance to the treatment, and redirection of specific immune cells to tumor cells [8]. In the past 30 years, fast evolving antibody engineering methods have helped to overcome many obstacles related to therapeutic antibodies, but a number of problems still remain, including BsAb chain mispairing issues and isotype selection problems [9]. Accordingly, in this thesis, we have studied 1) the anti-tumor therapeutic efficacy of BsAbs in a novel format which solved the chain mispairing issue, and 2) the anti-tumor therapeutic efficacy of antibodies in different isotypes.

A novel bispecific antibody format, Fab x sdAb-Fc, has overcome the potential light chain mis-pairing issue

Bispecific antibodies (BsAbs) are a vast family of molecules that can distinguish between two different antigens or epitopes. In order to simplify the manufacture of BsAbs, especially overcoming the chain mis-pairing issues, over 100 BsAb formats have been created and more than 30 of them were developed into mature commercial technology platforms [10]. A number of BsAbs have been developed by these platforms and evaluated in the clinical phase. What is more, several BsAbs developed by Art-Ig, BiTE, duobody, KiH or crossmab platform have been approved for marketing [11]. Since there are already many mature technologies such as KiH, SEED and DEEK platforms that have been invented to overcome heavy-heavy chain

mis-pairing, in this thesis (**Chapter 3**), we have focused on solving heavy-light mis-pairing issues. Y-body platform, developed by Wuhan YZY Biopharma, is based on a format combining Fab and Single-Chain Fragment Variable (scFv) to avoid potential heavy-light mis-pairing (**Chapter 1, Figure 3C**)[12]. SMAbody (Single-Domain Antibody fused to Monoclonal Ab) platform, developed by GenScript, is based on a format which fuses the single domain antibody(s) (sdAb) to a conventional monoclonal antibody to make a bispecific antibody in symmetric format (**Chapter 1, Figure 3L**). Inspired by these formats, we have developed a novel bispecific antibody format, combining a conventional Fab with a sdAb, which avoids potential heavy-light chain mis-pairing.

scFv is a fusion protein formed by engineering the association of the VH and VL domains of the antibodies with a short polypeptide linker. Therefore, combining Fab with an scFv would not have an issue of heavy-light chain mis-pairing. In contrast, camelid sdAb does not have a corresponding light chain naturally [13]. The VH region of an antibody contains three complementarity determining regions (CDR1-CDR3) and four conserved framework regions (FR1-FR4). In the conventional VH region, four highly conserved hydrophobic amino acids (Val37, Gly44, Leu45, and Trp47) make up the standard FR2, which together with Gln39, Gly44, Tyr91, and Trp103 form a conserved hydrophobic interface that makes it easier for VL joining [14]. However, in the camelid sdAb, these four hydrophobic residues are replaced by more hydrophilic amino acids (Phe37, Glu44, Arg45, and Gly47) [15–17], thus abrogating its binding to any VLs and displaying higher solubility comparing to scFv [18,19]. The properties of sdAb in comparison to scFv are summarized in table 1. Because of all above, we considered sdAb as a good compartment in forming BsAbs and developed a novel format Fab x sdAb-Fc. In chapter 3 we demonstrated that BsAbs in Fab x sdAb-Fc format were efficiently formed by applying any commonly used heterodimerization methods. The purity of the BsAbs was up to 95.9% and the aggregation was lower than 1%. In addition, the BsAbs still maintained the binding capacity to two different antigens simultaneously.

Table 1 [13]

Physiochemical properties	scFv	sdAb
Size	30-35KDa	12-15KDa
Water solubility	Medium	Very high
Aggregation	Medium	N/A
Stability	Medium	Very high
Affinity	High	High
Tissue penetration	Medium	High
Immunogenicity	Medium	Low

The application of Fab x sdAb-Fc format on T cell redirecting bispecific antibodies

T cell redirecting bispecific antibody (TbsAb) is a subclass of BsAb that bridges T cells and tumor cells and promotes immune synapse formation between these cells [20]. The most common TbsAb target is the CD3 subunit of the TCR, whereas the other arm targets a tumor associated antigen (TAA) expressed on the cell surface of tumors, such as the B cell antigen CD19. T cell redirecting bispecific antibodies have received a great deal of attention in recent years due to the approval of Blinatumomab, a CD19-directed T cell engager, by FDA for the treatment of refractory B-cell precursor acute lymphoblastic leukemia (ALL) patients in 2018 [21]. Among over 100 BsAbs currently being evaluated in clinical trials, the majority are TbsAbs [8]. TbsAbs can be roughly divided into two classes: fragment-based TbsAbs and IgG-like TbsAbs. The major problem of fragment-based TbsAbs is their short serum half-life, due to the lack of Fc. As a representative of fragment-based TbsAbs, Blinatumomab has a serum half-life of only ~2.11 hours [22]. In order to maintain certain serum drug concentration, Blinatumomab have to be administered via continuous intravenous infusion and delivered at a constant flow rate using a pump system. In contrast, IgG-like TbsAbs with Fc, display a similar serum half-life as conventional IgGs, which is usually around 10-21 days [23]. However, nonspecific activation of immune cells could be induced by the cross-linking of CD3 and Fc γ receptors, thus

mutations have to be introduced into Fc region to avoid Fc-FcγR association for TbsAbs [24–27]. Moreover, because of the Fc-in-presence architecture, chain association issues of IgG-like TbsAbs must be resolved [28]. Thus, the format we have described in chapter 3 could be applied to generate IgG-like TbsAbs. In addition, it has been demonstrated that the distance between T cells and tumor cells is a key factor that influences the anti-tumor efficacy of TbsAbs. For example, Bluemel et al. have generated two BiTE antibodies with similar binding affinity to melanoma chondroitin sulfate proteoglycan (MCSP) and epithelial cell adhesion molecule (EpCAM). However, these BiTEs displayed significant variations in their ability to redirect lysis CHO cells that had been transfected stably with engineered protein with various distances from the antigen to the cell membrane. BiTEs were more effective when they bound to the membrane-proximal domain D3 of MCSP than when they bound to the more distal domains [29]. Moreover, several studies have already successfully modulated the distance between TAA and CD3E binding sites of TbsAbs and enhanced tumor cell lysis by using alternative formats. For example, Wei Chen et al. produced and compared a bispecific diabody-Fc format, which displays a relatively short antigen-binding arm distance (3-6nm), with conventional IgG (9-15nm) format bispecific antibodies. A panel of cells were expressed with B cell maturation antigen (BCMA) fusing to various EGF-like domains as tethers to increase the distance to the membrane of target cells. It has been demonstrated that diabody-Fc is more effective than IgG format bispecific antibody in the case of targeting membrane distal antigen epitopes [30]. In addition, the flexibility of the two arms of the antibody is another key factor that relates to the potency of TbsAbs. Paul A. Moore and colleagues have developed a bispecific antibody platform termed dual affinity retargeting (DART). Their data has shown that DART molecules are much more potent in mediating tumor cell lysis than BiTE molecules. Since the same antigen recognition specificities were used, the increased tumor cell lysis mediated by DART molecules is most likely due to their lesser flexibility between the 2 binding domains in comparison to BiTE molecules [31].

Based on all these findings, we realized that the potency of TbsAb in the bispecific antibody format we have described in chapter 3 could be potentially enhanced by shortening the hinge between sdAb and Fc of the format. Therefore, in chapter 4, we generated two TbsAbs in Fab x sdAb-Fc format against mCD3 and mEGFR with two different hinges that differed in length termed TbsAb.long and TbsAb.short. The data of an in vitro tumor

cell lysis assay demonstrated that the TbsAb.short molecules induced better T-cell mediated cytotoxicity towards cells expressing mEGFR than the TbsAb.long form while inducing no specific cell lysis in mEGFR negative cell lines. In addition, our data showed that the TbsAb.short molecules could induce more effector cell/target cell clusters than TbsAb.long molecules. Previous studies demonstrated that TbsAbs could activate T cells which leads to the production of well-known activation markers such as CD69 and CD25 [32–35]. Consistent with these studies, in chapter 4, we have clearly shown that the expression of CD69 and CD25 were upregulated on T cells recruited by TbsAb.long or TbsAb.short molecules. Notably, the TbsAb.short molecules induced significantly higher expression of CD69 and CD25 than TbsAb.long molecules did. In comparison to other studies, instead of using alternative bispecific antibody formats, we have only deleted a few amino acids in the hinge region of the same format and resulting in significantly improved potency. Together, our data demonstrated that shortening the distance between T cells and tumor cells by engineering the hinge region could potentially improve the anti-tumor activity of TbsAb molecules. The underlying mechanism might be that the shortened distance between T cells and tumor cells could facilitate the formation of T cell/tumor cell clusters, thus extensively activating T cells. Nevertheless, in particular scenarios, such as when the targeted epitope is masked by elongated structural spacer domains, a longer arm of TbsAb might facilitate the TbsAb molecule to effectively bridge the epitope and T cells [30]. A BsAb format suitable for all applications does not exist, in this case, a longer hinge of Fab x sdAb-Fc format should be designed for desired applications specifically.

Isotype selection of therapeutic antibodies as cancer therapy

Fc tail is the domain where antibodies interact with the complement system and different effector cells to mediate antibody-dependent cell-mediated cytotoxicity (ADCC), antibody-dependent cell-mediated phagocytosis (ADCP) and complement-dependent cytotoxicity (CDC) against tumor cells [36,37]. The downstream effector function is mostly influenced by antibody isotype since the immunological responses brought on by various antibody isotypes are primarily caused by variable affinities for activating and inhibitory FcRs, also known as the activating-to-inhibitory (A/I) ratio [38]. IgG is the most abundant type of antibody found in blood circulation in humans which represents approximately 75% of serum

antibodies [39]. Currently, all marketed therapeutic antibodies are in IgG isotype based on practical and functional concerns. The human IgG class can be further subdivided into four isotypes: hIgG1, hIgG2, hIgG3 and hIgG4. Within this class, IgG3 and IgG1 have the highest A/I ratio reflecting their high affinity for activating FcRs and low affinity for the inhibitory one. However, due to several unfavored physico-chemical properties of IgG3 such as high allotypic polymorphism, susceptibility to proteolysis and aggregate formation during production, IgG1 has been the most selected isotype for antibodies as tumor targeting therapy [40–43]. Similarly, the counterpart of human IgG1 in the mouse immune system, mouse IgG2a has the highest A/I ratio, whereas mouse IgG1 shows the lowest A/I ratio among all mouse IgGs. Thus, in the very early development phase of a tumor targeting therapeutic antibody, mIgG2a has been usually selected as the antibody isotype to test in mouse tumor models and will be subsequently switched to hIgG1 by humanization after entering clinical trials [44].

The previous study has demonstrated that tumor-targeting mIgG2a showed superior tumor control to mIgG1 in a B16 lung metastasis model in a prophylactic setting since the antibody treatment started on the same day when the tumor cells were injected. However, in a clinical setting, treatment of human cancer is always in a therapeutic setting (treatment to be performed after the establishment of tumors). Therefore, in chapter 5, we generated monoclonal antibodies of the very same specificity, targeting a surface tumor antigen Thy1.1 with either a mIgG2a, mIgG1 or mIgE isotype and compared the *in vivo* efficacy in a therapeutic setting. Our results demonstrated that the IgG2a isotype offers superior tumor control in comparison to antibodies with an IgG1 or IgE isotype in a therapeutic setting in mice. The observed effect was entirely Fc-mediated as it was completely lost using IgG2a featuring Fc silencing LALA-PG mutations. Surprisingly, IgE antibodies did not show any anti-tumor activity in this experiment although we hypothesized it could potentially induce Treg suppression via histamine released from degranulating MCs [45].

Concluding remarks

Most studies described in this thesis investigate antibody engineering of tumor-targeting antibodies leading to either optimal antibody production or tumor cell eradication. To facilitate the production of IgG-like bispecific antibodies, a novel format (Fab x sdAb-Fc) is described in **Chapter 3**. We demonstrate that this format could avoid potential heavy-light chain mis-

pairing, thus increasing the purity of bispecific antibody products to above 95%. To further optimize this format for T-cell redirecting application, two CD3 x EGFR T-cell redirecting bispecific antibodies designed with different hinge lengths are evaluated. Our data show that optimal tumor cell killing can be achieved by the bispecific antibody using a shorter hinge design in Fab x sdAb-Fc format (**Chapter 4**). In addition, we also investigate the anti-tumor activity of antibodies in different isotypes (mouse IgG1, mouse IgG2a and mouse IgE) in a therapeutic setting. Mouse IgG2a is demonstrated to be the optimal choice for antibodies used as tumor targeting therapy (**Chapter 5**).

Taken together, our studies focus on improving the efficacy of antibody-based cancer therapy by antibody engineering. Future developments in engineering of therapeutic mAbs would be of benefit for cancer therapies and thereby for human health.

References

1. Kaplon, H.; Reichert, J.M. Antibodies to Watch in 2019. *mAbs* **2019**, *11*, 219–238, doi:10.1080/19420862.2018.1556465.
2. Smith, G.P. Filamentous Fusion Phage: Novel Expression Vectors That Display Cloned Antigens on the Virion Surface. *Science* **1985**, *228*, 1315–1317, doi:10.1126/science.4001944.
3. Gao J.; He J.; Wang Q.; Liu W. Monoclonal antibodies: Emergence, present and outlook. *Kexue Tongbao/Chinese Science Bulletin* **2020**, 3085–3090.
4. Frenzel, A.; Schirrmann, T.; Hust, M. Phage Display-Derived Human Antibodies in Clinical Development and Therapy. *mAbs* **2016**, *8*, 1177–1194, doi:10.1080/19420862.2016.1212149.
5. Nixon, A.E.; Sexton, D.J.; Ladner, R.C. Drugs Derived from Phage Display. *mAbs* **2014**, *6*, 73–85, doi:10.4161/mabs.27240.
6. Lyu, X.; Zhao, Q.; Hui, J.; Wang, T.; Lin, M.; Wang, K.; Zhang, J.; Shentu, J.; Dalby, P.A.; Zhang, H.; et al. The Global Landscape of Approved Antibody Therapies. *Antibody Therapeutics* **2022**, *5*, 233–257, doi:10.1093/abt/tbac021.
7. Godar, M.; de Haard, H.; Blanchetot, C.; Rasser, J. Therapeutic Bispecific Antibody Formats: A Patent Applications Review (1994-2017). *Expert Opinion on Therapeutic Patents* **2018**, *28*, 251–276, doi:10.1080/13543776.2018.1428307.
8. Huang, S.; van Duijnhoven, S.M.J.; Sijts, A.J.A.M.; van Elsas, A. Bispecific Antibodies Targeting Dual Tumor-Associated Antigens in Cancer Therapy. *J Cancer Res Clin Oncol* **2020**, *146*, 3111–3122, doi:10.1007/s00432-020-03404-6.
9. Li, H.; Er Saw, P.; Song, E. Challenges and Strategies for Next-Generation Bispecific Antibody-Based Antitumor Therapeutics. *Cell Mol Immunol* **2020**, *17*, 451–461, doi:10.1038/s41423-020-0417-8.
10. Ma, J.; Mo, Y.; Tang, M.; Shen, J.; Qi, Y.; Zhao, W.; Huang, Y.; Xu, Y.; Qian, C. Bispecific Antibodies: From Research to Clinical Application. *Frontiers in Immunology* **2021**, *12*.
11. Segués, A.; Huang, S.; Sijts, A.; Berraondo, P.; Zaiss, D. Opportunities and Challenges of Bi-Specific Antibodies. In *International Review of Cell and Molecular Biology*; 2022; Vol. 369 ISBN 978-0-323-99402-6.
12. Zhou, P.; Zhang, J.; Yan, Y. Bispecific Antibody 2017.

13. Asaadi, Y.; Jouneghani, F.F.; Janani, S.; Rahbarizadeh, F. A Comprehensive Comparison between Camelid Nanobodies and Single Chain Variable Fragments. *Biomark Res* **2021**, *9*, 87, doi:10.1186/s40364-021-00332-6.
14. Padlan, E.A. Anatomy of the Antibody Molecule. *Mol Immunol* **1994**, *31*, 169–217, doi:10.1016/0161-5890(94)90001-9.
15. Muyldermans, S.; Atarhouch, T.; Saldanha, J.; Barbosa, J.A.; Hamers, R. Sequence and Structure of VH Domain from Naturally Occurring Camel Heavy Chain Immunoglobulins Lacking Light Chains. *Protein Eng* **1994**, *7*, 1129–1135, doi:10.1093/protein/7.9.1129.
16. Muyldermans, S. Nanobodies: Natural Single-Domain Antibodies. *Annu Rev Biochem* **2013**, *82*, 775–797, doi:10.1146/annurev-biochem-063011-092449.
17. Vu, K.B.; Ghahroudi, M.A.; Wyns, L.; Muyldermans, S. Comparison of Llama VH Sequences from Conventional and Heavy Chain Antibodies. *Molecular Immunology* **1997**, *34*, 1121–1131, doi:10.1016/S0161-5890(97)00146-6.
18. Muyldermans, S.; Cambillau, C.; Wyns, L. Recognition of Antigens by Single-Domain Antibody Fragments: The Superfluous Luxury of Paired Domains. *Trends in Biochemical Sciences* **2001**, *26*, 230–235, doi:10.1016/S0968-0004(01)01790-X.
19. Davies, J.; Riechmann, L. “Camelising” Human Antibody Fragments: NMR Studies on VH Domains. *FEBS Lett* **1994**, *339*, 285–290, doi:10.1016/0014-5793(94)80432-x.
20. Goebeler, M.-E.; Bargou, R.C. T Cell-Engaging Therapies — BiTEs and Beyond. *Nat Rev Clin Oncol* **2020**, *17*, 418–434, doi:10.1038/s41571-020-0347-5.
21. Przepiorka, D.; Ko, C.-W.; Deisseroth, A.; Yancey, C.L.; Candau-Chacon, R.; Chiu, H.-J.; Gehrke, B.J.; Gomez-Broughton, C.; Kane, R.C.; Kirshner, S.; et al. FDA Approval: Blinatumomab. *Clinical Cancer Research* **2015**, *21*, 4035–4039, doi:10.1158/1078-0432.CCR-15-0612.
22. Mocquot, P.; Mossazadeh, Y.; Lapierre, L.; Pineau, F.; Despas, F. The Pharmacology of Blinatumomab: State of the Art on Pharmacodynamics, Pharmacokinetics, Adverse Drug Reactions and Evaluation in Clinical Trials. *Journal of Clinical Pharmacy and Therapeutics* **2022**, *47*, 1337–1351, doi:10.1111/jcpt.13741.
23. Booth, B.J.; Ramakrishnan, B.; Narayan, K.; Wollacott, A.M.; Babcock, G.J.; Shriver, Z.; Viswanathan, K. Extending Human IgG Half-Life Using

Structure-Guided Design. *MAbs* **2018**, *10*, 1098–1110, doi:10.1080/19420862.2018.1490119.

24. Klupsch, K.; Baeriswyl, V.; Scholz, R.; Dannenberg, J.; Santimaria, R.; Senn, D.; Kage, E.; Zumsteg, A.; Attinger-Toller, I.; von der Bey, U.; et al. COVA4231, a Potent CD3/CD33 Bispecific FynomAb with IgG-like Pharmacokinetics for the Treatment of Acute Myeloid Leukemia. *Leukemia* **2019**, *33*, 805–808, doi:10.1038/s41375-018-0249-z.

25. Liu, L.; Lam, C.-Y.K.; Long, V.; Widjaja, L.; Yang, Y.; Li, H.; Jin, L.; Burke, S.; Gorlatov, S.; Brown, J.; et al. MGD011, A CD19 x CD3 Dual-Affinity Retargeting Bi-Specific Molecule Incorporating Extended Circulating Half-Life for the Treatment of B-Cell Malignancies. *Clin Cancer Res* **2017**, *23*, 1506–1518, doi:10.1158/1078-0432.CCR-16-0666.

26. Xu, H.; Cheng, M.; Guo, H.; Chen, Y.; Huse, M.; Cheung, N.-K.V. Retargeting T Cells to GD2 Pentasaccharide on Human Tumors Using Bispecific Humanized Antibody. *Cancer Immunol Res* **2015**, *3*, 266–277, doi:10.1158/2326-6066.CIR-14-0230-T.

27. Lopez-Albaitero, A.; Xu, H.; Guo, H.; Wang, L.; Wu, Z.; Tran, H.; Chandarlapaty, S.; Scaltriti, M.; Janjigian, Y.; de Stanchina, E.; et al. Overcoming Resistance to HER2-Targeted Therapy with a Novel HER2/CD3 Bispecific Antibody. *Oncoimmunology* **2017**, *6*, e1267891, doi:10.1080/2162402X.2016.1267891.

28. Klein, C.; Sustmann, C.; Thomas, M.; Stubenrauch, K.; Croasdale, R.; Schanzer, J.; Brinkmann, U.; Kettenberger, H.; Regula, J.T.; Schaefer, W. Progress in Overcoming the Chain Association Issue in Bispecific Heterodimeric IgG Antibodies. *mAbs* **2012**, *4*, 653–663, doi:10.4161/mabs.21379.

29. Bluemel, C.; Hausmann, S.; Fluhr, P.; Sriskandarajah, M.; Stallcup, W.B.; Baeuerle, P.A.; Kufer, P. Epitope Distance to the Target Cell Membrane and Antigen Size Determine the Potency of T Cell-Mediated Lysis by BiTE Antibodies Specific for a Large Melanoma Surface Antigen. *Cancer Immunol Immunother* **2010**, *59*, 1197–1209, doi:10.1007/s00262-010-0844-y.

30. Chen, W.; Yang, F.; Wang, C.; Narula, J.; Pascua, E.; Ni, I.; Ding, S.; Deng, X.; Chu, M.L.-H.; Pham, A.; et al. One Size Does Not Fit All: Navigating the Multi-Dimensional Space to Optimize T-Cell Engaging Protein Therapeutics. *mAbs* **2021**, *13*, 1871171, doi:10.1080/19420862.2020.1871171.

31. Moore, P.A.; Zhang, W.; Rainey, G.J.; Burke, S.; Li, H.; Huang, L.; Gorlatov, S.; Veri, M.C.; Aggarwal, S.; Yang, Y.; et al. Application of Dual Affinity Retargeting Molecules to Achieve Optimal Redirected T-Cell Killing

of B-Cell Lymphoma. *Blood* **2011**, *117*, 4542–4551, doi:10.1182/blood-2010-09-306449.

32. Brandl, C.; Haas, C.; d'Argouges, S.; Fisch, T.; Kufer, P.; Brischwein, K.; Prang, N.; Bargou, R.; Suzich, J.; Baeuerle, P.A.; et al. The Effect of Dexamethasone on Polyclonal T Cell Activation and Redirected Target Cell Lysis as Induced by a CD19/CD3-Bispecific Single-Chain Antibody Construct. *Cancer Immunol Immunother* **2007**, *56*, 1551–1563, doi:10.1007/s00262-007-0298-z.

33. Choi, B.D.; Kuan, C.-T.; Cai, M.; Archer, G.E.; Mitchell, D.A.; Gedeon, P.C.; Sanchez-Perez, L.; Pastan, I.; Bigner, D.D.; Sampson, J.H. Systemic Administration of a Bispecific Antibody Targeting EGFRvIII Successfully Treats Intracerebral Glioma. *Proceedings of the National Academy of Sciences* **2013**, *110*, 270–275, doi:10.1073/pnas.1219817110.

34. Mack, M.; Gruber, R.; Schmidt, S.; Riethmüller, G.; Kufer, P. Biologic Properties of a Bispecific Single-Chain Antibody Directed against 17-1A (EpCAM) and CD3: Tumor Cell-Dependent T Cell Stimulation and Cytotoxic Activity. *The Journal of Immunology* **1997**, *158*, 3965–3970.

35. Labrijn, A.F.; Meesters, J.I.; Bunce, M.; Armstrong, A.A.; Somani, S.; Nesspor, T.C.; Chiu, M.L.; Altıntaş, I.; Verploegen, S.; Schuurman, J.; et al. Efficient Generation of Bispecific Murine Antibodies for Pre-Clinical Investigations in Syngeneic Rodent Models. *Sci Rep* **2017**, *7*, 2476, doi:10.1038/s41598-017-02823-9.

36. Chenoweth, A.M.; Wines, B.D.; Anania, J.C.; Mark Hogarth, P. Harnessing the Immune System via FcγR Function in Immune Therapy: A Pathway to next-Gen MAbs. *Immunology & Cell Biology* **2020**, *98*, 287–304, doi:10.1111/imcb.12326.

37. Gaetano, N.D.; Cittera, E.; Nota, R.; Vecchi, A.; Grieco, V.; Scanziani, E.; Botto, M.; Introna, M.; Golay, J. Complement Activation Determines the Therapeutic Activity of Rituximab In Vivo. *The Journal of Immunology* **2003**, *171*, 1581–1587, doi:10.4049/jimmunol.171.3.1581.

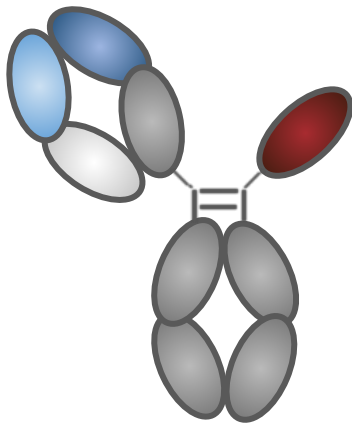
38. Nimmerjahn, F.; Anthony, R.M.; Ravetch, J.V. Agalactosylated IgG Antibodies Depend on Cellular Fc Receptors for in Vivo Activity. *Proceedings of the National Academy of Sciences* **2007**, *104*, 8433–8437, doi:10.1073/pnas.0702936104.

39. Vidarsson, G.; Dekkers, G.; Rispen, T. IgG Subclasses and Allotypes: From Structure to Effector Functions. *Front Immunol* **2014**, *5*, 520, doi:10.3389/fimmu.2014.00520.

40. Jefferis, R. Antibody Therapeutics: *Expert Opinion on Biological Therapy* **2007**, *7*, 1401–1413, doi:10.1517/14712598.7.9.1401.

41. Salfeld, J.G. Isotype Selection in Antibody Engineering. *Nat Biotechnol* **2007**, *25*, 1369–1372, doi:10.1038/nbt1207-1369.
42. Carter, P.J. Potent Antibody Therapeutics by Design. *Nat Rev Immunol* **2006**, *6*, 343–357, doi:10.1038/nri1837.
43. Human Gm, Km, and Am Allotypes and Their Molecular Characterization: A Remarkable Demonstration of Polymorphism - PubMed Available online: <https://pubmed.ncbi.nlm.nih.gov/22665258/> (accessed on 2 April 2023).
44. Nimmerjahn, F.; Ravetch, J.V. Divergent Immunoglobulin G Subclass Activity Through Selective Fc Receptor Binding. *Science* **2005**, *310*, 1510–1512, doi:10.1126/science.1118948.
45. De Vries, V.C.; Wasiuk, A.; Bennett, K.A.; Benson, M.J.; Elgueta, R.; Waldschmidt, T.J.; Noelle, R.J. Mast Cell Degranulation Breaks Peripheral Tolerance. *American Journal of Transplantation* **2009**, *9*, 2270–2280, doi:10.1111/j.1600-6143.2009.02755.x.

7



Summary/Overzicht

Summary

Bispecific antibodies (BsAbs) are a class of monoclonal antibodies that can target two different antigens/epitopes simultaneously. It has been more than a decade since the first BsAb was approved by the European Medicines Agency (EMA) in 2009, and during this time, emerging data have demonstrated the huge advantage of BsAb over conventional monospecific antibodies. As a result, BsAbs have become a popular medication class for treating cancer, and their potential for therapeutic application has grown in recent years. The number of marketed BsAbs in the year 2022 has already exceeded the number of approved BsAbs ever before, thus BsAbs have finally reached their golden age.

BsAbs can be roughly divided into two classes: IgG-like BsAbs and fragment-based BsAbs. Fragment-based BsAbs have a much shorter serum half-life due to the absence of the Fc fragment, which has limited their application in the clinic. In contrast, IgG-like BsAbs have relatively long serum half-lives, however, generating pure IgG-like BsAbs and improving their yield is still challenging due to chain association issues. The production of a BsAb in one expression cell line is very difficult and unfavourable due to challenges in extracting the desired BsAb from the lysates and the inherently low yield (**Chapter 1, Figure 2**). Thus, the aim of the research described in **chapter 3** was to design a novel format to improve the purity and yield of BsAb during production. We have combined a conventional antigen-binding fragment with a single-domain antibody and generated BsAbs in a Fab x sdAb-Fc format. Our data show that this format can avoid potential heavy-light chain mis-pairing during the production of BsAbs, and increases the purity of BsAbs to above 95%. Further characterization assays showed that the BsAbs in this configuration nevertheless maintained the ability of binding to two distinct antigens concurrently.

During the design of this novel BsAb format, we found that the hinge region can be adapted for different application scenarios. There are already several studies indicating that enhanced T-cell mediated tumor cell elimination can be achieved by decreasing the distance between T cells and tumor cells. In our case, the distance between tumor cells and T cells can be modulated by different hinge designs. Thus, we modulated the hinge region in T-cell redirecting bispecific antibodies (TRBAs) and studied their anti-tumor activity in in vitro assays. Our data show that with less space separating the two arms of the TRBA, tumor cells and effector T cells can bridge more tightly,

which strengthens T cell activation and, in turn, increases tumor cell death. Therefore, our data indicate that the modulation of the 'hinge region length' parameter can possibly contribute to future design of similar molecules **(Chapter 4)**.

Since the antibody Fc-tail activates specific immune effector mechanisms, antibody isotype plays an important role in cancer therapy. Previous studies in a mouse tumor model showed the efficacy of prophylactic application of mIgG2a isotype antibodies. However, human cancer patients usually receive antibodies in a therapeutic setting. Thus, in the last study, we developed a panel of anti-Thy1.1 antibodies with various isotypes (mIgG1, mIgG2a, mIgE and Fc-silenced) and evaluated their effectiveness in a therapeutic setting in mouse tumor models. Our data demonstrated that mIgG2a is the most effective isotype in treating cancer in a therapeutic setting in mice. Therefore, isotype selection is a critical parameter determining the efficacy of tumor-targeting antibody therapy. We believe future research in tumor immunotherapy may benefit from the knowledge we gained in designing tumor antigen targeting antibodies for cancer therapy **(Chapter 5)**.

Overzicht

Bispecifieke antilichamen (BsAb) zijn een klasse van monoklonale antilichamen die twee verschillende antigenen/epitopen tegelijkertijd kunnen binden. Meer dan tien jaar geleden, in 2009, werd het eerste BsAb goedgekeurd door het Europees Geneesmiddelenbureau (EMA) en sinds deze tijd hebben nieuwe gegevens het enorme voordeel van BsAb ten opzichte van conventionele monospecifieke antilichamen aangetoond. Als gevolg hiervan zijn BsAbs een populaire medicatieklasse geworden voor de behandeling van kanker, en hun potentieel voor therapeutische toepassing is de laatste jaren sterk gegroeid. Het aantal op de markt gebrachte BsAbs in 2022 is al groter dan het aantal goedgekeurde BsAbs ooit tevoren, erop duidend dat BsAbs hun Gouden Eeuw hebben bereikt.

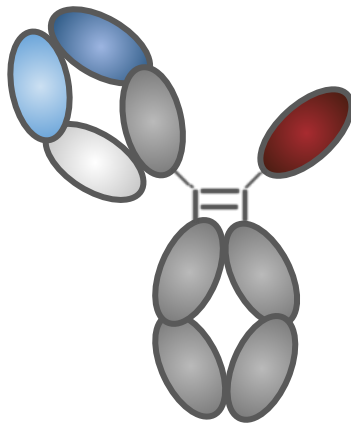
BsAbs kunnen grofweg in twee klassen worden onderverdeeld: 'IgG-like' BsAbs en op fragmenten gebaseerde BsAbs. Op fragmenten gebaseerde BsAbs hebben een korte serumhalfwaardetijd vanwege de afwezigheid van een Fc-staart, wat hun toepassing in de kliniek beperkt. 'IgG-like' BsAbs daarentegen hebben een relatief lange serumhalfwaardetijd, maar het genereren van zuivere 'IgG-like' BsAbs en het verbeteren van de opbrengst hiervan is vanwege problemen met ketenassociatie nog steeds een uitdaging. De productie van een BsAb in één expressiecellijn wordt verder bemoeilijkt door uitdagingen bij het extraheren van het gewenste BsAb en de inherent lage opbrengst (**Hoofdstuk 1, Figuur 2**). Het doel van het onderzoek beschreven in **hoofdstuk 3** was dus om een nieuw formaat te ontwerpen om de zuiverheid en opbrengst van BsAb tijdens de productie te verbeteren. We hebben een conventioneel antigeenbindend fragment gecombineerd met een antilichaam met één domein, en BsAbs gegenereerd met Fab x sdAb-Fc-formaat. Wij hebben gevonden dat dit formaat mogelijke miskoppeling van zware en lichte ketens tijdens de productie kan voorkomen en de zuiverheid van BsAbs kan verhogen tot meer dan 95%. Verdere karakteriseringstesten hebben aangetoond dat BsAbs in deze configuratie het vermogen behielden om twee verschillende antigenen tegelijkertijd te binden.

Tijdens het ontwerpen van dit nieuwe BsAb-formaat ontdekten we dat de 'hinge region' aangepast kan worden voor verschillende toepassingsscenario's. Verschillende onderzoeken lieten al zien dat T-cel-gemedieerde tumorceleliminatie verbeterd kan worden door de afstand tussen T-cellen en tumorcellen te verkleinen. Ook in ons geval kon de afstand tussen tumorcellen en T-cellen worden gemoduleerd door

manipulatie van de 'hinge region'. Dit hebben we toegepast in zogenaamde 'T-cell-redirecting' bispecifieke antilichamen (TRBA's), waarvan we vervolgens de antitumoractiviteit in *in vitro* testen bestudeerd hebben. We vonden dat reductie van de afstand tussen de twee armen van TRBA, tumorcellen en effector-T-cellen in staat stelde een strakkere brug te vormen, wat T-celactivering versterkte en tumorcel dood verhoogde. Dus modulatie van de parameter 'hinge region length' kan mogelijk bijdragen aan het toekomstige ontwerp van vergelijkbare moleculen (**Hoofdstuk 4**).

Aangezien het Fc-deel van antilichamen een specifiek immuun-effectormechanisme activeert, speelt het isotype van antilichamen een belangrijke rol in kankertherapie. Eerdere studies hebben de werkzaamheid van mIgG2a-isotype-antilichamen aangetoond bij profylactische toepassing in muizentumormodellen. Behandeling van menselijke kankerpatiënten met antilichamen vindt echter meestal plaats in een therapeutische setting. Daarom hebben we in de laatste studie een panel van anti-Thy1.1-antilichamen met verschillende isotypen (mIgG1, mIgG2a, mIgE en Fc-silenced) ontwikkeld en hun effectiviteit in muizentumormodellen geëvalueerd, in een therapeutische setting. Onze resultaten tonen aan dat mIgG2a het meest effectieve isotype is bij behandeling van kanker in muizen in een therapeutische setting. Daarom is isotypeselectie een kritische parameter die de werkzaamheid van tumorspecifieke antilichaamtherapie bepaalt. Wij menen dat toekomstig onderzoek naar tumorimmunotherapie mogelijk gebaat is bij onze resultaten (**Hoofdstuk 5**).

Appendix



Acknowledgements
Curriculum vitae
List of publications

Acknowledgements

During my PhD journey over the past four years, I met many people who offered me their endless support, help and friendship, and without the help and support from them, this thesis would not have been possible.

I would like to thank all my supervisors, **Dietmar Zaiss**, **Alice Sijts**, **Andrea van Elsas**, **Sander van Duijnhoven**, **Pedro Berraondo** and **Ignacio Melero** for their supervision and guidance of the research project as described in the thesis.

My supervisor, **Dietmar Zaiss**, for helping me by supervising research of two of my papers (Chapter 4 and chapter 5). I am always impressed by your extensive immunology knowledge and great ideas.

My supervisor, **Alice Sijts**, for supporting my project and all the paperwork at Utrecht University. Many thanks for your valuable advice, kind help and always being patient.

My co-supervisor, **Andrea van Elsas**, for helping me settle down in the Netherlands and supporting my projects (chapter 2 and chapter 3) with all your expertise in immunology and monoclonal antibody engineering at Aduro Biotech.

My daily supervisor **Sander van Duijnhoven**, for helping me by supervising research of two of my papers (chapter 2 and chapter 3). You are always nice, approachable and have great ideas on antibody designation and engineering.

My co-supervisors, **Nacho** and **Kepa** for their valuable advice and guidance.

To the great **Aduro team**, my immunology teacher **Paul Vink**, for setting up an immunology course for us; **Aduro CMC team (Marc Snippert, Salim Harraou and Thomas Guyomard)** for teaching me antibody purification and quality control; **Aduro molecular biology team (Mark Parade, Lilian Driessen, Ingeborg de Breet and Inge Reinieren Beeren)** for their practical guidance on molecular biology experiments; **Joost** for setting up a course on the overview of drug development and running a biotech; **Mary**

for helping us furnish our house in Oss, **Jos, Peter, Tu-Anh, Maarten, Teun, Erik and everybody else** for helping me with my project at Aduro Biotech.

To my colleagues, also flat mates (**Aina** and **Natasa**): We have had a memorable time together and become best friends. You are the correct persons with whom I can express my joy and sorrow. I appreciate your kindness and support of both my life and my research.

My project was part of the EU Marie Curie Initial Training Network (ITN) on the Tumor Treg Targeting. I would like to thank the **European Commission** for funding the whole project and the rest of members: **Belén** for her administrative support and the rest of the students –**Claudia and Susy**, for being good friends and for mental support.

To Edinburgh colleagues,

To **Rose Zamoyska**, for her valuable advice and support. To **Patricia and Alex** for sharing their experiences and knowledge in immunology, **David Wright** for helping me with CRISPR-Cas9 technology. To the rest of the **Zamoyska team**, for sharing their knowledge and making me a member of the team. To **Samer**, for valuable help with molecular cloning and arranging a Pymol course for us. To **Martin Waterfall**, for helping me with his expertise in flow cytometry.

致谢

这里，我想从 2016 年我出国后的生涯开始写起，因为这些经历帮助我开启了后来的博士生涯并产生了重要影响。

雷润博士，在美国最早认识的朋友，感谢你在我做 visiting scientist 期间以及后来我在上海 Inmagene Biopharmaceuticals 实习期间对我提供的指导和帮助。

臧星星教授，作为我的肿瘤免疫学启蒙导师，感谢您在我做 visiting scientist 期间对我的悉心指导带领我走进肿瘤免疫学的世界，以及后来申请玛丽居里博士奖学金提供的支持。同时也感谢在 Zanglab 一起学习工作的小伙伴们，魏瑶，任晓新，汪浩，石磊，崔微，索琳娜，邢鹏，苏莹珍，张晓雨，Peter John, Damini Chand, Elodie Picarda，感谢你们对我的帮助和照顾，祝愿你们一切顺利。

邹俊韬，在美期间的 flat mate，感谢你像大哥一样对我的照顾，非常怀念这段时光。

感谢 UU 的吕庆康师兄，虽然我们在一起工作的时间不长，但是你给我提供了非常多的便利和帮助。再次恭喜你和王燕师姐一起拿到 PhD 学位并祝愿你们在美国生活工作一切顺利。

感谢 Aduro Biotech 的孙恬大哥。感谢你在此期间给我提供的帮助，感谢你给我人生，学习上的建议，使我受益匪浅。非常羡慕你的人生态度，希望有一天也能像你一样一边写书一边走遍世界。

感谢 **Andrea Van Elsas** 和 **Sander Van Duijnhoven**，作为我在工业界导师，您们总是耐心倾听，悉心指导；总是保持优雅乐观，从不把负面情绪传导给别人。祝愿 **Andrea** 在 Third Rock Venture，**Sander** 在 ImmunoPrecise Antibodies 一切顺利。

感谢 **Alice Sijts, Dietmar Zaiss** 作为我在高校的导师，对我的指导和帮助。祝愿 **Alice** 在 Utrecht University, **Dietmar** 在 Regensburg University 一切顺利。

感谢我的**父母**，我的女朋友**李亚茹**（现在是黄太太），给我无条件的支持和信任，永远做我的坚强的后盾。

最后，回望过去的六年，跨越了三个大洲，五个国家，期间遇到了公司被收购并关闭荷兰的 site, COVID-19, 英国脱欧等种种困境，万幸结识了许多朋友，承蒙大家的帮助才能够顺利走到今天,衷心感谢所有帮助过我的人！

Curriculum vitae

Shuyu Huang (黄书煜) was born on July 3rd, 1992 in Ji'an city, Jiangxi Province, China. He was raised there and completed elementary, middle, and high school there. The Hebei University's undergraduate curriculum allowed him to study biology science for four years, from September 2009 to June 2013, and he graduated with a bachelor's degree in 2013. He began his master's degree program in Biochemistry and Molecular Biology at Dalian Medical University in Liaoning, China, in September 2013. He mainly concentrated on the study of non-coding RNA and DNA methylation in cancer. He received his master's in science degree in June 2016. He served as a visiting researcher in Prof. Xingxing Zang's lab at the Albert Einstein College of Medicine in May 2017 in New York, USA. Under the direction of Prof. Xingxing Zang, he worked on the project "Development of anti-human B7x antibodies for cancer immunotherapies." He had the chance to apply to the PhD program in November 2018 that was supported by Aduro Biotech (Now is Chinook Therapeutics), Utrecht University, Edinburgh University, and Navara University and funded by Marie Sklodowska-Curie Actions under Horizon 2020. Here, he created a brand-new configuration for a bispecific antibody that prevents the possibility of heavy-light chain mis-pairing. He also investigated how the hinge design of Fab x sdAb-Fc bispecific antibodies affected the destruction of tumor cells by redirected T lymphocytes.

List of publications

Vukovic, N*, Segués, A*, **Huang, S***, Waterfall, M, Sijts, A. J, & Zaiss, D. M. Mouse IgG2a isotype therapeutic antibodies elicit superior tumor growth control compared to mIgG1 or mIgE. **Cancer Research Communications** (2023) 3 (1): 109–118.

Huang S*, Segués A*, Waterfall M, Wright D, Vayssiere C, van Duijnhoven SMJ, van Elsas A, Sijts AJAM, Zaiss DM. Shortened Hinge Design of Fab x sdAb-Fc Bispecific Antibodies Enhances Redirected T-Cell Killing of Tumor Cells. **Biomolecules**. 2022; 12(10):1331.

Segués A*, **Huang S***, Sijts A, Berraondo P, Zaiss DM. Opportunities and challenges of bi-specific antibodies. **Int Rev Cell Mol Biol**. 2022;369:45-70. doi: 10.1016/bs.ircmb.2022.05.001. Epub 2022 May 30. PMID: 35777864.

Yuan, Z., Gardiner, J. C., Maggi, E. C., **Huang, S.**, Adem, A., Bagdasarov, S., Li, G., Lee, S., Slegowski, D., Exarchakis, A., Howe, J. R., Lattime, E. C., Zang, X., & Libutti, S. K. (2021). B7 immune-checkpoints as targets for the treatment of neuroendocrine tumors. **Endocrine-related cancer**, 28(2), 135–149.

Huang, S., van Duijnhoven, S.M.J., Sijts, A.J.A.M. et al. Bispecific antibodies targeting dual tumor-associated antigens in cancer therapy. **J Cancer Res Clin Oncol** (2020). <https://doi.org/10.1007/s00432-020-03404-6>.

Huang S, Segués A, Hulsik DL, Zaiss DM, Sijts AJAM, van Duijnhoven SMJ, van Elsas A. A novel efficient bispecific antibody format, combining a conventional antigen-binding fragment with a single domain antibody, avoids potential heavy-light chain mis-pairing. **J Immunol Methods**. 2020 Aug;483:112811. doi: 10.1016/j.jim.2020.112811. Epub 2020 Jun 19. PMID: 32569598.

Saha A, Taylor PA, Lees CJ, Panoskaltsis-Mortari A, Osborn MJ, Feser CJ, Thangavelu G, Melchinger W, Refaeli Y, Hill GR, Munn DH, Murphy WJ, Serody JS, Maillard I, Kreymborg K, van den Brink M, Dong C, **Huang S**, Zang X, Allison JP, Zeiser R, Blazar BR. Donor and host B7-H4 expression

Appendix

negatively regulates acute graft-versus-host disease lethality. *JCI Insight*. 2019 Oct 3;4(19):e127716. doi: 10.1172/jci.insight.127716. PMID: 31578305; PMCID: PMC6795410.